Aus dem Institut für Klinische Pharmakologie und Toxikologie
der Medizinischen Fakultät Charité – Universitätsmedizin Berlin

DISSERTATION

Molekulare Mechanismen mit Einfluss auf kardiorenale Endorganschäden bei arterieller Hypertonie

zur Erlangung des akademischen Grades
Doctor medicinae (Dr. med.)

vorgelegt der Medizinischen Fakultät Charité –
Universitätsmedizin Berlin

von

Jana Šubrová

Datum der Promotion: 30.11.2023

Inhaltsverzeichnis

Abbildungsverzeichnis

Abkürzungsverzeichnis

CPXM2	Carboxypeptidase X Member 2
DAPI	4',6-Diamidin-2-Phenylindol
DMEM	*Dulbecco's Modified Eagle Medium*
F344	Rattenstamm Fischer 344
FBS	*Fetal Bovine Serum*
FITC	Fluoresceinisothiocyanat
FLuc	*Firefly*-Luciferase
GAPDH	Glyceraldehyd-3-Phosphat-Dehydrogenase
HEK293	humane embryonale Nierenzellen
HPRT	Hypoxanthinphosphoribosyltransferase
LIM	Proteindomäne, ursprünglich beschrieben in den Proteinen LIN-11, Isl1m und MEC-3
miRNA	microRNA, *micro ribonucleic acid*, micro-Ribonukleinsäure
mut	mutiert
n.s.	kein signifikanter Unterschied
p-Wert	*probability value*, Überschreitungswahrscheinlichkeit
PCR	*polymerase chain reaction*, Polymerase-Kettenreaktion
Pdlim3	*PDZ and LIM domain 3* Protein
PDZ	Proteindomäne charakterisiert durch *postsynaptic density 95*, *discs large* und *zonula occludens-1*
RLuc	*Renilla*-Luciferase
RNA	*ribonucleic acid*, Ribonukleinsäure
SDS-PAGE	Natriumdodecylsulfat-Polyacrylamidgelelektrophorese
SHRSP	*stroke-prone spontaneously hypertensive rats* (Rattenstamm mit Prädisposition für arterielle Hypertonie)
TGF-β	*Transforming growth factor-β*
TMEM63c	Transmembranprotein 63c
UTR	untranslatierte Region
vec	Vektor

Zusammenfassung

Abstract (deutsch)

Arterielle Hypertonie führt als Zivilisationskrankheit auf Dauer zu multiplen Endorganschäden bei großen Teilen der Weltbevölkerung. Zu den häufigen Folgeerkrankungen bei chronisch erhöhtem Blutdruck gehören beispielsweise die linksventrikuläre Hypertrophie und hypertensive Nephropathie. Im Rahmen dieser Arbeit wurden molekulare Mechanismen der Entstehung von kardiorenalen Endorganschäden bei arterieller Hypertonie untersucht.

Die linksventrikuläre Hypertrophie ist ein Hauptrisikofaktor für kardiovaskuläre Ereignisse und Sterblichkeit. Ein kürzlich entdecktes Kandidatengen mit Einfluss auf die Entstehung der Hypertonie-induzierten linksventrikulären Hypertrophie ist das Gen für Carboxypeptidase X Member 2 (CPXM2). CPXM2 gehört in die M14-Familie der Metallocarboxypeptidasen, allerdings weist dieses Protein keine nachweisbare enzymatische Aktivität auf und seine genaue Funktion ist bisher unklar.

Die Expression von CPXM2 in verschiedenen kardialen Zellkulturen wurde mit Hilfe von *Real-Time polymerase chain reaction* (PCR), *Western Blotting* und Immunofluoreszenzfärbung charakterisiert. Ein besonderer Schwerpunkt dieser Arbeit lag bei der Analyse der posttranskriptionellen Regulation der CPXM2-Expression mittels microRNA (miRNA).

Die Ergebnisse der Untersuchungen zeigen, dass CPXM2 sowohl in primären Rattenkardiomyozyten als auch -fibroblasten exprimiert und unter hypertensiven Bedingungen hochreguliert wird. Eine Transfektion von H9C2-Zellen mit miRNA-29b, miRNA-195 oder miRNA-497 führte zur verminderten CPXM2-Expression auf mRNA- und Proteinebene. Die Ergebnisse des *Dual Luciferase Assays* zeigten, dass die posttranskriptionelle Regulation der Expression von CPXM2 durch miRNA-29b und miRNA-497 über eine direkte Bindung dieser miRNAs an die 3'-untranslatierte Region (3'-UTR) der CPXM2-mRNA vermittelt wird.

In einer weiteren Studie wurde ebenfalls der Einfluss von bestimmten miRNAs (miRNA-30b, miRNA-564) auf die Expression eines renal bedeutsamen Proteins (Transmembranprotein 63c; TMEM63c) in glomerulären Epithelzellen untersucht. Erste Studien deuten darauf hin, dass TMEM63c möglicherweise an der Entwicklung einer Albuminurie beteiligt ist.

Im Rahmen der hier vorliegenden Arbeit wurden miRNAs mit direktem Einfluss auf die posttranskriptionelle CPXM2- und TMEM63c-Expression identifiziert. Die hier erhobenen Daten können potenziell in späteren Studien zur Entschlüsselung der Expressionsteuerung und der genauen Funktionen von CPXM2 und TMEM63c sowie deren Rolle bei der molekularen Pathophysiologie der linksventrikulären Hypertrophie und renalen Endorganschädigung bei arterieller Hypertonie beitragen.

Abstract (englisch)

High blood pressure is one of the most prevalent diseases worldwide. It leads to various hypertension mediated organ damages such as left ventricular hypertrophy and hypertensive nephropathy. This study examines different molecular mechanisms involved in the development of cardiorenal organ damage in hypertension.

Left ventricular hypertrophy is one of the main risk factors for adverse cardiovascular events and mortality. Recently, a novel candidate gene encoding the carboxypeptidase X member 2 (CPXM2) was found to be associated with hypertension-induced cardiac hypertrophy. CPXM2 belongs to the M14 family of metallocarboxypeptidases although it lacks detectable enzyme activity and its function remains unknown.

CPXM2 expression was characterized in several cardiac cell cultures via Real-time polymerase chain reaction (PCR), western blotting and immunofluorescence staining. Additionally, we analysed the posttranscriptional regulation of CPXM2 via microRNA (miRNA).

Our results show that CPXM2 is expressed in both primary rat cardiomyocytes and cardiofibroblasts and is upregulated under hypertensive conditions. Transfection of H9C2 cells with miRNA-29b, miRNA-195, and miRNA-497, respectively, led to decreased levels of CPXM2 mRNA and protein. The performed dual luciferase assay indicated a direct posttranscriptional expression regulation of CPXM2 by binding of miRNA-29b and miRNA-497 to the 3' untranslated region of the CPXM2 mRNA.

In another study we examined the impact of selected miRNAs (miRNA-30b and miRNA-564) on the posttranscriptional regulation of an important renal protein i.e., Transmembrane Protein 63c (TMEM63c). According to recent studies, TEMEM63c could be involved in the development of albuminuria.

We identified miRNAs capable of direct influence on the posttranscriptional expression of CPXM2 and TMEM63c. Our results may help to inform future studies assessing the function of CPXM2 and TMEM63c and their role in the molecular pathology of left ventricular hypertrophy as well as renal damage in hypertension.

1 Einleitung

Arterielle Hypertonie ist eine bei der erwachsenen Weltbevölkerung weit verbreitete Erkrankung (GBD 2013 Mortality and Causes of Death Collaborators 2015). Chronisch erhöhte Blutdruckwerte führen zur Entstehung von funktionellen und strukturellen, initial asymptomatischen und potentiell reversiblen Veränderungen verschiedener Organe (Williams B 2018). Als Beispiele für diese Hypertonie-bedingten Endorganschäden gelten die linksventrikuläre Hypertrophie, hypertensive Retinopathie sowie renale Schädigungen mit daraus folgender Albuminurie (Williams B 2018).

Linksventrikuläre Hypertrophie stellt einen bedeutenden Risikofaktor für die Entstehung vieler kardiovaskulären Folgeerkrankungen, wie beispielsweise Herzinsuffizienz, Myokardinfarkt oder Herzrhythmusstörungen sowie für ein erhöhtes Sterberisiko dar (Lovic D 2017, Nwabuo CC 2020). Die Erforschung der molekularen Entstehungsmechanismen der hypertensiven Herzerkrankung ist somit von besonderem Interesse für die medizinische Forschung. Die Ergebnisse verschiedener Studien deuten darauf hin, dass unterschiedliche genetische Faktoren Einfluss auf die Entwicklung einer Herzhypertrophie haben können (Grabowski K 2013, Patel SK 2018).

Erst vor kurzem wurde ein Zusammenhang zwischen der Expression von Carboxypeptidase X Member 2 (CPXM2) und der Entwicklung einer Hypertonie-induzierten linksventrikulären Hypertrophie beschrieben (Grabowski K 2016). CPXM2 ist ein Protein aus der M14 Familie der Metallocarboxypeptidasen, jedoch weist es keine enzymatische Aktivität auf und seine genaue biologische Funktion bleibt bis heute unbekannt (Xin X 1998, Grabowski K 2022). Grabowski *et al.* zeigten, dass bei einem Rattenstamm mit Prädisposition zur arteriellen Hypertonie (*stroke-prone spontaneously hypertensive rats*, SHRSP) die CPXM2-Expression signifikant erhöht ist. Dies wurde auch im Rahmen der vorliegenden Arbeit bestätigt. CPXM2-defiziente Knockout-Mäuse entwickelten wiederum nach 8 Wochen unter hypertensiven Bedingungen im Vergleich zu Kontrolltieren weniger ausgeprägte Zeichen einer kardialen Hypertrophie und Dysfunktion (Grabowski K 2022). Zusätzlich wurden erhöhte CPXM2-Spiegel bei Patienten mit Herzhypertrophie beobachtet (Grabowski K 2022). Diese Daten machen CPXM2 zu einem interessanten Objekt für die medizinische Forschung.

Arterielle Hypertonie ist eine der häufigsten Ursachen für linksventrikuläre Hypertrophie (Yildiz M 2020). Der durch Bluthochdruck bedingte mechanische Stress führt zu Veränderungen der Genexpression in kardialen Zellen. Dieser Prozess wird als Mechanotransduktion bezeichnet und beeinflusst unter anderem verschiedene Proteine

der Z-Scheibe, wie zum Beispiel das Protein Pdlim3 (*PDZ and LIM domain 3 Protein*; PDZ steht für *postsynaptic density 95*, *discs large* und *zonula occludens*-1, LIM wurde ursprünglich in den Proteinen LIN-11, Isl1m und MEC-3 beschrieben) (Frank D 2011).

Neben der hypertensiven Herzerkrankung gehört auch die chronische Niereninsuffizienz zu den Langzeitfolgen von chronisch erhöhtem Blutdruck (Webster AC 2017). Arterielle Hypertonie führt auf Dauer zur Schädigung der renalen Glomeruli und damit verbundener Albuminurie (Leoncini G 2010, Lambers Heerspink HJ 2015). Die glomeruläre Filtration findet im Bereich der Blut-Harn-Schranke statt. Diese besteht aus dem Endothel der glomerulären Kapillaren, der glomerulären Basalmembran und einer Schicht von Podozyten (Lüllmann-Rauch R 2009). Schulz *et al.* zeigten kürzlich, dass das in Podozyten exprimierte Transmembranprotein 63C (TMEM63C) eine wichtige Rolle für die Funktionsfähigkeit der Blut-Harn-Schranke spielt und möglicherweise bei der Entwicklung von Albuminurie beteiligt ist (Schulz A 2019). Die von TMEM63C vermittelten molekularen Mechanismen sowie die Regulation seiner Expression sind bisher unbekannt. Die im Rahmen dieser Arbeit durchgeführten Experimente trugen dazu bei, dies näher zu beleuchten (Orphal M 2020).

Ferner erlauben die Ergebnisse dieser Arbeit neue Einblicke in die posttranskriptionelle micro (mi)RNA-vermittelte Regulation der Expression von CPXM2 und TMEM63C. MiRNAs sind kurze, nicht-proteinkodierende RNAs, die spezifisch an eine regulatorische Sequenz in der 3'-untranslatierten Region (3'-UTR) ihrer korrespondierenden messenger (m)RNAs binden und somit deren Translation beeinflussen. Dies führt zu einer verringerten Bildung des finalen Proteins (Eisenreich A 2014).

MiRNAs beeinflussen verschiedene zelluläre Prozesse, die u.a. an der Entstehung kardiovaskulärer Erkrankungen beteiligt sind (Eisenreich A 2013, Olson EN 2014). Beispielsweise wirkt miRNA-29b der Organfibrose entgegen, indem sie die Expression von Kollagen und anderen Proteinen der Extrazellulärmatrix in kardialen Fibroblasten inhibiert (Abonnenc M 2013). Ein anderes Beispiel für miRNAs mit Beteiligung an der Entstehung von kardiovaskulären Erkrankungen sind die Mitglieder der miRNA-15 Familie (Xiao J 2012, Porrello ER 2013, Li X 2015, Zhang X 2018). Sie sind u.a. in die Prozesse der kardialen Fibrose und Hypertrophie involviert (Tijsen AJ 2014).

Auch die Pathophysiologie renaler Erkrankungen wird von verschiedenen miRNAs beeinflusst (Trionfini P 2017). So ist beispielsweise miRNA-21 an der Entstehung der

Fibrose in Nieren und von Nierenzellkarzinomen beteiligt (Chung AC 2015, Fan B 2020).

Im Rahmen dieser Arbeit wurden mehrere miRNA-Kandidaten identifiziert, die potenziell die CPXM2-Expression regulieren können. Anschließend wurde der Einfluss von miRNA-29b, miRNA-195 und miRNA-497 auf die Expression von CPXM2 in Rattenkardiomyozyten untersucht. Ferner wurde die posttranskriptionelle Regulation der TMEM63C-Expression mittels miRNA in renalen Zellen analysiert. Die hier gewonnenen Erkenntnisse bieten neue Einblicke in die miRNA-vermittelte posttranskriptoionelle Regulation der Expression von CPXM2 und TMEM63C. Somit können die im Rahmen dieser Arbeit dargestellten Ergebnisse zur weiteren Charakterisierung der möglichen (patho-)physiologisch-relevanten zellulären Funktionen dieser Proteine und deren möglicher Rolle bei der Genese kardiorenaler Endorganschäden beitragen.

2 Material und Methoden

2.1 Zellkultur

Rattenkardiomyozyten der Zelllinie H9C2 sowie humane embryonale Nierenzellen (HEK293) wurden in Dulbecco's Modified Eagle Medium (DMEM) mit 10% *Fetal Bovine Serum* (FBS) und 1% Penicillin/Streptomycin (DMEM und Supplemente von Biochrom GmbH, Berlin, Deutschland) bei 37°C und 5% CO_2 kultiviert. Vor der Transfektion wurden die Zellen für mindestens 12h im nährstoffarmen Medium gehalten (DMEM ohne FBS). Zur Transfektion der H9C2-Zellen wurden jeweils 200nM miRNA-mimics für miRNA-29b, miRNA-195, miRNA-497 und Nonsense-miRNA-Kontrolle (Sigma-Aldrich Chemie GmbH, München, Deutschland) sowie Lipofectamine® 2000 (Thermo Fisher Scientific, Carlsbad, CA, USA) angewendet. Die HEK293-Zellen wurden jeweils mit 200nM miRNA-mimics für miRNA-30b, miRNA-564 sowie Nonsense-miRNA-Kontrolle (Sigma-Aldrich Chemie GmbH, München, Deutschland) ebenfalls mit Lipofectamine® 2000 transferiert. Die Transfektionseffizienz für H9C2-Zellen sowie für HEK293-Zellen lag jeweils bei 62% (getestet mittels *Fluorescence-activated Cell Sorting*-Analyse nach Transfektion der Zellen mit 200nM Dy547 *transfection control*; Dharmacon, Lafayette, CO, USA).

Linksventrikuläres Gewebe sowie isolierte primäre Kardiomyozyten und -fibroblasten erwachsener Ratten der Stämme SHRSP und Fischer 344 (F344) wurden uns zur weiteren Analyse freundlicherweise von unserer Kollegin Dr. med. Katja Grabowski zur Verfügung gestellt. SHRSP-Ratten gelten als ein etabliertes Modell für arterielle Hypertonie (Nabika T 2012). Die F344-Ratten stellen eine geeignete Kontrollgruppe dar (Grabowski K 2013).

2.2 *In silico*-Analyse

Zur Identifizierung von miRNAs, die potenziell mit der CPXM2- beziehungsweise der TMEM63c- mRNA interagieren könnten, wurden mehrere voneinander unabhängige Datenbanken verwendet, wie zum Beispiel TargetScan (http://www.TargetScan.org), miRDB (http://miRDB.org) und microRNA.org – Targets and Expression (http://www.microRNA.org). Die *in silico*-Analyse der räumlichen miRNA-mRNA-Wechselwirkungen wurde mit Hilfe der RNAhybrid 2.2 database (https://bibiserv.cebitec.uni-bielefeld.de/rnahybrid/) durchgeführt (Rehmsmeier, 2004).

2.3 Immunofluoreszenzfärbung

Für die Immunofluoreszenzfärbung wurden folgende Antikörper verwendet:

- polyklonale Kaninchen-Antikörper gegen CPXM2 in 1:100 Verdünnung (Thermo Fisher, Carlsbad, CA, USA)
- mit Fluoresceinisothiocyanat (FITC)-markierte goat-anti-rabbit-Antikörper in 1:200 Verdünnung (#12-507, Millipore, Darmstadt, Germany)
- polyklonale ALEXA FLUOR® 594-konjugierte anti-Pdlim3-Antikörper in 1:200 Verdünnung (#bs-2928R-A594, Bioss, Woburn, MA, USA)

Die Zellen wurden nacheinander mit den genannten Antikörpern jeweils für 1h bei Raumtemperatur inkubiert. Für die Inkubation mit fluoreszenzmarkierten Antikörpern wurden die Proben verdunkelt. Die nukleäre DNA wurde zur Darstellung der Zellkerne mit 4',6-Diamidin-2-Phenylindol (DAPI, #D1306, Thermo Fisher, Carlsbad, CA, USA) in 1:5000 Verdünnung markiert. Die Immunofluoreszenz wurde mit Hilfe eines Konfokalmikroskops (Leica TCS SPE, Wetzlar, Germany) dargestellt und mit EVOS® FL Auto Imaging System (Thermo Fisher, Carlsbad, CA, USA) analysiert.

2.4 *Real-Time polymerase chain reaction*

Die Gesamt-RNA wurde 48h nach Transfektion der Zellen mit Hilfe von Universal RNA Purification Kit (Roboklon GmbH, #E3598-02, Berlin, Germany) isoliert. Jeweils 1µg der gewonnenen RNA wurde revers transkribiert, dafür wurde ein *High-Capacity cDNA Reverse Transcription Kit* (Thermo Fisher Scientific, #4368814, Carlsbad, CA, USA) verwendet. Anschließend wurden Messungen für CPXM2 und das *Housekeeping*-Gen Hypoxanthinphosphoribosyltransferase (HPRT) mittels 7500 Fast *Real-Time polymerase chain reaction* (PCR) System (Thermo Fisher Scientific, Carlsbad, CA, USA) unter Einsatz von Fast SYBR® Green Master Mix (Applied Biosystems, Darmstadt, Germany) durchgeführt. Alle Proben wurden als Triplikate getestet. Zur Auswertung wurde die ΔΔ-ct-Methode angewendet.

2.5 Western Blot-Analysen

Für die Bestimmung der relativen CPXM2- beziehungsweise TMEM63c-Proteinexpression wurden Western Blot-Analysen durchgeführt. 48h nach der Transfektion wurden die Gesamtproteine aus den H9C2- oder HEK293-Zellen isoliert, mittels Natriumdodecylsulfat-Polyacrylamidgelelektrophorese (SDS-PAGE) aufgetrennt und auf eine Polyvinylidenfluorid-Membran (Carl Roth GmbH, Karlsruhe, Germany)

übertragen. Anschließend wurden die Proteine mittels anti-CPXM2-Antikörpern (Thermo Fisher, Carlsbad, CA, USA), anti-TMEM63c-Antikörpern (Sigma-Aldrich Chemie GmbH, München, Deutschland) sowie Antikörpern gegen das *Housekeeping*-Protein Glyceraldehyd-3-Phosphat-Dehydrogenase (GAPDH, Calbiochem, Darmstadt, Deutschland) markiert. Die relative Proteinexpression von CPXM2 und TMEM63c zu GAPDH wurde mittels der Gel-Pro Analyzer Software Version 4.0.00.001 (Media Cybernetics, Bethesda, Maryland, USA) bestimmt.

2.6 *Dual Luciferase Reporter Assay*

Um zu untersuchen, ob die getesteten miRNAs ihre Wirkung über eine direkte Bindung an die *in silico* identifizierten Bindungsstellen der CPXM2- beziehungsweise der TMEM63c-mRNA ausüben, wurde ein *Dual Luciferase Reporter Assay* durchgeführt. Dafür wurden die H9C2-Zellen mit einem *Target Clone* mit der 3'-UTR von CPXM2 (miRNA 3'-UTR *Target Clone* pEZX-MT06) beziehungsweise einem Negativkontrolle-Vektor (beide von GeneCopoeia, Rockville, MD, USA) sowie den getesteten miRNAs transfiziert. Ergänzend wurde das Experiment mit zwei CPXM2-3'-UTR-Klonen mit mutierten Bindungsstellen für miRNA-29b oder miRNA-497 wiederholt. Zur Herstellung dieser Klone wurde der Q5® *Site-Directed Mutagenesis Kit* (New England BioLabs, Ipswich, MA, USA) benutzt. 48h nach der Transfektion der H9C2-Zellen mit den getesteten miRNAs sowie den Luciferase-Vektoren wurde der *Luciferase Reporter Assay* (Dual-Glo® *Luciferase Assay System*, Promega, Madison, WI, USA) durchgeführt. Die durch die miRNAs beeinflusste *Firefly*-Luciferase-Aktivität wurde dabei relativ zur *Renilla*-Luciferase-Aktivität (Basisaktivitäts-Kontrolle) gemessen und dargestellt. Die Testung der TMEM63c-3'-UTR-Interaktion mit den entsprechenden miRNA-Kandidaten erfolgte analog in den HEK293-Zellen.

2.7 Statistische Analyse

Alle Ergebnisse wurden als Durchschnitt ± Standardabweichung angegeben. Unsere Daten wurden mit dem *Student's t-test* beziehungsweise *one-way ANOVA* (*analysis of variance*, Varianzanalyse) analysiert. Die statistischen Analysen erfolgten mit Hilfe von GraphPad Prism v4.03 (GraphPad Software, Inc., La Jolla, CA, USA). Ergebnisse mit einem Signifikanzwert (*probability value*, p-Wert) ≤ 0,05 wurden als signifikant betrachtet.

3 Ergebnisse

3.1 CPXM2 wird in kardialen Zellen der Ratte exprimiert

Mittels Immunofluoreszenzfärbung konnten wir nachweisen, dass CPXM2 in den H9C2-Zellen exprimiert wird und mit Pdlim3 ko-lokalisiert ist (Abbildung 1 A-C). Die Expresion des CPXM2-Proteins in H9C2-Zellen wurde mittels Western Blot-Analysen bestätigt (Abbildung 1 D). Zusätzlich wiesen wir CPXM2-mRNA und CPXM2-Protein im linksventrikulären Gewebe sowie in isolierten primären Kardiomyozyten und Kardiofibroblasten aus dem linken Ventrikel von SHRSP- und F344-Ratten nach. Abbildung 2 zeigt die erhöhte CPXM2-mRNA-Expression im kardialen Gewebe der zur arteriellen Hypertonie neigenden SHRSP-Ratten im Vergleich zu den Kontrolltieren (F344).

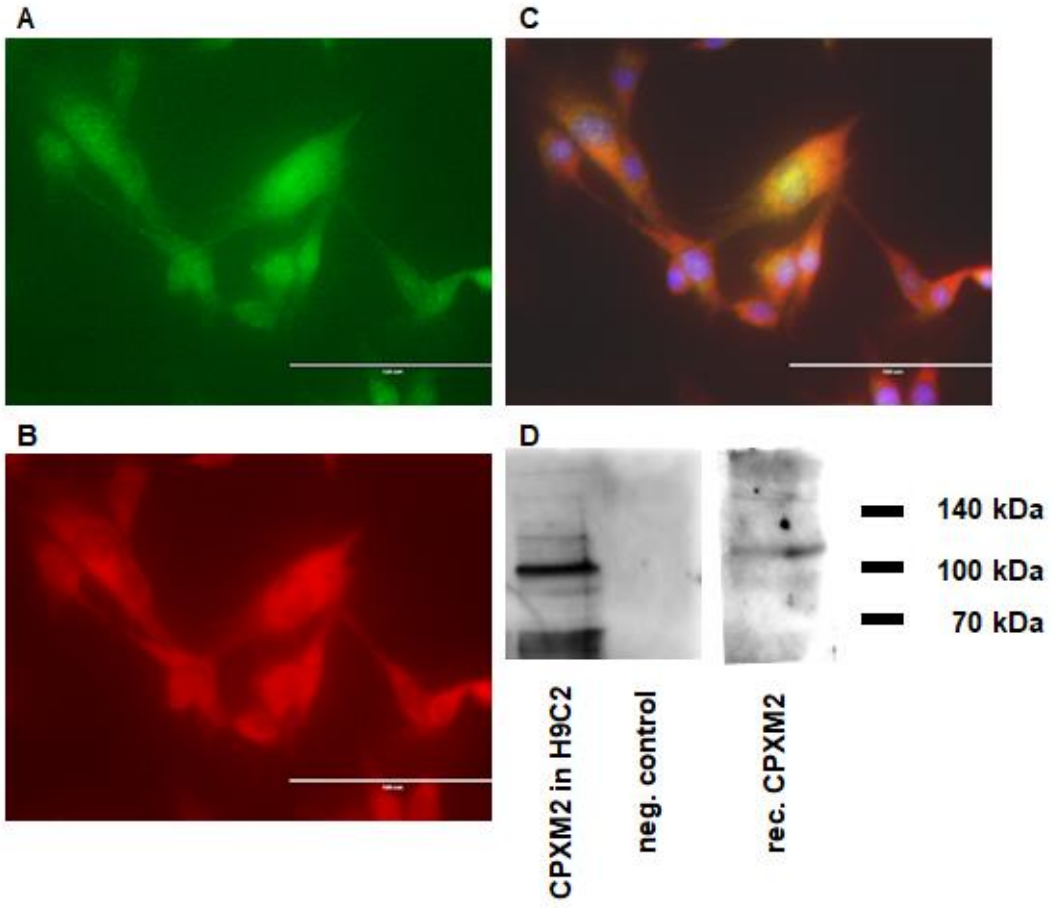

Abbildung 1. Expression von CPXM2 und Pdlim3 in Rattenkardiomyozyten.
Konfokalmikroskopische Aufnahme von H9C2-Zellen mit immunofluoreszenter Markierung von CPXM2 (A) und Pdlim3 (B). In der *Overlay*-Darstellung wird die Ko-Lokalisation von CPXM2 und Pdlim3 gezeigt (C). Nukleäre DNA wurde mit DAPI gefärbt (Zellkerne stellen sich blau dar). Der Balken entspricht 100µm. Unter (D) sind Western Blot-Ausschnitte zum Nachweis von CPXM2-Protein in H9C2-Zellen sowie eine Positivkontrolle (rekombinantes CPXM2-Protein, rec. CPXM2) und eine Negativkontrolle (leere Bande, neg. control) dargestellt. (Subrova J 2022)

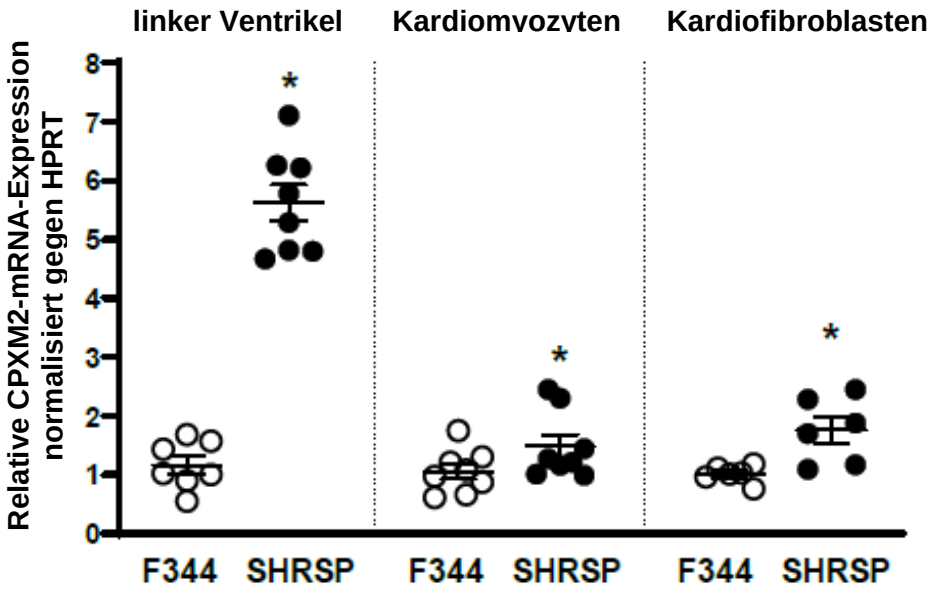

Abbildung 2. CPXM2-mRNA-Expression im kardialen Gewebe von F344- und SHRSP-Ratten.
Dargestellt ist die unterschiedlich starke CPXM2-mRNA-Expression im linksventrikulären Gewebe, in primär isolierten Kardiomyozyten und -fibroblasten aus dem linken Ventrikel von 14 Wochen alten F344- (weiß) und SHRSP-Ratten (schwarz). Die CPXM2-mRNA-Expression wurde in Relation zur HPRT-mRNA-Expression (*Housekeeping*-Gen) normalisiert. (*) $p < 0,05$. (Grabowski K 2022)

3.2 *In silico*-Identifizierung der miRNAs mit potentiellem Einfluss auf die posttranskriptionelle Expression von CPXM2

Mit Hilfe von mehreren unabhängigen miRNA-Datenbanken wurden etwa 20 verschiedene miRNAs identifiziert, die potenziell an die 3'-UTR der CPXM2-mRNA binden könnten. Für drei davon (miRNA-29b, miRNA-195 und miRNA-497) ergaben die durchgeführten *in silico*-Strukturanalysen Hinweise auf eine stabile miRNA/Ziel-mRNA-Bindung (Eisenreich A 2014, Subrova J 2022). Für miRNA-29b und miRNA-497 konnten zwei wichtige Eigenschaften bezüglich der Bindung an die 3'-UTR der CPXM2-mRNA gezeigt werden. Dies waren eine vollständige Komplementarität der *Seed Region* (miRNA-Nukleotide 2-8) mit der korrespondierenden mRNA sowie die Ausbildung einer zentralen Blase (*central bulge*) bei der miRNA/mRNA-Interaktion (Abbildung 3 A-B). Für miRNA-195 wurde nur die Ausbildung einer zentralen Blase vorhergesagt, die *Seed Region* stellte sich als nicht perfekt komplementär bezüglich der korrespondierenden Sequenz in der 3'-UTR der CPXM2-mRNA dar (Abbildung 3 C).

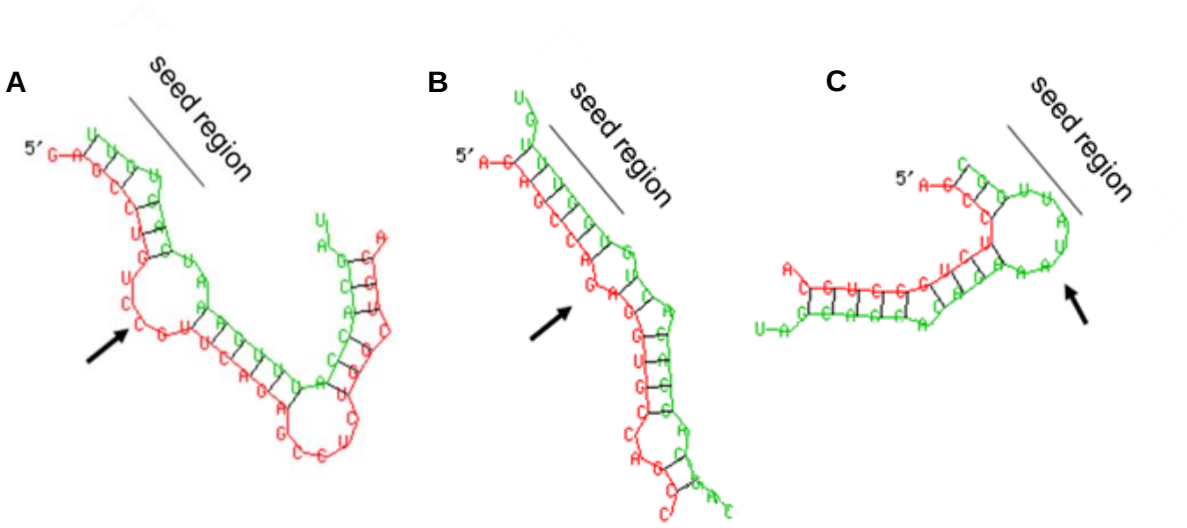

Abbildung 3. Strukturelle *in silico*-Analyse der miRNA/Ziel-mRNA-Interaktion.
Computergestützte Modelle der miRNA/mRNA-Interaktion zwischen (A) miRNA-29b, (B) miRNA-497 und (C) miRNA-195 mit der korrespondierenden Sequenz in der 3'-UTR der CPXM2-mRNA. MiRNAs sind grün und der entsprechende Abschnitt der CPXM2-mRNA rot dargestellt. Als *Seed Region* werden die Nukleotide 2-8 der miRNAs bezeichnet, diese sind entscheidend für die miRNA/mRNA-Bindung. Ebenfalls wichtig für die Interaktion ist die Ausbildung einer zentralen Blase (*central bulge*, markiert durch Pfeile). (Subrova J 2022, modifiziert)

3.3 Einfluss der getesteten miRNA-Kandidaten auf die CPXM2-Expression in H9C2-Zellen

48h nach der Transfektion der H9C2-Zellen mit miRNA-29b, miRNA-195 oder miRNA-497 beobachteten wir eine signifikant reduzierte CPXM2-Expression auf mRNA-Ebene verglichen mit Zellen, die mit einer Nonsense-miRNA-Kontrolle transfiziert wurden (Abbildung 4 A). Auch der CPXM2-Protein-Spiegel war nach der Transfektion der H9C2-Zellen mit den getesteten miRNAs signifikant vermindert (Abbildung 4 B).

3.4 MiRNA-29b und miRNA-497 binden an die *in silico* vorhergesagten Sequenzen der CPXM2-mRNA-3'-UTR

Um herauszufinden, ob die oben beschriebenen inhibitorischen Effekte der getesteten miRNAs auf die CPXM2-Expression durch ihre Bindung an die 3'-UTR der CPXM2-mRNA zustande kommen, führten wir einen *Dual Luciferase Reporter Assay* durch. Hierfür wurden die H9C2-Zellen mit einer der zu untersuchenden miRNAs sowie einem *Luciferase Reporter Vector*, der die 3'-UTR der CPXM2-mRNA beinhaltet, transfiziert. Für miRNA-29b und miRNA-497 konnten wir eine signifikante Reduktion der Luciferase-Aktivität nachweisen (Abbildung 5 A). MiRNA-195 zeigte keinen signifikanten Einfluss auf die Luciferase-Aktivität (Abbildung 5 A). Um zu bestätigen, dass die beobachtete Suppression der Luciferase-Aktivität durch direkte Bindung der miRNAs an die CPXM2-

mRNA-3'-UTR bedingt ist, mutierten wir die *in silico* identifizierten Bindesequenz und wiederholten den *Dual Luciferase Reporter Assay* mit den mutierten Vektoren. Unter diesen Bedingungen zeigten miRNA-29b und miRNA-497 keinen Einfluss auf die Luciferase-Aktivität (Abbildung 5 B).

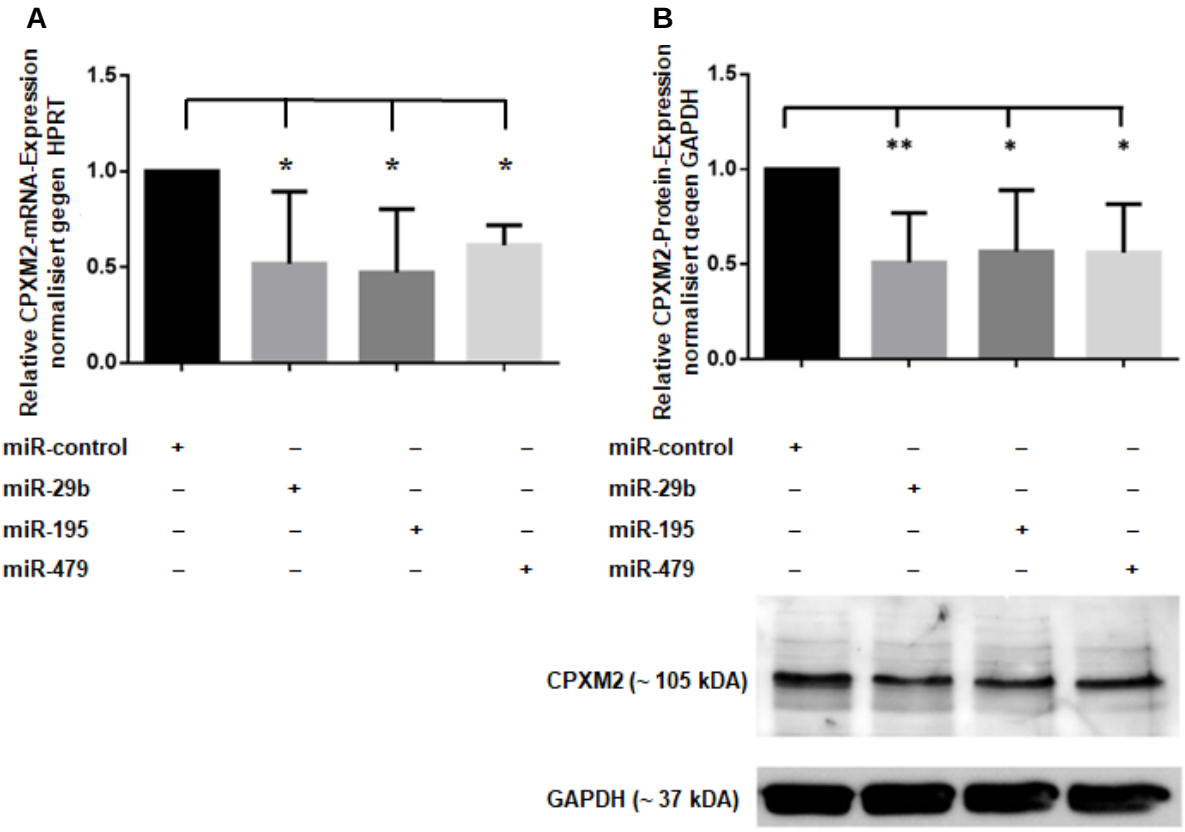

Abbildung 4. Einfluss von miRNA-29b, miRNA-195 und miRNA-497 auf die CPXM2-Expression in H9C2-Zellen.
Gezeigt wird die relative Reduktion der CPXM2-Expression auf (A) mRNA- und (B) Protein-Ebene 48h nach Transfektion der H9C2-Zellen mit miRNA-29b, miRNA-195, miRNA-497 oder einer Nonsense-miRNA-Kontrolle (miR-control). Die CPXM2-mRNA-Expression wurde gegen HPRT normalisiert. Die CPXM2-Protein-Expression wurde gegen GAPDH normalisiert. (*) $p < 0,05$; (**) $p < 0,01$; Anzahl der durchgeführten Experimente für einzelne miRNAs ≥ 3. (Subrova J 2022, modifiziert)

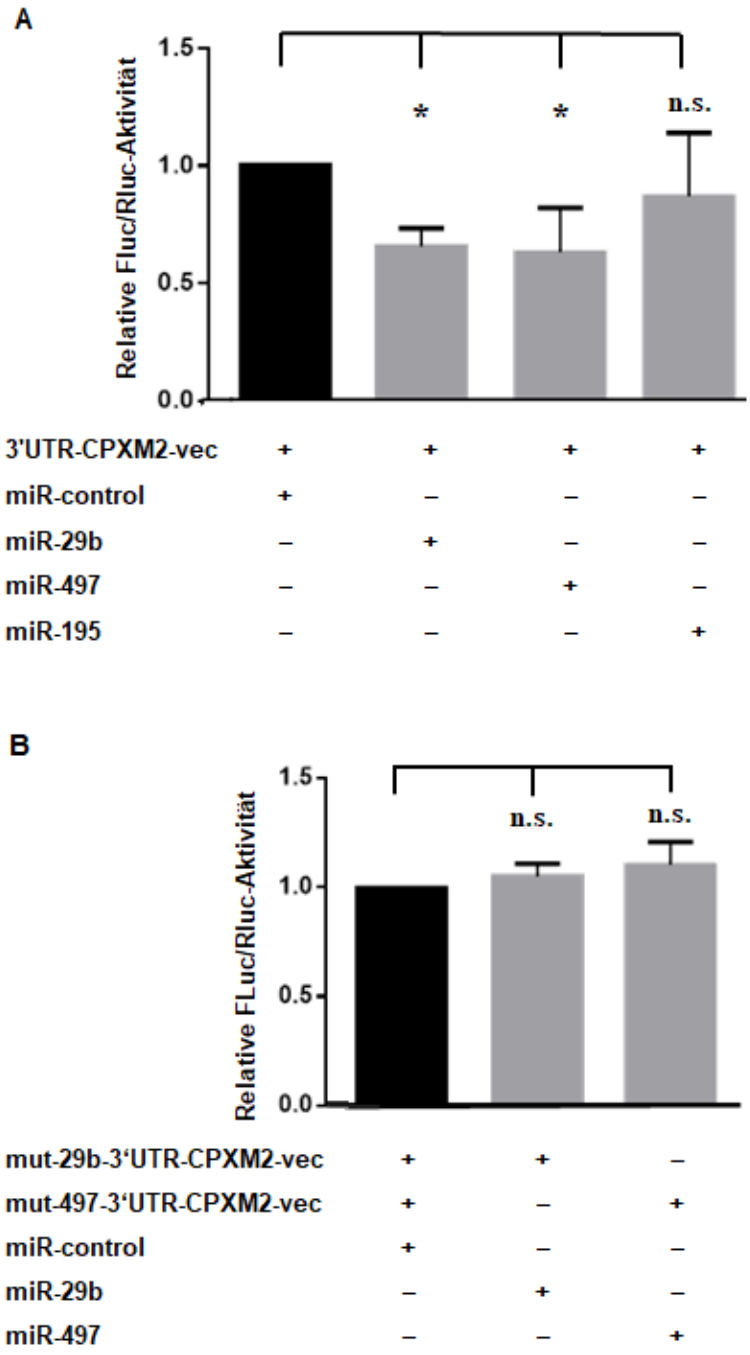

Abbildung 5. *Dual Luciferase Reporter Assay* in H9C2-Zellen zum Nachweis der Bindung der Kandidaten-miRNAs an die 3'-UTR der CPXM2-mRNA.
(A) Gezeigt wird der Einfluss von miRNA-29b, miRNA-497 und miRNA-195 auf die relative Luciferase-Aktivität des miRNA 3'-UTR *Target Clone* pEZX-MT06 mit der CPXM2-3'-UTR (3'UTR-CPXM2-vec) 48h nach der Transfektion. (B) Wird ein CPXM2-3'-UTR-Vektor mit mutierter Bindungsstelle für miRNA-29b (mut-29b-3'UTR-CPXM2-vec) oder miRNA-497 (mut-497-3'UTR-CPXM2-vec) verwendet, wird keine Reduktion der Luciferase-Aktivität durch die entsprechenden miRNAs 48h nach Transfektion beobachtet. (*) $p < 0,05$; (n.s.) kein signifikanter Unterschied; Anzahl der durchgeführten Experimente für einzelne miRNAs ≥ 3; FLuc, *Firefly*-Luciferase; RLuc, *Renilla*-Luciferase. (Subrova J 2022)

3.5 Der Einfluss von miRNA-30b und miRNA-564 auf die TMEM63C-Expression in HEK293-Zellen

Die durchgeführten *in silico*-Analysen zeigten, dass miRNA-30b und miRNA-564 mögliche Kandidaten für eine posttranskriptionelle Regulation der Expression von TMEM63C sind. *In vitro* konnten wir diesen Einfluss in HEK293-Zellen auf Protein-Ebene für beide miRNA-Kandidaten bestätigen (Abbildung 6). Im anschließenden *Dual Luciferase Reporter Assay* mit einem TMEM63C-3'-UTR-Vektor konnte nur für miRNA-564 eine signifikante Reduktion der Luciferase-Aktivität nachgewiesen werden (Orphal M 2020).

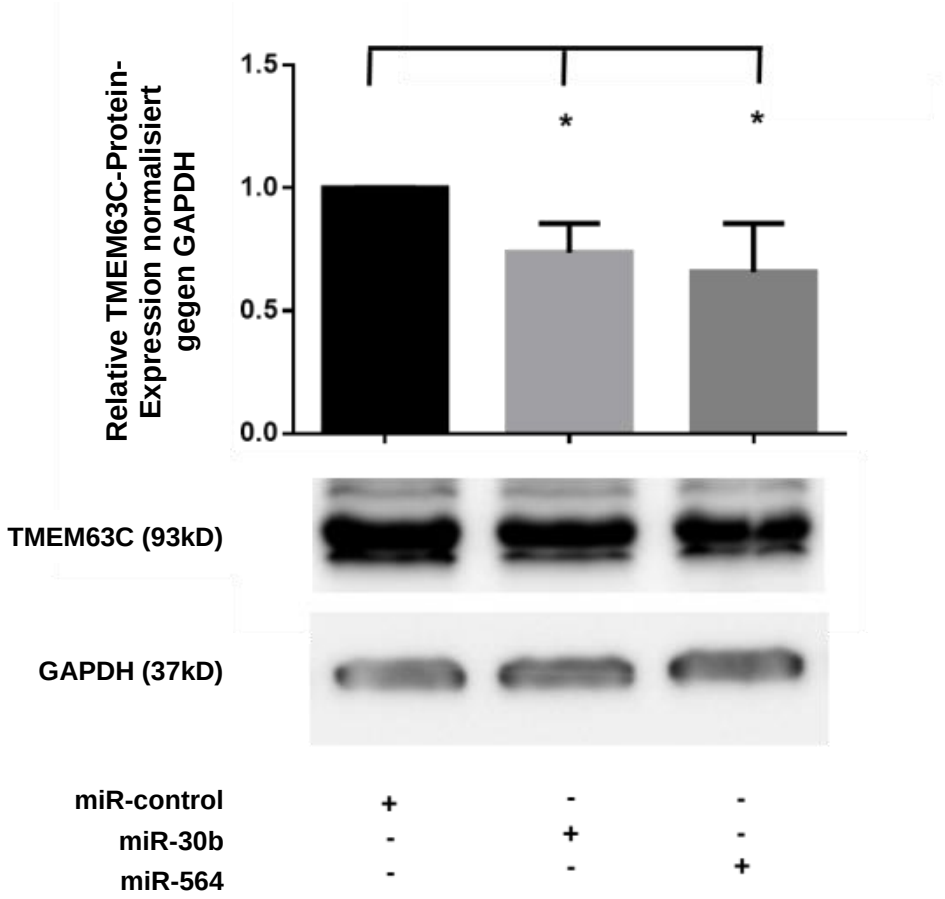

Abbildung 6. Einfluss der miRNA-30b und miRNA-564 auf die TMEM63C-Expression in HEK293-Zellen.
Gezeigt wird die relative Reduktion der TMEM63C-Expression auf Protein-Ebene 48h nach der Transfektion der HEK293-Zellen mit miRNA-30b, miRNA-564 beziehungsweise einer Nonsense-miRNA-Kontrolle (miR-control). Die TMEM63C-Proteinexpression wurde gegen GAPDH normalisiert. (*) $p < 0,05$; Anzahl der durchgeführten Experimente für einzelne miRNAs ≥ 3. (Orphal M 2020)

4 Diskussion

Im Rahmen der vorliegenden Arbeit wurden molekulare Mechanismen näher beleuchtet, die möglicherweise einen Einfluss auf die Pathophysiologie kardiorenaler Endorganschäden bei arterieller Hypertonie haben könnten.

Der Fokus der Experimente lag insbesondere auf der Charakterisierung der CPXM2-Expression in kardialen Zellen der Ratte, um die mögliche Rolle dieses Proteins bei der Entwicklung einer Hypertonie-bedingten linksventrikulären Hypertrophie zu untersuchen (Grabowski K 2022, Subrova J 2022). Obwohl CPXM2 bereits vor über 20 Jahren entdeckt wurde (Xin X 1998), sind die biologischen Funktionen dieses Proteins immer noch weitgehend unbekannt.

Wir konnten mittels Western Blot und Immunofluoreszenz nachweisen, dass CPXM2 in Rattenkardiomyozyten der Zelllinie H9C2 exprimiert wird (Abbildung 1). Es konnte ebenfalls gezeigt werden, dass CPXM2-mRNA im linksventrikulären Gewebe sowie in isolierten primären Rattenkardiomyozyten und -kardiofibroblasten vorhanden ist. Darüber hinaus ließen sich im kardialen Gewebe der SHRSP-Ratten - mit Prädisposition für arterielle Hypertonie - signifikant höhere CPXM2-Spiegel im Vergleich zu den F344-Kontrolltieren feststellen. Dies galt sowohl für das linksventrikuläre Gewebe als auch für Kardiomyozyten und Kardiofibroblasten (Abbildung 2). Überdies wiesen CPXM2-*Knock out*-Mäuse eine - im Vergleich zu *Wild type*-Tieren - signifikant geringere Neigung zur linksventrikulären Hypertrophie unter hypertensiven Bedingungen auf (Grabowski K 2022). Zusammengenommen deuten diese Ergebnisse darauf hin, dass CPXM2 eine wichtige Rolle beim kardialen *Remodelling* als Folgeerkrankung bei arterieller Hypertonie spielen könnte.

Weiterhin deuten die Ergebnisse der immunohistologischen Experimente darauf hin, dass CPXM2 mit Pdlim3 ko-lokalisiert sein könnte (Abbildung 1A-C). Bei arterieller Hypertonie sind Herzmuskelzellen einem erhöhten mechanischen Stress ausgesetzt und reagieren darauf durch Anpassungen auf Genexpressions-Ebene. Dieser Prozess wird als Mechanotransduktion bezeichnet (Knöll R 2003). Daran sind unter anderem verschiedene Z-Disk-assoziierte Proteine, wie zum Beispiel Pdlim3 beteiligt (Frank D 2011, Xue K 2014, Dixon DM 2015). Ein Zusammenhang zwischen Pdlim3 und vermehrter Kollagenablagerung im Herzen wurde betreits von Lodder *et al.* im Jahr 2014 beschrieben (Lodder EM 2014). Die Ko-Lokalisation könnte möglicherweise auf eine funktionelle Wechselwirkung von CPXM2 und Pdlim3 hindeuten, was in weiterführenden Studien untersucht werden könnte. Zusammen untermauern diese

Befunde die Vermutung, dass CPXM2 an der Entstehung kardialer Fibrose beteiligt sein könnte.

Um die Rolle von CPXM2 in kardialen Zellen besser zu verstehen, haben wir die posttranskriptionelle Regulation der CPXM2-Expression durch miRNAs untersucht. MiRNAs üben durch die spezifische Downregulation ihrer korrespondierenden mRNAs Einfluss auf zahlreiche zelluläre Prozesse aus (Eisenreich A 2013). Unter anderem tragen miRNAs zur Entstehung verschiedener kardiovaskulärer Erkrankungen bei (Huang Y 2017, Panizo S 2017). Von besonderer Relevanz für diese Arbeit ist der Zusammenhang zwischen miRNAs und kardialer Hypertrophie sowie Fibrose, der bereits in verschiedenen Studien beschrieben wurde (Xiao Y 2016, Chiang MH 2020).

Um miRNAs zu identifizieren, die potentiell die CPXM2-Expression beeinflussen können, führten wir eine *in silico* Analyse durch. Mit Hilfe mehrerer miRNA-Datenbanken wurden etwa 20 miRNAs mit einem potentiellen Einfluss auf die CPXM2-Expression identifiziert. Für drei dieser miRNA-Kandidaten (miRNA-29b, miRNA-195 und miRNA-497) ließ sich die Ausbildung stabilisierender Strukturen bei der miRNA-mRNA-Bindung *in silico* vorhersagen (Abbildung 3). Anschließend konnten wir *in vitro* bestätigen, dass diese drei miRNA-Kandidaten die Expression von CPXM2 auf mRNA- und Protein-Ebene vermindern (Abbildung 4). Weiterhin konnte im Rahmen dieser Arbeit gezeigt werden, dass miRNA-29b und miRNA-497 direkt mit der *in silico* vorhergesagten Bindesequenzen in der 3'-UTR der CPXM2-mRNA interagieren (Abbildung 5). Wohingegen der miRNA-195-assoziierte Einfluss auf die Expression von CPXM2 eher indirekt vermittelt wurde (Subrova J 2022).

Die hier gewonnen Erkenntnisse bieten neue Einblicke in die miRNA-vermittelte posttranskriptoionelle Regulation der Expression von CPXM2. Somit können sie zur weiteren Charakterisierung der möglichen (patho-)physiologisch-relevanten zellulären Funktionen dieses Proteins und seiner möglichen Rolle bei der Genese Hypertonie-bedingter Endorganschäden im kardialen Gewebe beitragen. Beispielsweise werden erhöhte Spiegel von miRNA-29b mit antifibrotischen Effekten im Herzen und anderen Geweben assoziiert (Qin W 2011, Zhang Y 2014, Yang F 2015, Yamada Y 2017, Monaghan MG 2018, Widlansky ME 2018). Monaghan *et al.* zeigten, dass die Applikation von miRNA-29b kurzfristig nach einem Myokardinfarkt das postischämische kardiale *Remodelling* in Mäusen positiv beeinflusste (Monaghan MG 2018). Dass miRNA-29b der fibrotischen Umwandlung vom Herzgewebe entgegenwirkt, könnte möglicherweise zum Teil durch ihren inhibitorischen Einfluss auf die Expression von

CPXM2 vermittelt werden, was allerdings zunächst in weiterführenden Studien näher beleuchtet werden sollte. Dies ist ein weiterer Hinweis dafür, dass CPXM2 eine Rolle bei der Entstehung einer kardialen Fibrose spielen könnte.

Von Xiao *et al.* wurde ein Zusammenhang zwischen miRNA-497 und der Herzhypertrophie beschrieben (Xiao Y 2016). In einem zellulären Modell für kardiale Hypertrophie (mit Angiotensin II behandelte Kardiomyozyten), wurden verminderte miRNA-497-Spiegel gemessen, wohingegen eine miRNA-497-Überexpression in Kardiomyozyten zum Rückgang bestimmter Hypertrophie-Marker (wie zum Beispiel der Zellgröße und des atrialen natriuretischen Peptids) führte (Xiao Y 2016). Dies unterstützt die Hypothese, dass CPXM2 im Prozess der kardialen Hypertrophie involviert sein könnte.

Neben kardialer Hypertrophie ist die chronische Niereninsuffizienz mit Albuminurie eine weit verbreitete Folgeerkrankung bei arterieller Hypertonie. Im Rahmen dieser Arbeit untersuchten wir auch Regulationsmechanismen, die bei den renalen Albuminverlusten involviert sein könnten. Wir charakterisierten die posttranskriptionelle Regulation der TMEM63c-Proteinexpression in Podozyten. TMEM63c ist nach Erkenntnissen von Schultz *et al.* an der renalen Filtrationsfunktion beteiligt (Schulz A 2019).

Wir konnten zeigen, dass miRNA-30b und miRNA-564 zu einer signifikanten Reduktion der TMEM63c-Expression in renalen HEK293-Zellen auf mRNA- und Proteinebene führen (Abbildung 6). Allerdings konnten wir nur für miRNA-564 zeigen, dass dieser Effekt durch ihre direkte Interaktion mit der *in silico* vorhergesagten Bindungsstelle in der 3'-UTR der TMEM63c-mRNA erfolgt (Orphal M 2020). Interessanterweise haben mehrere Forschungsgruppen beobachtet, dass miRNA-564 Apoptose in verschiedenen Krebsarten induziert sowie die epithelial-mesenchymale Transition und somit das Entartungspotential vermindern kann (Ru N 2018, Mutlu M 2016). Außerdem scheint miRNA-564 einen Einfluss auf die *Transforming growth factor-β* (TGF-β)-Signaltransduktion auszuüben (Jiang C 2016, Xiao L 2019). Erste *in vitro*-Befunde deuten darauf hin, dass eine TGF-β-induzierte Überexpression von TMEM63c potentiell zur Verbesserung renaler Fibrose beitragen könnte (Orphal M 2020).

Zusammengefasst zeigten wir, dass verschiedene miRNAs Einfluss auf pathophysiologische Prozesse in Herz und Nieren haben könnten. Beispielsweise sind miRNA-29b und miRNA-497 in der Lage, die CPXM2-Expression in Rattenkardiomyozyten auf posttranskriptioneller Ebene über eine direkte Interaktion mit der 3'-UTR der CPXM2-mRNA zu regulieren (Subrova J 2022). Diese Erkenntnisse

könnten möglicherweise bei weiterführenden Untersuchungen zu den biologischen Funktionen von CPMX2 eingesetzt werden. Vom besonderen Interesse ist dabei die Beteiligung von CPXM2 an pathophysiologisch-relevanten Prozessen, wie der Hypertonie-induzierten linksventrikulären Hypertrophie und der kardialen Fibrose. Auch im renalen Gewebe spielen miRNAs eine wichtige Rolle, was wir am Beispiel der posttranskriptionellen Regulation vom TMEM63c demonstieren konnten.

Weiterführende Untersuchungen sollten sich mit der CPXM2-Überexpression in kardialen Zellen und den damit verbundenen Veränderungen des zellulären Stoffwechsels sowie des Zellüberlebens befassen. Außerdem könnte der Einfluss der miRNA-vermittelten CPXM2-Downregulation auf die Entwicklung Hypertonie-induzierter kardiovaskulärer Erkrankungen im Tiermodell untersucht werden.

Literaturverzeichnis

Abonnenc M, Nabeebaccus AA, Mayr U, Barallobre-Barreiro J, Dong X, Cuello F, Sur S, Drozdov I, Langley SR, Lu R, Stathopoulou K, Didangelos A, Yin X, Zimmermann WH, Shah AM, Zampetaki A, Mayr M. (2013). "Extracellular matrix secretion by cardiac fibroblasts: role of microRNA-29b and microRNA-30c." Circulation Research 113(10): 1138-1147.

Chiang MH, Liang CJ, Lin LC, Yang YF, Huang CC, Chen YH, Kao HL, Chen YC, Ke SR, Lee CW, Lin MS, Chen YL. (2020). "miR-26a attenuates cardiac apoptosis and fibrosis by targeting ataxia-telangiectasia mutated in myocardial infarction." J Cell Physiol.

Chung AC, Lan HY. (2015). "MicroRNAs in renal fibrosis." Front Physiol. 6: 50.

Dixon DM, Choi J, El-Ghazali A, Park SY, Roos KP, Jordan MC, Fishbein MC, Comai L, Reddy S. (2015). "Loss of muscleblind-like 1 results in cardiac pathology and persistence of embryonic splice isoforms." Sci Rep. 5:9042.

Eisenreich A. (2013). "Regulation of Vascular Function on Posttranscriptional Level." Thrombosis

Eisenreich A, Leppert U. (2014). "The impact of microRNAs on the regulation of tissue factor biology." Trends Cardiovasc Med. 24(3): 128-132.

Eisenreich A, Rauch U. (2013). "Regulation of the Tissue Factor Isoform Expression and Thrombogenicity of HMEC-1 by miR-126 and miR-19a." Cell Biol: Res Ther. 2(1).

Fan B, Jin Y, Zhang H, Zhao R, Sun M, Sun M, Yuan X, Wang W, Wang X, Chen Z, Liu W, Yu N, Wang Q, Liu T, Li X. (2020). "MicroRNA-21 contributes to renal cell carcinoma cell invasiveness and angiogenesis via the PDCD4/c-Jun (AP-1) signalling pathway." Int J Oncol. 56(1):178-192.

Frank D, Frey N. (2011). "Cardiac Z-disc Signaling Network." J Biol Chem. 286(12): 9897-9904.

GBD 2013 Mortality and Causes of Death Collaborators. (2015). "Global, regional, and national age-sex specific all-cause and cause-specific mortality for 240 causes of death, 1990-2013: a systematic analysis for the Global Burden of Disease Study 2013." Lancet 385 (9963): 117-171.

Grabowski K, Koplin G, Aliu B, Schulte L, Schulz A, Kreutz R. (2013). "Mapping and Confirmation of a Major Left Ventricular Mass QTL on Rat Chromosome 1 by Contrasting SHRSP and F344 Rats." Physiol Genomics 45(18): 827-833.

Grabowski K, Herlan L, Eisenreich A, Schulz A, Müller DN, Plehm R, Bader M, Kreutz R. (2016). [OP.8C.01] "A novel candidate gene identified in stroke-prone spontaneously hypertensive rats has a major impact on adverse left ventricular remodeling in salt-induced hypertension." Journal of Hypertension 34: e102.

Grabowski K, Herlan L, Witten A, Qadri F, Eisenreich A, Lindner D, Schädlich M, Schulz A, Subrova J, Mhatre KN, Primessnig U, Plehm R, van Linthout S, Escher F, Bader M, Stoll M, Westermann D, Heinzel FR, Kreutz R. (2022). "Cpxm2 as a novel candidate for cardiac hypertrophy and failure in hypertension." Hypertens Res. 45(2): 292-307.

Huang Y, Tang S, Huang C, Chen J, Li J, Cai A, Feng Y. (2017). "Circulating miRNA29 family expression levels in patients with essential hypertension as potential markers for left ventricular hypertrophy." Clin Exp Hypertens. 39(2): 119-125.

Jiang C, Shen F, Du J, Hu Z, Li X, Su J, Wang X, Huang X. (2016). ”MicroRNA-564 is downregulated in glioblastoma and inhibited proliferation and invasion of glioblastoma cells by targeting TGF-β1.” Oncotarget. 7(35): 56200–56208.

Knöll R, Hoshijima M, Chien K. (2003). "Cardiac mechanotransduction and implications for heart disease." J Mol Med (Berl) 81(12): 750-756.

Lambers Heerspink HJ, Gansevoort RT. (2015). "Albuminuria Is an Appropriate Therapeutic Target in Patients with CKD: The Pro View." Clin J Am Soc Nephrol. 10(6):1079-88.

Leoncini G, Viazzi F, Pontremoli R. (2010). "Chronic kidney disease and albuminuria in arterial hypertension." Curr Hypertens Rep. 12(5): 335-41.

Li X, Zeng Z, Li Q, Xu Q, Xie J, Hao H, Luo G, Liao W, Bin J, Huang X, Liao Y. (2015). "Inhibition of microRNA-497 ameliorates anoxia/reoxygenation injury in cardiomyocytes by suppressing cell apoptosis and enhancing autophagy." Oncotarget 6(22): 18829-18844.

Lodder EM, Scicluna BP, Beekman L, Arends D, Moerland PD, Tanck MW, Adriaens ME, Bezzina CR. (2014). "Integrative genomic approach identifies multiple genes involved in cardiac collagen deposition." Circ Cardiovasc Genet. 7(6): 790-798.

Lovic D, Narayan P, Pittaras A, Faselis C, Doumas M, Kokkinos P. (2017). "Left ventricular hypertrophy in athletes and hypertensive patients." J Clin Hypertens (Greenwich) 19(4): 413-417.

Lüllmann-Rauch R. (2009). "Taschenlehrbuch Histologie." (3. Auflage). Thieme.

Monaghan MG, Holeiter M, Brauchle E, Layland SL, Lu Y, Deb A, Pandit A, Nsair A, Schenke-Layland K. (2018). "Exogenous miR-29B Delivery Through a Hyaluronan-Based Injectable System Yields Functional Maintenance of the Infarcted Myocardium." Tissue Eng Part A. 24(1-2): 57-67.

Mutlu M, Saatci Ö, Ansari SA, Yurdusev E, Shehwana H, Konu Ö, Raza U, Şahin Ö. (2016). “miR-564 acts as a dual inhibitor of PI3K and MAPK signaling networks and inhibits proliferation and invasion in breast cancer.” Sci Rep. 6(1): 32541.

Nabika T, Ohara H, Kato N, Isomura M. (2012). "The stroke-prone spontaneously hypertensive rat: still a useful model for post-GWAS genetic studies?" Hypertens Res. 35(5): 477-484.

Nwabuo CC, Vasan RS. (2020). "Pathophysiology of Hypertensive Heart Disease: Beyond Left Ventricular Hypertrophy." Curr Hypertens Rep. 22(2).

Olson EN. (2014). "MicroRNAs as therapeutic targets and biomarkers of cardiovascular disease." Sci Transl Med. 6(239): 239ps233.

Orphal M, Gillespie A, Böhme K, Subrova J, Eisenreich A, Kreutz R. (2020). "TMEM63C, a Potential Novel Target for Albuminuria Development, Is Regulated by MicroRNA-564 and Transforming Growth Factor beta in Human Renal Cells." Kidney Blood Press Res. 45(6): 850-862.

Panizo S, Carrillo-López N, Naves-Díaz M, Solache-Berrocal G, Martínez-Arias L, Rodrigues-Díez RR, Fernández-Vázquez A, Martínez-Salgado C, Ruiz-Ortega M, Dusso A, Cannata-Andía JB, Rodríguez I. (2017). "Regulation of miR-29b and miR-30c by vitamin D receptor activators contributes to attenuate uraemia-induced cardiac fibrosis." Nephrol Dial Transplant. 32(11): 1831-1840.

Patel SK, Ramchand J, Crocitti V, Burrell LM. (2018). "Kruppel-Like Factor 15 Is Critical for the Development of Left Ventricular Hypertrophy." Int J Mol Sci. 19(5): pii: E1303.

Porrello ER, Mahmoud AI, Simpson E, Johnson BA, Grinsfelder D, Canseco D, Mammen PP, Rothermel BA, Olson EN, Sadek HA. (2013). "Regulation of neonatal and adult mammalian heart regeneration by the miR-15 family." Proc Natl Acad Sci U S A 110(1): 187-192.

Qin W, Chung ACK, Huang XR, Meng XM, Hui DSC, Yu CM, Sung JJY, Lan HY. (2011). "TGF-β/Smad3 signaling promotes renal fibrosis by inhibiting miR-29." J Am Soc Nephrol 22(8): 1462-1474.

Ru N, Zhang F, Liang J, Du Y, Wu W, Wang F, Liu X. (2018). “MiR-564 is down-regulated in osteosarcoma and inhibits the proliferation of osteosarcoma cells via targeting Akt.” Gene. 645:163–9.

Schulz A, Müller NV, van de Lest NA, Eisenreich A, Schmidbauer M, Barysenka A, Purfürst B, Sporbert A, Lorenzen T, Meyer AM, Herlan L, Witten A, Rühle F, Zhou W, de Heer E, Scharpfenecker M,

Panáková D, Stoll M, Kreutz R. (2019). "Analysis of the genomic architecture of a complex trait locus in hypertensive rat models links Tmem63c to kidney damage." Elife. 22;8: e42068.

Subrova J, Böhme K, Gillespie A, Orphal M, Plum C, Kreutz R, Eisenreich A. (2022). “MiRNA-29b and miRNA-497 Modulate the Expression of Carboxypeptidase X Member 2, a Candidate Gene Associated with Left Ventricular Hypertrophy.” Int J Mol Sci. 23(4): 2263-2276.

Tijsen AJ, van der Made I, van den Hoogenhof MM, Wijnen WJ, van Deel ED, de Groot NE, Alekseev S, Fluiter K, Schroen B, Goumans MJ, van der Velden J, Duncker DJ, Pinto YM, Creemers EE. (2014). "The microRNA-15 family inhibits the TGFβ-pathway in the heart." Cardiovasc Res. 104(1): 61-71.

Trionfini P, Benigni A. (2017). "MicroRNAs as Master Regulators of Glomerular Function in Health and Disease." J Am Soc Nephrol. 28(6):1686-1696.

Webster AC, Nagler EV, Morton RL, Masson P. (2017). "Chronic Kidney Disease." Lancet. 389(10075):1238-1252.

Widlansky ME, Jensen DM, Wang J, Liu Y, Geurts AM, Kriegel AJ, Liu P, Ying R, Zhang G, Casati M, Chu C, Malik M, Branum A, Tanner MJ, Tyagi S, Usa K, Liang M. (2018). "miR-29 contributes to normal endothelial function and can restore it in cardiometabolic disorders." EMBO Mol Med. 10(3).

Williams B, Mancia G, Spiering W, Agabiti Rosei E, Azizi M, Burnier M, Clement DL, Coca A, de Simone G, Dominiczak A, Kahan T, Mahfoud F, Redon J, Ruilope L, Zanchetti A, Kerins M, Kjeldsen SE, Kreutz R, Laurent S, Lip GYH, McManus R, Narkiewicz K, Ruschitzka F, Schmieder RE, Shlyakhto E, Tsioufis C, Aboyans V, Desormais I. (2018). "2018 ESC/ESH Guidelines for the management of arterial hypertension." European Heart Journal. 39: 3021-3104.

Xiao J, Meng XM, Huang XR, Chung AC, Feng YL, Hui DS, Yu CM, Sung JJ, Lan HY. (2012). "miR-29 inhibits bleomycin-induced pulmonary fibrosis in mice." Mol Ther. 20(6): 1251-1260.

Xiao L, Tang T, Huang Y, Guo J. (2019). “MiR-564 promotes hypertrophic scar formation through TGF-β1 upregulation.” G Ital Dermatol Venereol. 154(2):186–191.

Xiao Y, Zhang X, Fan S, Cui G, Shen Z. (2016). "MicroRNA-497 Inhibits Cardiac Hypertrophy by Targeting Sirt4." PLoS One 11(12).

Xin X, Day R, Dong W, Lei Y, Fricker LD. (1998). "Identification of Mouse CPX-2, a Novel Member of the Metallocarboxypeptidase Gene Family: cDNA Cloning, mRNA Distribution, and Protein Expression and Characterization. ." DNA Cell Biol. 17(10): 897-909.

Xue K, Wang Y, Hou Y, Wang Y, Zhong T, Li L, Zhang H, Wang L. (2014). "Molecular characterization and expression patterns of the actinin-associated LIM protein (ALP) subfamily genes in porcine skeletal muscle." Gene 539(1): 111-116.

Yamada Y, Takanashi M, Sudo K, Ueda S, Ohno SI, Kuroda M. (2017). "Novel form of miR-29b suppresses bleomycin-induced pulmonary fibrosis." PLoS One. 12(2).

Yang F, Li P, Li H, Shi Q, Li S, Zhao L. (2015). "microRNA-29b Mediates the Antifibrotic Effect of Tanshinone IIA in Postinfarct Cardiac Remodeling." J Cardiovasc Pharmacol. 65(5): 456-464.

Yildiz M, Oktay AA, Stewart MH, Milani RV, Ventura HO, Lavie CJ. (2020). “Left ventricular hypertrophy and hypertension.” Prog Cardiovasc Dis. 63: 10-21.

Zhang X, Ji R, Liao X, Castillero E, Kennel PJ, Brunjes DL, Franz M, Möbius-Winkler S, Drosatos K, George I, Chen EI, Colombo PC, Schulze PC. (2018). "MicroRNA-195 Regulates Metabolism in Failing Myocardium Via Alterations in Sirtuin 3 Expression and Mitochondrial Protein Acetylation. ." Circulation. 137(19): 2052-2067.

Zhang Y, Huang XR, Wei LH, Chung AC, Yu CM, Lan HY. (2014). "miR-29b as a therapeutic agent for angiotensin II-induced cardiac fibrosis by targeting TGF-β/Smad3 signaling." Mol Ther. 22(5): 974-985.

Eidesstattliche Versicherung

„Ich, Jana Šubrová, versichere an Eides statt durch meine eigenhändige Unterschrift, dass ich die vorgelegte Dissertation mit dem Thema: „Molekulare Mechanismen mit Einfluss auf kardiorenale Endorganschäden bei arterieller Hypertonie“ (englisch: „Molecular mechanisms involved in the development of hypertension mediated cardiorenal organ damage“) selbstständig und ohne nicht offengelegte Hilfe Dritter verfasst und keine anderen als die angegebenen Quellen und Hilfsmittel genutzt habe.
Alle Stellen, die wörtlich oder dem Sinne nach auf Publikationen oder Vorträgen anderer Autoren/innen beruhen, sind als solche in korrekter Zitierung kenntlich gemacht. Die Abschnitte zu Methodik (insbesondere praktische Arbeiten, Laborbestimmungen, statistische Aufarbeitung) und Resultaten (insbesondere Abbildungen, Graphiken und Tabellen) werden von mir verantwortet.
Ich versichere ferner, dass ich die in Zusammenarbeit mit anderen Personen generierten Daten, Datenauswertungen und Schlussfolgerungen korrekt gekennzeichnet und meinen eigenen Beitrag sowie die Beiträge anderer Personen korrekt kenntlich gemacht habe (siehe Anteilserklärung). Texte oder Textteile, die gemeinsam mit anderen erstellt oder verwendet wurden, habe ich korrekt kenntlich gemacht.

Meine Anteile an etwaigen Publikationen zu dieser Dissertation entsprechen denen, die in der untenstehenden gemeinsamen Erklärung mit dem/der Erstbetreuer/in, angegeben sind. Für sämtliche im Rahmen der Dissertation entstandenen Publikationen wurden die Richtlinien des ICMJE (International Committee of Medical Journal Editors; www.icmje.og) zur Autorenschaft eingehalten. Ich erkläre ferner, dass ich mich zur Einhaltung der Satzung der Charité – Universitätsmedizin Berlin zur Sicherung Guter Wissenschaftlicher Praxis verpflichte.

Weiterhin versichere ich, dass ich diese Dissertation weder in gleicher noch in ähnlicher Form bereits an einer anderen Fakultät eingereicht habe.

Die Bedeutung dieser eidesstattlichen Versicherung und die strafrechtlichen Folgen einer unwahren eidesstattlichen Versicherung (§§156, 161 des Strafgesetzbuches) sind mir bekannt und bewusst.“

Datum	Unterschrift

Anteilserklärung an den erfolgten Publikationen

Jana Šubrová hatte folgenden Anteil an den folgenden Publikationen:

Publikation 1:
Subrova J, Böhme K, Gillespie A, Orphal M, Plum C, Kreutz R, Eisenreich A.
MiRNA-29b and miRNA-497 Modulate the Expression of Carboxypeptidase X Member 2, a Candidate Gene Associated with Left Ventricular Hypertrophy. Int J Mol Sci. 2022.

Insgesamte Beteiligung: 85%
Beitrag im Einzelnen: Durchführung der Real-time PCR- und Western Blot-Analysen sowie der Immunofluoreszenzfärbung und des Dual luciferase reporter Assay. Zusätzlich Beteiligung an der statistischen Auswertung und Interpretation der gewonnenen Daten. Verfassung des Papers und Erstellung von allen darin enthaltenen Abbildungen (Bildmaterial für Abbildung 3 wurde durch Andreas Eisenreich erstellt und durch Jana Šubrová zu der finalen Version bearbeitet).

Publikation 2:
Grabowski K, Herlan L, Witten A, Qadri F, Eisenreich A, Lindner D, Schädlich M, Schulz A, **Subrova J**, Mhatre KN, Primessnig U, Plehm R, van Linthout S, Escher F, Bader M, Stoll M, Westermann D, Heinzel FR, Kreutz R.
Cpxm2 as a novel candidate for cardiac hypertrophy and failure in hypertension. Hypertens Res. 2022.

Insgesamte Beteiligung: 15%
Beitrag im Einzelnen: Durchführung der Real-time PCR- und Western Blot-Analysen zur Bestimmung der CPXM2-mRNA- und -Protein-Spiegel in primären Kardiomyozyten und Kardiofibroblasten der SHRSP- und F344-Ratten. Unterstützung bei der Erstellung des graphischen Abstracts, Bereitstellung der Daten für Abbildung 1c. Kritisches Korrekturlesen vor Veröffentlichung des Manuskripts.

Publikation 3:
Orphal M, Gillespie A, Böhme K, **Subrova J**, Eisenreich A, Kreutz R.
TMEM63C, a Potential Novel Target for Albuminuria Development, Is Regulated by MicroRNA-564 and Transforming Growth Factor beta in Human Renal Cells. Kidney Blood Press Res. 2020.

Insgesamte Beteiligung: 10%
Beitrag im Einzelnen: Durchführung der Western Blot-Analysen zur Bestimmung der Podoplanin-Spiegel in renalen HEK293-Zellen nach Transfektion mit ausgewählten miRNAs. Mitwirkung an der Datengewinnung für die Abbildungen 1 und 3. Kritisches Korrekturlesen vor Veröffentlichung des Manuskripts.

_____
Unterschrift, Datum und Stempel des erstbetreuenden Hochschullehrers

_____
Unterschrift der Doktorandin

Ausgewählte Publikationen

Die finalen, publizierten Versionen der nachfolgenden Open-Access-Artikel sind unter diesen Links zu finden:

„Cpxm2 as a novel candidate for cardiac hypertrophy and failure in hypertension”

https://doi.org/10.1038/s41440-021-00826-8

„MiRNA-29b and miRNA-497 Modulate the Expression of Carboxypeptidase X Member 2, a Candidate Gene Associated with Left Ventricular Hypertrophy”

https://doi.org/10.3390/ijms23042263

„ TMEM63C, a Potential Novel Target for Albuminuria Development, Is Regulated by MicroRNA-564 and Transforming Growth Factor beta in Human Renal Cells”

https://karger.com/?doi=10.1159/000508477

Hypertension Research (2022) 45:292–307
https://doi.org/10.1038/s41440-021-00826-8

ARTICLE

Cpxm2 as a novel candidate for cardiac hypertrophy and failure in hypertension

Katja Grabowski[1] · Laura Herlan[1] · Anika Witten[2] · Fatimunnisa Qadri[3] · Andreas Eisenreich[1] · Diana Lindner[4,5] · Martin Schädlich[2] · Angela Schulz[1] · Jana Subrova[1] · Ketaki Nitin Mhatre[6] · Uwe Primessnig[6,7] · Ralph Plehm[3] · Sophie van Linthout[7,8] · Felicitas Escher[6,7,9] · Michael Bader[3,7,10,11] · Monika Stoll[2,12] · Dirk Westermann[4,5] · Frank R. Heinzel[6,7] · Reinhold Kreutz[1]

Received: 21 June 2021 / Revised: 8 October 2021 / Accepted: 29 October 2021 / Published online: 16 December 2021

Abstract

Treatment of hypertension-mediated cardiac damage with left ventricular (LV) hypertrophy (LVH) and heart failure remains challenging. To identify novel targets, we performed comparative transcriptome analysis between genetic models derived from stroke-prone spontaneously hypertensive rats (SHRSP). Here, we identified carboxypeptidase X 2 (Cpxm2) as a genetic locus affecting LV mass. Analysis of isolated rat cardiomyocytes and cardiofibroblasts indicated Cpxm2 expression and intrinsic upregulation in genetic hypertension. Immunostaining indicated that CPXM2 associates with the t-tubule network of cardiomyocytes. The functional role of Cpxm2 was further investigated in Cpxm2-deficient (KO) and wild-type (WT) mice exposed to deoxycorticosterone acetate (DOCA). WT and KO animals developed severe and similar systolic hypertension in response to DOCA. WT mice developed severe LV damage, including increases in LV masses and diameters, impairment of LV systolic and diastolic function and reduced ejection fraction. These changes were significantly ameliorated or even normalized (i.e., ejection fraction) in KO-DOCA animals. LV transcriptome analysis showed a molecular cardiac hypertrophy/remodeling signature in WT but not KO mice with significant upregulation of 1234 transcripts, including Cpxm2, in response to DOCA. Analysis of endomyocardial biopsies from patients with cardiac hypertrophy indicated significant upregulation of CPXM2 expression. These data support further translational investigation of CPXM2.

Keywords Cardiac hypertrophy · Cpxm2 · DOCA-salt hypertension · Genetics · Knock-out mice

Supplementary information The online version contains supplementary material available at https://doi.org/10.1038/s41440-021-00826-8.

✉ Reinhold Kreutz
Reinhold.kreutz@charite.de

[1] Charité—Universitätsmedizin Berlin, corporate member of Freie Universität Berlin, Humboldt-Universität zu Berlin, and Berlin Institute of Health (BIH), Institut für Klinische Pharmakologie und Toxikologie, 10178 Berlin, Germany

[2] Department of Genetic Epidemiology, Institute of Human Genetics, University Hospital Münster, Münster, Germany

[3] Max-Delbrück Center for Molecular Medicine (MDC), Berlin-Buch, Berlin, Germany

[4] German Center for Cardiovascular Research (DZHK), Partner site Hamburg/Kiel/Lübeck, Hamburg, Germany

[5] Clinic for Cardiology, University Heart and Vascular Center Hamburg, University Hospital Hamburg-Eppendorf, Hamburg, Germany

[6] Charité—Universitätsmedizin Berlin, corporate member of Freie Universität Berlin, Humboldt-Universität zu Berlin, and Berlin Institute of Health (BIH), Department of Cardiology, Campus Virchow Klinikum, 10178 Berlin, Germany

[7] German Center for Cardiovascular Research (DZHK), Partner Site Berlin, Berlin, Germany

[8] Charité—Universitätsmedizin Berlin, BCRT—Berlin Institute of Health Center for Regenerative Therapies, Berlin, Germany

[9] Institute of Cardiac Diagnostics and Therapy, IKDT GmbH, Berlin, Germany

[10] Charité—Universitätsmedizin Berlin, corporate member of Freie Universität Berlin, Humboldt-Universität zu Berlin, and Berlin Institute of Health (BIH), 10178 Berlin, Germany

[11] University of Lübeck, Institute for Biology, Ratzeburger Allee 160, 23562 Lübeck, Germany

[12] Department of Biochemistry, Cardiovascular Research Institute Maastricht, Maastricht University, Maastricht, The Netherlands

Graphical Abstract

Differential increased cardiac expression of *Cpxm2* was assigned to cardiac hypertrophy in SHRSP rats. *Cpxm2* knock-out (KO) in mice reduced cardiac hypertrophy and remodeling in DOCA salt hypertension

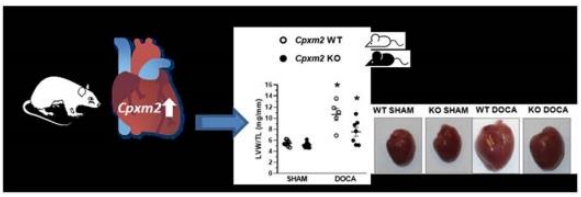

Introduction

Hypertension-mediated organ damage (HMOD), including cardiac hypertrophy, has a major impact on the morbidity and mortality of hypertensive patients [1, 2]. Thus, sustained hypertension can result in maladaptive cardiac changes, including left ventricular (LV) structural remodeling with LV hypertrophy (LVH) and fibrosis, impaired (diastolic and systolic) LV function, left atrial enlargement and atrial fibrillation and, importantly, the development of heart failure with preserved ejection fraction (HFpEF) or reduced ejection fraction [2–4]. Approximately half of all patients presenting with HF have HFpEF [3], and hypertension is particularly prevalent in this condition [5], for which no established pharmacological therapies exist beyond blood pressure control [1, 2].

The development of LVH represents a pivotal early step in the pathophysiology of progression toward HF [3, 4], which is modulated by multiple individual and environmental factors, including genetic susceptibility variants that influence LV mass [6–8]. Animal models, including inbred hypertensive rat models [9], have proven to be an effective complementary tool for analyzing cardiovascular disease mechanisms, including the role of genetic factors in LV remodeling [10–14]. The stroke-prone spontaneously hypertensive rat (SHRSP) strain represents such a well-established inbred hypertension model with an inherited predisposition to developing HMOD [15, 16]. Regarding LV remodeling, Fischer (F344) rats are a suitable reference strain for the analysis of LVH because this strain features a contrasting phenotype with low LV mass and normal blood pressure levels [17]. Previous genetic studies in the SHRSP/F344 model confirmed the presence of a major quantitative trait locus (QTL) for LV mass on rat chromosome (RNO) 1 (Supplementary Fig. 1) [17]. Building on these previous findings, we set out to identify potential novel targets for LVH and LV remodeling in the SHRSP/F344 rat model. Our data support a functional role of CPXM2 as a novel candidate for LVH and adverse cardiac remodeling in hypertension.

Methods

The authors declare that all supporting data are available within the article and in the Supplementary Material with an expanded Material and Methods section.

Animal models

All animals were maintained under standard conditions of regular 12 h diurnal cycles using an automated light switching device and climate-controlled conditions at a constant room temperature of 22 °C. Animals had access to food and water ad libitum. All animal experiments were approved by the responsible local government committee and performed in accordance with the guidelines of the Charité-Universitätsmedizin Berlin and the local authority for animal protection (Landesamt für Gesundheit und Soziales, LaGeSo, Berlin, Germany). The registration numbers are G0354-13, T 0189-02, and O0052/03.

Rats

Male SHRSP and F344 rats were obtained from our colonies at the Forschungseinrichtung für Experimentelle Medizin (FEM), Charité—Universitätsmedizin, Berlin [17]. To develop the consomic strain SHRSP-1^{F344} (Rat Genome Database (RGD)-ID: SHRSP-Chr 1^{F344}/Rkb), we crossed the SHRSP strain with the F344 strain in accordance with our linkage results and introgressed the whole rat chromosome (RNO)1 from F344 into the SHRSP background as previously described [17].

Mice

Cpxm2 knock-out (KO) mice were obtained as heterozygous B6;129S5-*Cpxm2*^{tm1Lex}/Mmucd/rk mice from the Mutant Mouse Regional Resource Center, University of California, Davis, USA, and were inbred to produce homozygous KO (*Cpxm2*$^{-/-}$) and wild-type (WT) mice (*Cpxm2*$^{+/+}$). Genotyping of the KO and WT alleles was

performed by PCR (Supplementary Table 1). Only homozygous KO mice and corresponding WT mice were used in this study.

DOCA-salt hypertension in Cpxm2 KO and WT mice - in vivo study

Baseline phenotypic characterization of all mice under control conditions was performed at ~12 weeks of age. Animals were subsequently followed for 8 weeks under either deoxycorticosterone acetate (DOCA) DOCA-salt or SHAM conditions.

DOCA and SHAM experimental groups

At 12 weeks of age, unilateral nephrectomy was performed under anesthesia (isoflurane 3.5% induction followed by 1.5% maintenance dose) in WT and KO mice ($n = 8$/group), and a pellet containing DOCA was implanted in each mouse subcutaneously (DOCA pellet, 75 mg, 60-day release, Innovative Research of America, Sarasota, Florida, USA). Subsequently, these mice were exposed to salt by adding 1% NaCl to drinking water (DOCA groups). Unilateral nephrectomy was also performed in an additional group of WT and KO mice ($n = 10$/group), but these animals received no DOCA pellet and were given normal drinking water (SHAM groups). Animals were treated for 8 weeks overall.

Radiotelemetry

Telemetry devices for continuous blood pressure and heart rate monitoring (TA11PA-C10, Data Sciences International, St. Paul, Minnesota, USA) were implanted in the DOCA mouse groups (WT DOCA $n = 8$, KO DOCA $n = 8$) under isoflurane (isoflurane 3.5% initially followed by 1.5%) anesthesia when the mice were 10 weeks of age [18]. The catheter was inserted into the right carotid artery, tunneled subcutaneously and placed in a subcutaneous pocket along the right flank. After a recovery period of 10 days, baseline recordings for blood pressure and heart rate were monitored for 3 days, and mice were subsequently followed with continuous 24 h blood pressure and heart rate monitoring for ~8 weeks under DOCA treatment.

Analysis of cardiac and renal fibrosis and structural kidney damage

Hearts and kidneys were fixed in formalin (4%), embedded in paraffin and sectioned into 3 µm slices. Collagen was stained with picrosirius red for assessment of perivascular and interstitial fibrosis as reported [19]. The glomerulosclerosis index and tubulointerstitial damage index were determined as reported for the analysis of structural kidney damage [20].

Isolation and analysis of primary cardiac cells

Cardiomyocytes were enzymatically isolated from adult SHRSP and F344 rats as previously described [21].

Rat primary cardiac fibroblasts were isolated via outgrowth culture as described for murine cardiac fibroblasts [22], with slight modifications. The outgrowing cardiac fibroblasts were cultured in Iscove's medium (Biochrom, Berlin, Germany) containing 20% fetal calf serum (Biochrom), 100 U/ml penicillin and 100 µg/ml streptomycin (both PAA, Cölbe, Germany) at 37 °C with 95% air and 5% CO2.

Expression analysis of human endomyocardial biopsies

Between 2003 and 2012, all patients with suspected cardiomyopathy were screened using clinical and endomyocardial biopsy-based diagnostics. The diagnosis of cardiac hypertrophy was made as recommended by the European Association of Cardiovascular Imaging and the American Society of Echocardiography [23]. In all patients, coronary artery disease and other possible causes of myocardial dysfunction were excluded by angiography and echocardiography before endomyocardial biopsy. All patients gave their written informed consent for data storage and evaluation. The study conformed to the principles outlined in the Declaration of Helsinki and was approved by the local institutional review committee of the University Clinic Benjamin Franklin, Berlin, Germany (approval 225-07). Patients' data were anonymized for analyses.

Patients presenting with signs of acute myocarditis with recent onset of symptoms were excluded, as were those with proof of intramyocardial enterovirus, adenovirus, human herpesvirus 6, Epstein–Barr virus, or erythrovirus (B19V) genomes, as described previously [24]. Other exclusion criteria were a history of antiviral or immunosuppressive therapy, clinical or biochemical evidence of concomitant chronic inflammatory disease, inability to understand the consent form, or participation or consent to participate in another study. In addition, 16 patients without signs of congestive heart failure who underwent coronary angiography and endomyocardial biopsy to evaluate chest pain were also enrolled in this study and served as controls. Endomyocardial biopsies were obtained from the right ventricular septum. Out of the patients, we selected controls ($n = 16$ (38% male), median age 38.5 years, 95% CI 34.8–49.1) without any proven cardiac dysfunction and patients with hypertrophic cardiomyopathy or hypertrophic

obstructive cardiomyopathy ($n = 20$ (75% male), median age 58 years, 95% CI 49.5–61.6).

Total RNA was isolated from endomyocardial biopsies during routine biopsy diagnostic analysis using TRIzol reagent (Life Technologies, Darmstadt, Germany), treated with DNase (PeqLab, Erlangen, Germany) to remove any traces of genomic DNA, and reverse-transcribed into cDNA using a High Capacity Kit (Life Technologies, Darmstadt, Germany) as described previously [25]. For quantitative real-time TaqMan PCR, 5 µl gene expression Mastermix (Thermo Fisher Scientific, USA) and 0.5 µl TaqMan gene expression assay purchased from Life Technologies; *CDNK1B*: Hs00153277_m1; *CPXM2*: Hs00406866_m1) were used in a final volume of 10 µl including 1 µl of cDNA template (the assays were performed in duplicate). Data were normalized to the *CDKN1B* mRNA level as an endogenous control and plotted as mRNA expression using the $2^{-\Delta Ct}$ method [26].

Bioinformatic and statistical analysis

We assessed differences in gene expression between the three rat strains (SHRSP, F334, and SHRSP-1^{F334}), and in the genome-wide transcriptome analysis, all samples except two samples (SHRSP and SHRSP-1^{F334}) passed quality control and were subsequently analyzed (gene-level analysis with the R/Bioconductor packages systemsbio [27] and limma [28]; thresholds for differential expression: $p < 0.05$, Benjamini–Hochberg-corrected, and fold change > log2 (1.5)).

For genome-wide transcriptome analysis of the four experimental mouse groups (WT SHAM, KO SHAM, WT DOCA, and KO DOCA), microarray data were analyzed using TAC-console 4.0 from Affymetrix (parameters: analysis type "Expression (Gene)", summarization: "Gene Level – RMA", FDR corrected p value with fold change > 1, meta data loaded from "MoGene_2-0_st" array type). For mouse data, two outliers were identified and excluded from the analysis (one WT SHAM and one KO DOCA sample). Gene ontology (GO) enrichment analysis was performed on the transcriptome datasets as reported [29].

If not stated otherwise, data are presented as the means ± SEM. Differences between experimental groups were analyzed by Student's *t* test, Mann–Whitney test, or one-way ANOVA with post hoc Bonferroni adjustments. A probability of $p < 0.05$ was considered to be statistically significant. We used IBM SPSS Statistics 22 for statistical analysis, GraphPad Prism and OriginLab 8.1 G for graph preparation (GraphPad Prism version 8.0 for Windows, GraphPad Software, La Jolla California USA, www.graphpad.com; OriginLab Corporation, Northampton, MA, USA).

Results

Transcriptome analysis in hypertensive rat models identifies *Cpxm2* as a novel molecule related to LVH

In LV transcriptome analysis, 541 transcripts were differentially expressed between SHRSP and the two reference strains (Supplementary Tables 2 and 3). To reduce model complexity, we subsequently focused on mRNAs that were differentially expressed between the SHRSP and consomic SHSRP-1^{F344} strains (Fig. 1a and Supplementary Table 3) because both strains share the same genetic background, while RNO1 carries the LVH QTL. In this analysis, 41 genes with differential expression were detected, mainly on RNO1 but also on rat chromosomes 2, 5, 7, 9, 13, 18 and X. Of these, 28 transcripts were also differentially expressed between the SHRSP and F344 strains as well as between the SHRSP and consomic SHSRP-1^{F344} strains (Fig. 1b and Tables S2 and 3). For further downstream studies, we selected only positional candidates, i.e., those transcripts mapping within the LVH QTL on RNO1 between genetic markers D1Rat60 and D1Rat71 (the chromosomal region between nucleotides 186,936,140 and 230,420,772; Fig. S2). Accordingly, six differentially expressed genes were identified, including Bnip3, Slc22a18, Cpxm2, Eif1ad, Tpcn2, and Pola2 (Fig. 1a, Tables S2 and 3 in bold). The gene expression of Slc22a18 and Bnip3 was lower in the SHRSP strain (fold change of 0.9 and 1.9, respectively), while the expression of Cpxm2 (fold change −0.9), Pola2 (fold change −0.9), Tpcn2 (fold change −0.8) and Eif1ad (fold change −0.8) was higher in the SHRSP strain than in the consomic strain. Slc22a18, Bnip3, Cpxm2, Tpcn2 and Eif1ad but not Pola2 were also differentially expressed between the SHRSP and F344 strain. Only Cpxm2 was confirmed in validation experiments because it demonstrated consistent and significant differential expression between the SHRSP and SHSRP-1^{F344} strains in separate qPCR expression analysis of LV tissue in adult and young rats at 4 and 8 weeks of age without established hypertension (Supplementary Fig. 3). Cpxm2 mRNA expression was significantly upregulated in LV tissue in the SHRSP strain in comparison to the F344 strain (at least a 2-fold difference in all age groups). GO enrichment analysis revealed no significant differential regulation of GO terms, i.e., biological process terms, between groups after correction for multiple tests.

Cpxm2 is expressed in both cardiomyocytes and cardiofibroblasts

Data mining of *Cpxm2* (gene ID: 293566 [rat], 55987 [mouse], and 119587 [human]) revealed its original classification as a carboxypeptidase, which was only predicted based on structural analysis [30]. Importantly, subsequent biochemical enzyme activity analysis demonstrated that CPXM2

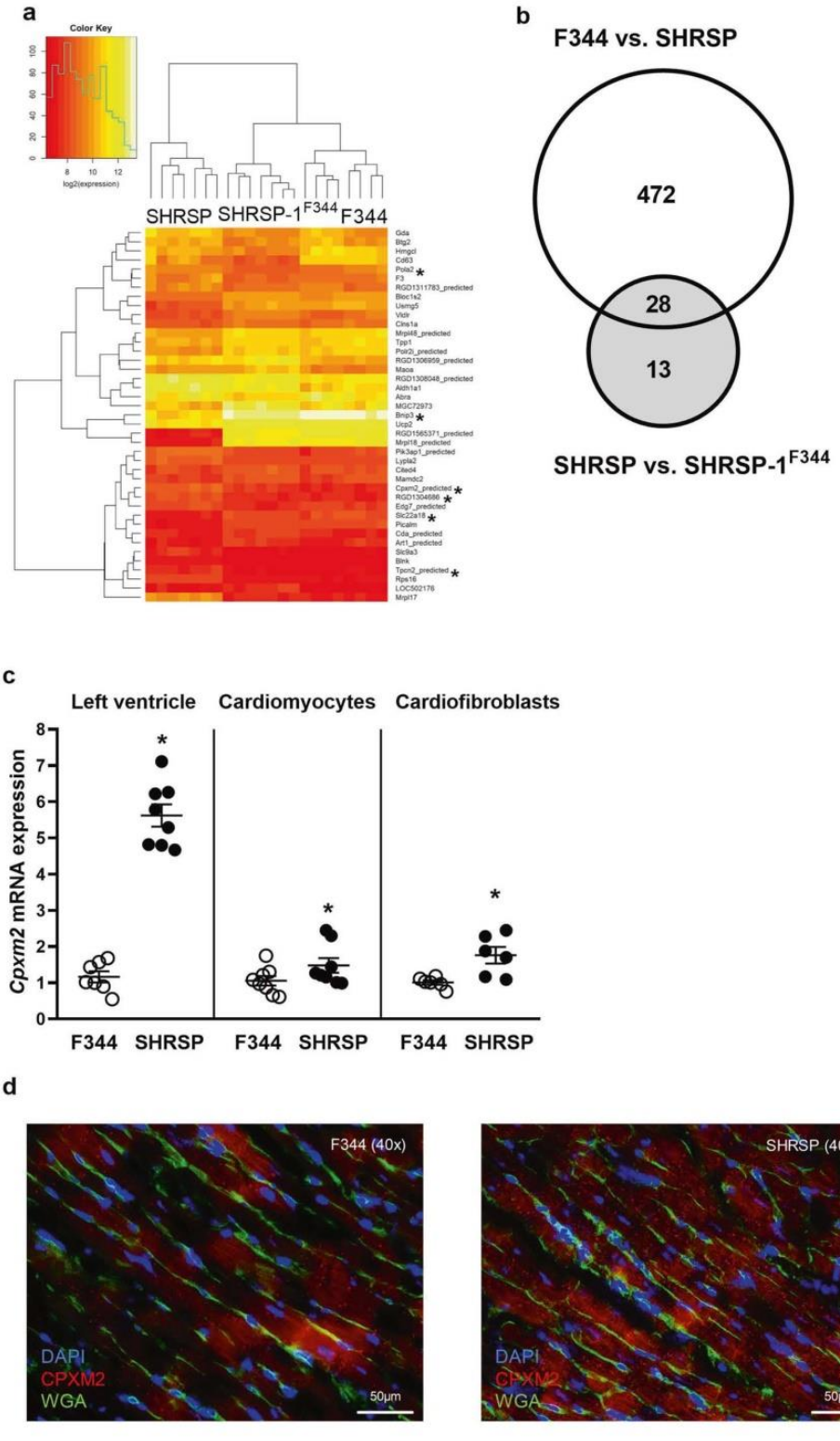

lacks—despite its predicted classification—enzymatic carboxypeptidase function [30, 31]. Currently, its biological function remains unclear. We therefore determined the cardiac cell type(s) in which it is expressed by analyzing primary cardiomyocytes and cardiofibroblasts isolated and separated from LV cardiac tissue from the rat model. This analysis

◀ **Fig. 1** Detection of differential *Cpxm2* expression in rats. **a** Heatmap of differentially expressed transcripts between 14-week-old male SHRSP ($n = 7$), SHRSP-1^{F344} ($n = 7$) and F344 ($n = 8$) rats. Transcripts mapping within the LVH QTL interval between the genetic markers D1Rat60 and D1Rat71 are marked with an asterisk. A heatmap was generated using R 3.6.1 (R Core Team, 2019) and gplots were generated (Gregory R. Warnes, Ben Bolker, Lodewijk Bonebakker, Robert Gentleman, Wolfgang Huber, Andy Liaw, Thomas Lumley, Martin Maechler, Arni Magnusson, Steffen Moeller, Marc Schwartz and Bill Venables (2019)) using the Gplots package (Various R Programming Tools for Plotting Data, R, package version 3.0.1.1 https://CRAN.R-project.org/package=gplots). **b** Venn diagrams displaying the number of differentially expressed transcripts between the SHRSP and F344 (500 transcripts) and SHRSP and SHRSP-1^{F344} (41 transcripts) strains. Common transcripts in both comparisons are emphasized ($n = 28$). **c** *Cpxm2* mRNA expression (diagram) in left ventricular tissue, in primary isolated rat cardiomyocytes, and in primary isolated rat cardiofibroblasts derived from 14-week-old F344 (white) and SHRSP (black) rats (LV *Cpxm2* mRNA, $n = 5$–8). *Cpxm2* mRNA expression in rat cardiomyocytes and rat cardiofibroblasts is shown. At least three independent experiments were performed. Expression levels are displayed as fold changes of Cpxm2 expression compared to the expression in the F344 strain ± SEM. The rat mRNA expression of *Cpxm2* was normalized against Hprt expression. **d** Paraffin sections of hearts from the SHRSP (right section) and F344 (left section) strains were analyzed with immunofluorescent staining of CPXM2 (red, cy3), the cardiomyocyte cell wall (green, WGA Alexa488) and nuclei (blue, DAPI) (magnification ×40; scale bar: 50 µM). The corresponding whole LV sections are shown in Supplementary Fig. 9. Comparison of CPXM2 staining between the SHRSP and F344 strains indicated higher expression in the SHRSP strain. Statistical analyses were performed using Student's *t* test in the rat experiments (*$p < 0.05$ vs. the F344 strain)

demonstrated that *Cpxm2* mRNA is expressed in both cardiomyocytes and cardiofibroblasts (Fig. 1c). In addition, the upregulation seen in total LV and heart paraffin tissue sections in the hypertensive model (Fig. 1c, d) was also confirmed for Cpxm2 mRNA expression in primary isolated cardiomyocytes and cardiofibroblasts obtained from the SHRSP strain compared to the F344 reference strain (Fig. 1c).

Expression analysis of CPXM2 in rat cardiomyocytes

Confocal fluorescence image analysis of isolated SHRSP rat cardiomyocytes indicated that CPXM2 was expressed along the t-tubule network and colocalized with dihydropyridine receptor (DHPR) (Fig. 2a). This was also confirmed by immunostaining of paraffin sections of rat hearts (Fig. 2b), which also indicated expression in the noncardiomyocyte compartment.

In vivo evaluation of *Cpxm2* effect on cardiac damage in *Cpxm2*-deficient mice with DOCA-salt hypertension

Body, heart, and kidney weight

Untreated KO mice did not demonstrate any morphological or behavioral differences in comparison with WT animals under normal conditions. In response to DOCA or SHAM treatment, no significant group differences in body weight were observed at the end of the observation period (after 8 weeks) (Table 1). Total heart weight was significantly increased in DOCA-treated mice compared to the corresponding SHAM mice (Table 1). Relative LV weight was markedly increased in WT DOCA compared to WT SHAM mice (+95%, Fig. 3a, b, $p = 0.000002$), and this increase was significantly lower in the KO DOCA group than in the KO SHAM group (+46%, Fig. 3a, b, $p = 0.01$) compared to the WT group. Relative kidney weights were also increased in DOCA-treated animals but without group differences (Table 1).

LV remodeling analysis

Histological analyses of cardiac tissue revealed a significant increase in LV perivascular and interstitial fibrosis (Fig. 3c–h) in WT DOCA mice vs. WT SHAM mice ($p = 0.01$ vs. SHAM groups). The increase in LV perivascular fibrosis observed in WT DOCA mice was not observed in KO DOCA mice (Fig. 3c), while LV interstitial fibrosis, although quantified as lower than that in WT DOCA mice, was still significantly elevated in KO DOCA mice compared to SHAM mice (Fig. 3f, $p = 0.048$). Collectively, an overall significant positive correlation between LV fibrosis and relative LV weight was found in all groups (perivascular fibrosis $r = 0.702$, $p = 0.000008$; interstitial fibrosis $r = 0.513$, $p = 0.003$). However, while further analysis confirmed the significant positive correlation between relative LV weight and perivascular fibrosis ($p = 0.0004$, Fig. 3e) and interstitial fibrosis in WT mice ($p = 0.04$, Fig. 3h), KO mice exhibited a significant correlation only between relative LV weight and interstitial fibrosis ($p = 0.03$, Fig. 3h).

Blood pressure and heart rate

Telemetric analysis in DOCA group animals at baseline, i.e., before DOCA and salt exposure, revealed no significant blood pressure difference between WT and KO mice (Fig. 4a). After uninephrectomy and DOCA implantation (Day 0), the mean arterial pressure (MAP) increased significantly by almost 40 mmHg in both strains (KO $p = 0.000004$ and WT $p = 0.001$, Fig. 4a). After 4 weeks, MAP decreased continuously during the observation period but did not differ between KO and WT DOCA mice. Heart rate (HR) was slightly but significantly lower at baseline in KO animals than in WT animals (−23 bpm at day −2, $p = 0.009$, Fig. 4a). During the first 4 weeks in which DOCA-salt-induced hypertension was present, HR increased significantly in both strains (KO $p = 0.004$ and WT $p = 0.0004$), which showed no significant difference, although HR remained numerically lower in KO DOCA mice.

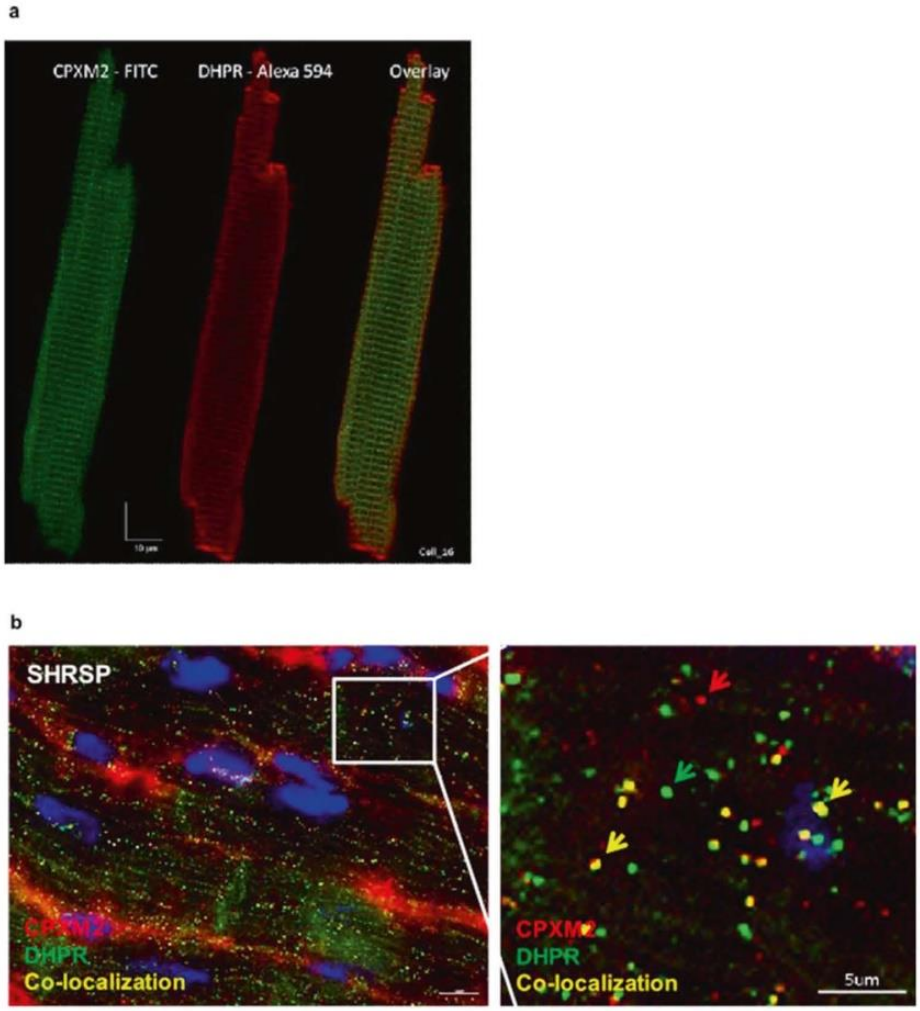

Fig. 2 Cardiac fluorescence imaging analysis in rats. **a** Freshly isolated rat cardiomyocytes were analyzed using Z stack confocal fluorescence imaging. Cardiomyocytes were stained for CPXM2 (FITC, green) and L-type Ca2+ channel dihydropyridine receptor (DHPR) (Alexa 594, red), and corresponding overlays were obtained using a Leica SP5 confocal microscope (LeicaMicrosystems, Mannheim, Germany). Immunostaining was performed as described previously [63]. Image analysis after CPXM2 staining indicated expression along t-tubules but not in intercalated disks (Z-line), which was confirmed by corresponding DHPR staining. **b** Paraffin sections of SHRSP rats were analyzed for colocalization of CPXM2 (red arrow) and DHRP (green arrow). Colocalization is marked with yellow arrows. Scale bar: 5 µM

Subsequently, between weeks 4 and 8 of DOCA exposure, between Days 33 and 43, HR was significantly lower in KO DOCA mice than in WT DOCA mice (Day 33 $p = 0.045$, Day 34 $p = 0.045$, Day 36 $p = 0.048$, Day 39 $p = 0.048$, Day 40 $p = 0.048$, Day 41 $p = 0.016$, Day 42 $p = 0.016$, Day 43 $p = 0.028$; Fig. 4a).

LV functional analysis

Echocardiography time course analysis demonstrated a significant and progressive enlargement of end-systolic (after 8 weeks + 69%, $p = 0.0000006$) and end-diastolic (after 8 weeks + 40%, $p = 0.00001$) LV internal diameters in DOCA-treated WT mice compared to SHAM WT mice (Fig. 4b). This LV enlargement was significantly attenuated in DOCA KO mice (end-systolic LV internal diameter $p = 0.002$ and end-diastolic LV internal diameter $p = 0.04$ vs. DOCA WT mice, respectively). WT DOCA mice showed significantly reduced LV ejection fraction (EF) after 4 and 8 weeks of DOCA treatment compared to WT SHAM mice (Fig. 4c, after 4 weeks $p = 0.00003$ and after 8 weeks $p = 0.00001$, respectively). This decline in EF was significantly attenuated in DOCA-treated KO mice ($p = 0.01$ vs. DOCA WT mice). Of interest, at 8 weeks of DOCA treatment, LV internal systolic diameter and EF were not significantly different between the DOCA KO groups and SHAM groups (Fig. 4b, c). Similarly, fractional shortening (FS) was significantly reduced in WT DOCA mice (after 4 weeks $p = 0.000005$ and after 8 weeks $p = 0.00003$, Table 1) but not in KO DOCA mice compared to the corresponding SHAM mice (Table 1).

Hemodynamic characterization at the end of the observation period by LV pressure-volume catheter analysis revealed that LV end-systolic volume (LVESV, +600%, $p = 0.0000000001$) and end-diastolic volume (LVEDV, + 146%, $p = 0.00000004$) were significantly elevated in the WT DOCA group compared with the SHAM group, in agreement with the echocardiography data. LVESV and LVEDV were

Table 1 Characteristics of WT SHAM, WT DOCA, KO SHAM and KO DOCA animals after 8 weeks of DOCA treatment

Phenotype	Strain	SHAM	DOCA	*p*-value (ANOVA)				
				Overall	WT SHAM vs. WT DOCA	KO SHAM vs. KO DOCA	WT SHAM vs. KO SHAM	WT DOCA vs. KO DOCA
BW (g)	WT	31.62 ± 0.99	29.19 ± 0.94	**0.040**	0.387	0.237	1.000	1.000
	KO	32.70 ± 0.54	30.24 ± 0.63					
HW (mg)	WT	125.40 ± 3.63	225.38 ± 23.31	**0.000001**	**0.000006**	**0.014**	1.000	**0.011**
	KO	118.06 ± 2.41	166.30 ± 16.58					
KW (mg)	WT	222.90 ± 7.03	277.80 ± 15.30	**0.00002**	**0.044**	**0.00006**	1.000	0.643
	KO	220.30 ± 5.62	311.50 ± 22.60					
KW/TL (mg/mm)	WT	12.31 ± 0.36	15.52 ± 0.85	**0.00003**	**0.037**	**0.0001**	1.000	1.000
	KO	12.05 ± 0.35	17.08 ± 1.32					
SV (µl)	WT	28.78 ± 1.46	31.67 ± 4.72	0.198	1.000	0.359	1.000	1.000
	KO	28.83 ± 1.86	35.72 ± 3.35					
CO (ml/min)	WT	13.33 ± 0.86	14.10 ± 2.32	0.598	1.000	1.000	1.000	1.000
	KO	12.29 ± 1.03	14.62 ± 1.54					
FS (%)	WT	28.10 ± 1.77	12.47 ± 1.01	**0.00008**	**0.00003**	1.000	0.391	**0.005**
	KO	23.74 ± 1.31	23.58 ± 2.52					

Phenotype values are means ± SEM. Significant *p*-values are presented in bold

BW body weight, *HW* heart weight, *KW* kidney weight, *TL* tibia length, *SV* stroke volume, *CO* cardiac output, *FS* fractional shortening, *WT* wild type, *KO* knock-out, *SHAM* SHAM-operated, *DOCA* Desoxycorticosterone acetate-treated

significantly lower (−61% and −51%) in KO DOCA mice than in WT DOCA mice (LVESV $p = 0.0000001$ and LVEDV $p = 0.00006$, respectively). LV end-diastolic pressure (LVEDP) was significantly elevated in WT DOCA but not in KO DOCA mice compared to SHAM mice ($p = 0.02$, Fig. 4d). In addition, both systolic (+dP/dt) and diastolic (−dP/dt) LV function were significantly impaired ($p = 0.04$ and $p = 0.01$, respectively) in WT DOCA but not in KO DOCA mice compared to SHAM mice (Fig. 4d).

When we analyzed the correlation between individual Cpxm2 mRNA expression and cardiac phenotypes in WT mice following DOCA treatment, a nonsignificant (possible due to the limited sample size) negative trend for correlation between the Cpxm2 mRNA level and relative LV weight ($r = -0.872$, $p = 0.054$) and the Nppa mRNA expression level ($r = -0.381$, $p = 0.527$) was observed, while the correlation with LV EF was blunted ($r = -0.003$, $p = 0.996$) due to the low level of variation of this phenotype in all WT DOCA mice (Supplementary Fig. 4).

Renal damage analysis

Analysis of structural glomerular and tubulointerstitial damage indices revealed a significant increase in both DOCA groups but no significant difference between WT and KO mice (Supplementary Fig. 5b, c). Renal interstitial fibrosis was also numerically higher in both DOCA groups, although this increase in KO DOCA compared with KO SHAM mice was not significant (Supplementary Fig. 5a).

Cardiac transcriptome analysis

Under SHAM conditions, no significant differences in LV transcriptome analysis data were observed between WT and KO mice. In contrast, 1243 transcripts were differentially expressed between WT SHAM and WT DOCA mice (Fig. 5 and Supplementary Table 4); a typical cardiac hypertrophy and remodeling expression pattern, e.g., significant upregulation of actin alpha 1 (Acta 1, −4.8-fold change), Nppa (−3.2-fold change), and periostin (Postn −7.9-fold change), was observed in DOCA-treated WT mice (Supplementary Table 4). Of interest, there were no differentially expressed transcripts between the KO SHAM and KO DOCA mice in the transcriptome analysis, underlining the impact of Cpxm2 on cardiac remodeling. In the separate qPCR analysis, we confirmed the significantly increased mRNA expression of natriuretic peptide A (Nppa) in WT DOCA compared to WT SHAM mice (FDR $p = 0.0000003$, Supplementary Fig. 5), while no significant increase was seen in KO DOCA compared to KO SHAM mice (FDR $p = 0.79$, Supplementary Fig. 6). However, Nppa mRNA expression was also significantly higher in WT DOCA than in KO DOCA mice ($p < 0.05$, Supplementary Fig. 6) in the targeted separate mRNA expression analysis by qPCR. Interestingly, Cpxm2 was one of the most differentially

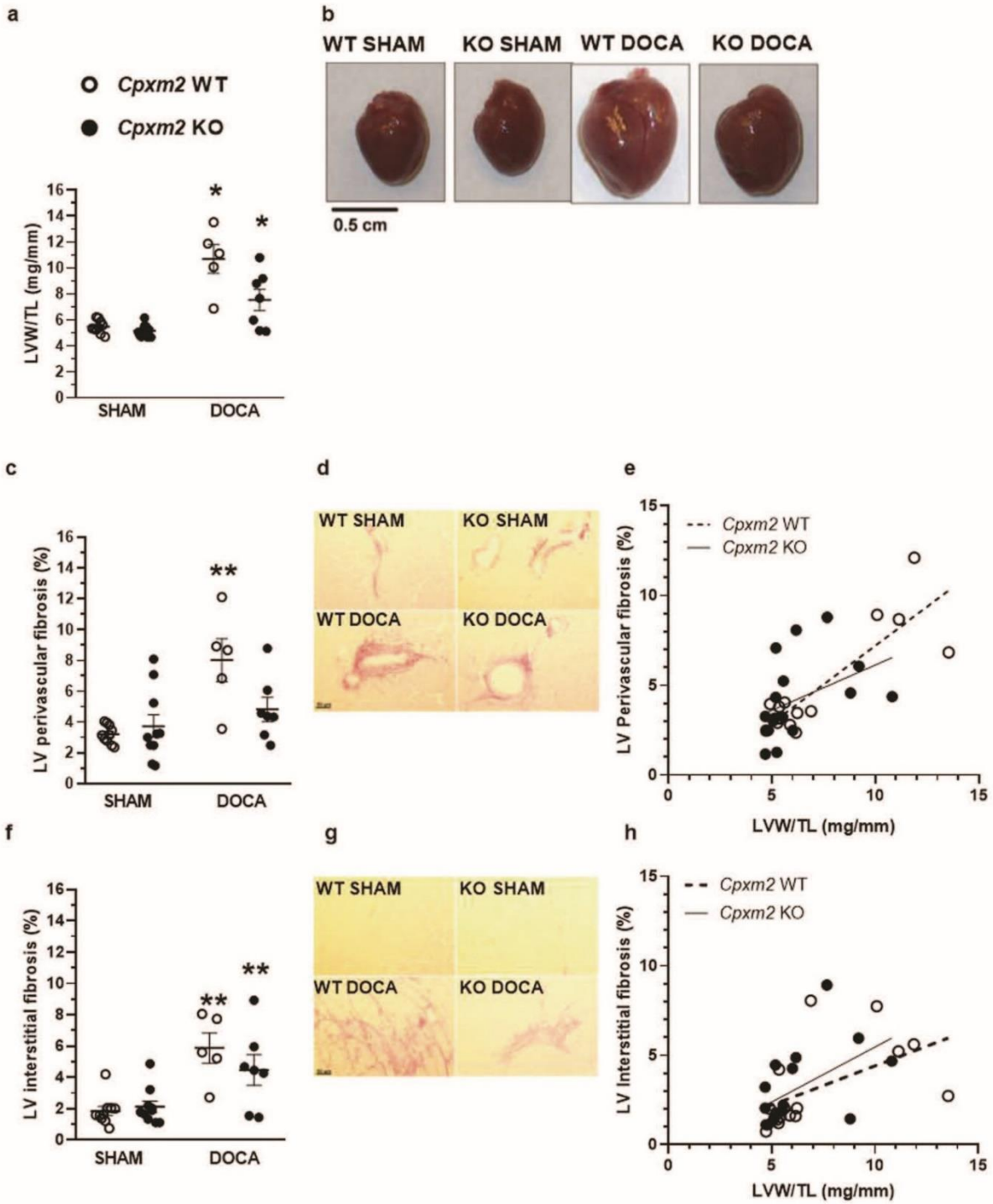

Fig. 3 Cardiac structural and molecular characteristics of *Cpxm2* wild-type (WT) and knock-out (KO) mice under SHAM and DOCA conditions. The left ventricular (LV) weight and LV fibrosis rate as well as genetic expression profile in WT (white) and KO (black) after 8 weeks of SHAM or DOCA treatment, $n = 3$–10. **a** Mean relative left ventricular weight [LVW/tibia length (TL)]. **b** Example whole hearts. **c–e** Mean perivascular fibrosis was analyzed after picrosirius red staining in three fields of view per animal; representative photographs are shown (**d**). Mean perivascular fibrosis was plotted against relative LV weight for *Cpxm2* WT ($r = 0.857$, $p = 0.00004$, **e**) and *Cpxm2* KO mice ($r = 0.417$, $p = 0.096$, **e**). **f–h** Mean interstitial fibrosis was analyzed after picrosirius red staining in three fields of view per animal; representative photographs are shown (**g**). Mean interstitial fibrosis was plotted against relative LV weight for *Cpxm2* WT ($r = 0.531$, $p = 0.04$, **h**) and *Cpxm2* KO ($r = 0.525$, $p = 0.03$, **h**). Statistical analyses were performed using one-way ANOVA with the Bonferroni post hoc test, $^{*}p < 0.05$ vs. all other groups, $^{**}p < 0.05$ vs. SHAM

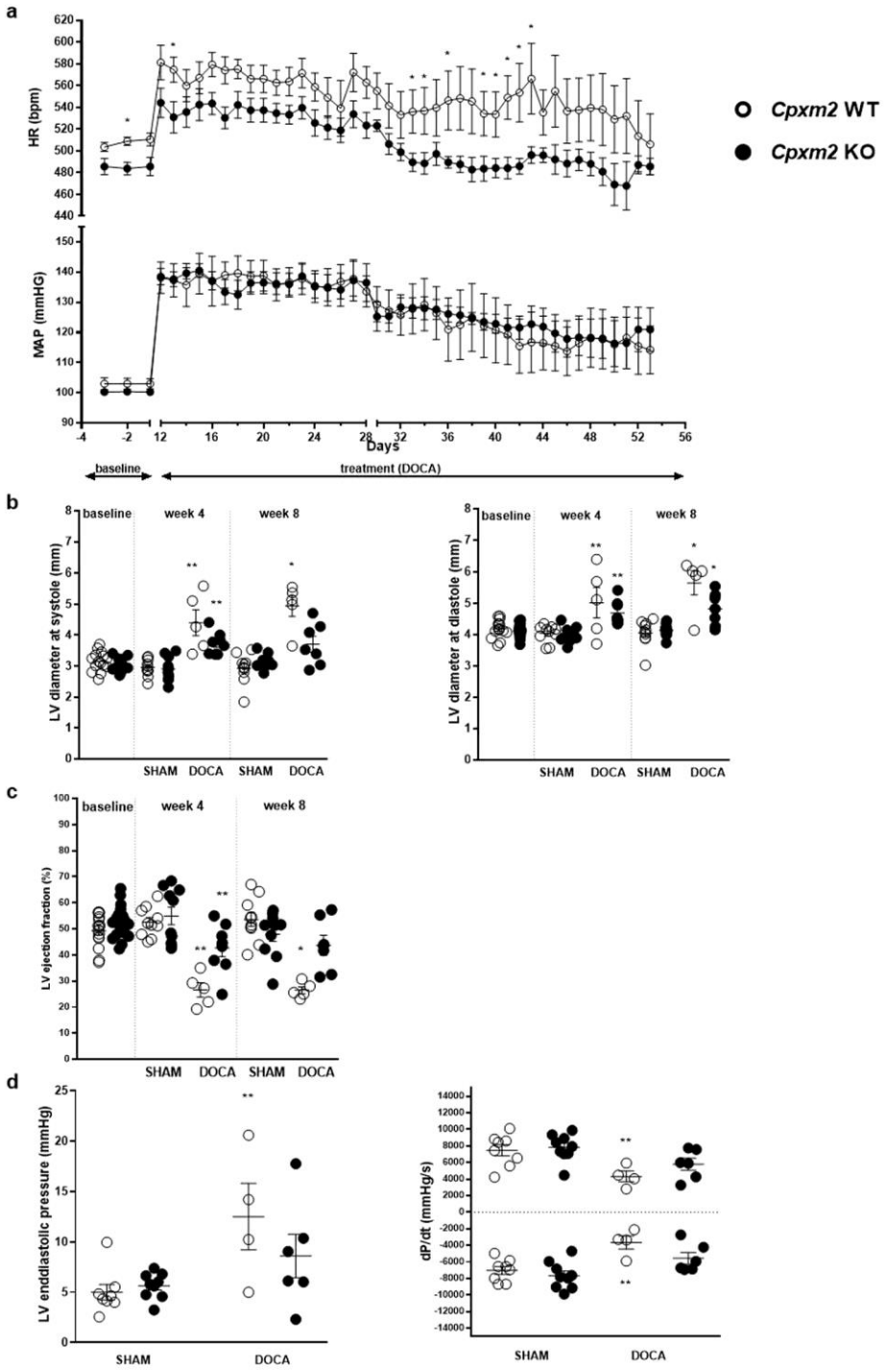

expressed transcripts between the two WT groups (fold change −4.9, FDR $p = 0.02$, Supplementary Table 4) and was upregulated in DOCA-treated WT mice; the latter finding was confirmed in separate qPCR analysis, while KO mice showed no LV Cpxm2 mRNA expression (Supplementary Fig. 7). In the direct comparison between WT DOCA and KO DOCA mice, only one transcript, encoding the gene Zdhhc2, was significantly upregulated after correction for multiple tests (−2.71-fold change, FDR $p = 0.04$) in WT DOCA mice. This transcript was also significantly upregulated in WT DOCA mice compared to WT SHAM mice (−3.12-fold change, FDR $p = 0.005$). GO

◀ **Fig. 4** Cardiac function characteristics of *Cpxm2* wild-type (WT) and knock-out (KO) mice under SHAM and DOCA conditions. **a** Mean arterial blood pressure (MAP) and heart rate (HR) in the DOCA mouse model. MAP (bottom) and HR (top) in WT (white, $n = 4$–7) and KO (black, $n = 7$–8) mice before DOCA pellet implantation and unilateral nephrectomy (baseline, Days −3 to −1) and after DOCA pellet implantation and unilateral nephrectomy (DOCA treatment, Day 12 to Day 53). MAP and HR are displayed as the mean ± SEM; statistical analyses were performed using the Mann–Whitney test, $*p < 0.05$ vs. WT DOCA (Days −2, 13, 33, 34, 36, and 39–43). **b**, **c** Left ventricular (LV) function according to echocardiographic analysis of WT (white) and KO (black) mice under SHAM and DOCA conditions after baseline (before DOCA pellet implantation and unilateral nephrectomy), after 4 weeks of DOCA treatment and after 8 weeks of DOCA treatment; $n = 5$–10. Mean LV diameter at systole (**b**, left diagram) and diastole (**b**, right diagram) and mean LV ejection fraction (EF, **c**) are displayed. **d** LV function according to hemodynamic analysis of WT (white) and KO (black) mice after 8 weeks of SHAM or DOCA treatment, $n = 5$–10. The mean LV end-diastolic pressure (left diagram) and mean maximum and minimum values of the pressure derivative during a loop (dP/dt, right diagram) are displayed. Statistical analyses were performed using Student's t test for the baseline data and one-way ANOVA with the Bonferroni post hoc test for data from 4 weeks and 8 weeks, $*p < 0.05$ vs. all other groups at the same time point, $**p < 0.05$ vs. the corresponding SHAM group

enrichment analysis indicated a significant association of GO terms with the response to DOCA in WT mice but not in KO mice, including the terms response to hypoxia, fatty acid beta-oxidation, heart development, cell adhesion, and response to mechanical stimulus (FDR $p < 0.03$).

CPXM2 expression is upregulated in patients with cardiac hypertrophy

We performed explorative analysis of CPXM2 mRNA expression in samples isolated from endomyocardial biopsies of human patients with cardiac hypertrophy and controls. CPXM2 mRNA expression was significantly higher in patients with cardiac hypertrophy ($n = 20$) than in patients without cardiac hypertrophy ($n = 16$, $p = 0.0054$, Fig. 6).

Discussion

In this study, we first performed comparative transcriptome analysis of LV tissues of rat models of hypertension, which mapped a novel candidate, i.e., *Cpxm2*, to a previously identified QTL for LV mass [17]. In subsequent validation experiments, we confirmed the expression and upregulation of Cpxm2 in primary cardiac fibroblasts, cardiomyocytes and total LV tissue in SHRSP rats.

The similar (in vivo) upregulation of Cpxm2 in the hearts of young animals at 4 weeks of age and before the development of sustained hypertension and in (in vitro) isolated cardiomyocytes and cardiofibroblasts corroborated a potential intrinsic role of Cpxm2 in LV remodeling in hypertension. In aging SHRSP rats, there was a subsequent further pronounced increase in Cpxm2 expression, which paralleled the reported increase in blood pressure in this strain (Fig. S3), suggesting additional upregulation in response to pressure overload. Nevertheless, other systemic effects, e.g., neurohumoral activation and cardiac infiltration of inflammatory cells, could also contribute to the further increase in Cpxm2 expression in the SHRSP strain. In a previous study, we clearly demonstrated that LV tissue levels of angiotensin II were not elevated in the SHRSP strain that we used in the current work [32]. Consequently, it appears that the upregulation of Cpxm2 expression in the SHRSP strain is not primarily induced by angiotensin II. This notion does not, however, exclude the possibility that inhibition of angiotensin II or aldosterone signaling with respective drug treatments can prevent the induction of Cpxm2 expression in the heart. Such strategies could be explored in future studies. Our subsequent studies in *Cpxm2*-deficient mice demonstrated a significant impact on maladaptive remodeling and heart failure development in DOCA-salt hypertension. DOCA-treated Cpxm2 KO mice showed attenuated LV dysfunction and enlargement as well as decreased LV fibrosis compared with DOCA-treated Cpxm2-WT mice [33]. In contrast, Cpxm2 deficiency had no protective effect on structural tissue damage in the kidney. The development of hypertension (mild to severe) and cardiac remodeling (diastolic to systolic dysfunction) in response to DOCA exposure may vary depending on the DOCA dose and time course of exposure, differences between species and strains, and combination with unilateral nephrectomy and increased dietary salt intake [34–37]. The DOCA protocol used in the current study in mice clearly induced severe hypertension and resulted in marked increases in LV masses and diameters as well as impairment of both diastolic and systolic LV function in WT mice. The lack of *Cpxm2* in KO mice significantly ameliorated this phenotype.

In the comparison between WT and KO mice, a significant, albeit modest, lower HR was noted at baseline in KO animals. This difference and the subsequent trend of a lower HR in Cpxm2-deficient mice might have contributed to the protective cardiac effect in response to DOCA. The lower HR in KO animals could be attributable either to intrinsic cardiac effects of Cpxm2 deficiency or to systemic effects, possibly related to the ability of the autonomic nervous system to control heart rate, in the general KO model. Future studies of conditional KO models could help dissect these effects; however, such studies would require targeting both cardiomyocytes and cardiofibroblasts based on the observed cardiac expression of Cpxm2.

Importantly, transcriptome analysis demonstrated a profound impact of *Cpxm2* KO on the LV transcriptome in response to DOCA hypertension. Hence, the induction of a characteristic LVH/remodeling transcriptome signature with a number of significant changes in response to DOCA in

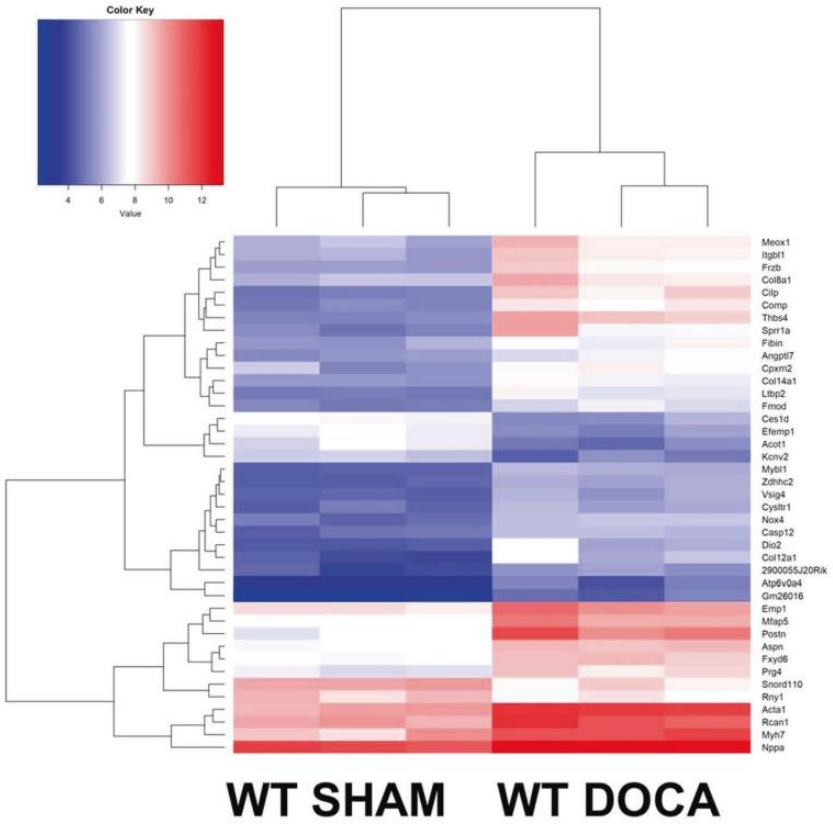

Fig. 5 Cardiac molecular characteristics of *Cpxm2* wild-type (WT) and knock-out (KO) mice under SHAM and DOCA conditions. Heatmap of differentially expressed transcripts between 8-week-old WT SHAM mice ($n = 3$) and WT DOCA mice ($n = 3$). The top 41 differentially expressed transcripts are displayed. A heatmap was generated using R 3.6.1 (R Core Team, 2019) and the gplots package (Gregory R. Warnes, Ben Bolker, Lodewijk Bonebakker, Robert Gentleman, Wolfgang Huber, Andy Liaw, Thomas Lumley, Martin Maechler, Arni Magnusson, Steffen Moeller, Marc Schwartz and Bill Venables (2019); Various R Programming Tools for Plotting Data. R, package version 3.0.1.1 https://CRAN.R-project.org/package=gplots)

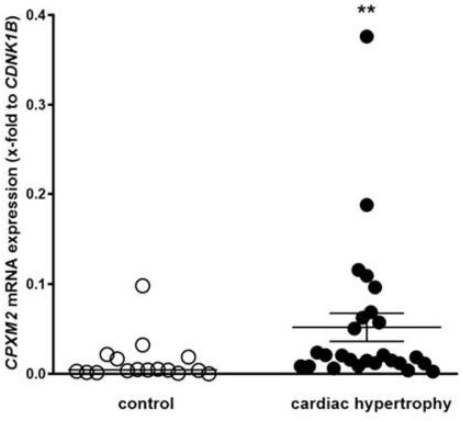

Fig. 6 Detection of differential *Cpxm2* expression in humans.*CPXM2* mRNA expression in control patients without cardiac hypertrophy ($n = 16$) and in patients with cardiac hypertrophy ($n = 20$). The human mRNA expression of *CPXM2* was normalized against *CDKN1B* expression. Statistical analyses were performed using the Mann–Whitney test in human samples, $^{**}p < 0.01$ vs. control

WT mice was abolished overall in *Cpxm2*-deficient DOCA mice. This result is in line with the moderate structural and functional cardiac remodeling phenotypes observed in the KO DOCA mice. However, a limitation of our microarray analysis is the limited sample size, which may have resulted in low statistical power for detecting differentially expressed genes (Supplementary Fig. 8).

Of interest, *Cpxm2* mRNA expression was also significantly upregulated in LV tissue of WT DOCA mice compared to control WT mice.

Our expression analysis of CPXM2 in endomyocardial biopsies of patients confirmed not only the expression of CPXM2 in the human heart but also significant CPXM2 upregulation in patients with various forms of cardiac hypertrophy. Our analysis of Cpxm2 expression in biopsies of patients should be considered explorative and for the purpose of generating hypotheses. Notwithstanding these limitations, it is important to confirm the expression of Cpxm2 in the human heart and to provide preliminary support for the differential regulation of CPXM2 in human heart diseases, which would provide a rationale for further clinical studies.

Carboxypeptidases by definition are enzymes with catalytic activity that remove protein C-terminal amino acids; they show diverse tissue distribution and biological functions [38, 39]. However, at least three members of the carboxypeptidase N/E subfamily lack catalytic function [31]: (i) carboxypeptidase × member 1 (CPXM1, CPX1, CPXM); (ii) carboxypeptidase × member 2 (CPXM2, CPX2); (iii) and aortic carboxypeptidase-like protein/

adipocyte enhancer binding protein 1 (ACLP, alias AE binding protein AEBP1). Thus, it is important to emphasize that CPXM2 also lacks enzymatic carboxypeptidase function for typical substrates [30, 31]. Currently, its biological function remains unclear. Moreover, the presence and potential function of CPXM2 in the circulation remain to be determined. CPXM1 was demonstrated to be involved in adipogenesis, osteoclastogenesis, and cancer [40–42]. Earlier studies showed AEBP1 to have a functional role in fibroblast organization and transition, wound healing, and neuromuscular development [43, 44]. More recently, AEBP1 was identified as a candidate gene in Ehlers-Danlos syndrome [45]. Previous studies have indicated a role of Cpxm2 in oncogenesis and development, as well as in disorders [46–50]. Interestingly, a mouse model with caloric restriction demonstrated reduced Cpxm2 expression in whole hearts [51]. These three proteins all contain an N-terminal domain with homology to the discoidin domain, i.e., discoidin 1, whereas none of the other members in the metallocarboxypeptidase family contain such a domain [31]. Thus, the potential interacting structure of Cpxm2 may lie in its discoidin or factor 5/8 type C domain [52]. These domains can bind to lipids, glycans, heparin-like molecules and proteins (reviewed in [52]). Proteins containing discoidin domains have been found to be related to cellular adhesion, migration, and aggregation events. These relationships could be associated with extracellular matrix function and thus influence cardiac remodeling [53–55]. The expression of CPXM2 in cardiofibroblasts appears to be in agreement with existing knowledge of discoidin domain-containing proteins and their role in extracellular remodeling. In contrast, the expression of CPXM2 in cardiomyocytes and its potential relevance are currently unclear. Nevertheless, GO enrichment analysis of the transcriptome dataset comparing the response to DOCA of the WT and KO mice indicated a significant association with the GO terms response to hypoxia, fatty acid beta-oxidation, heart development, cell adhesion, and response to mechanical stimulus. These biological processes are linked to cardiac function, cardiac remodeling and cardiac failure, and their associations thereby substantiate a putative role of CPXM2 in cardiac failure. Furthermore, our immunostaining analysis revealed that expression of CPXM2 in cardiomyocytes was associated with the t-tubule network and colocalized with DHPR. Of interest, a recent systematic analysis of the proteome of cardiac t-tubules indicated that a few proteins (1.8%) of all extracellular (matrisome) proteins of the heart had a tubule-staining immunohistochemistry pattern [56]. In this regard, Cpxm2 may represent a novel member of this small group of proteins that maintain the structure and function of t-tubules by being expressed in both compartments [56, 57]. Cpxm2 could link mechanical signals that act on the extracellular matrix and cardiomyocyte cell membranes of the t-tubule network and may play an important role in cardiac tissue remodeling in hypertension, as recently reviewed by Saucerman et al. [57].

The identified localization of the Cpxm2 protein at t-tubules indicates its potential role in the homeostatic function of the t-tubule structure or calcium handling, which should be investigated in future functional studies on calcium-handling proteins. Although limited in sample size, our microarray transcriptome analysis revealed no significant differences in mRNA expression levels between WT and Cpxm2-deficient mice during SHAM conditions for genes involved in calcium handling, including Atp2a2 (SR Ca2+ -ATPase [(SERCA2], Cav3 (cavelolin 3), Ncx (sodium/calcium exchanger), Ryr2 (ryanodine receptor 2), Pln (phosholamban) and Sln (sarcolipin).

Our LV transcriptome analysis in the mouse model indicated that only Zdhhc2 was differentially expressed between WT DOCA and KO DOCA mice after correction for multiple tests, while for example, Nppa mRNA also showed significantly higher levels in WT DOCA mice in the separate targeted analysis comparing WT DOCA and KO DOCA mice using qPCR. This result points to a potential link between Cpxm2 and the enzymes of the zinc-finger aspartate-histidine-histidine-cysteine family (zDHHC enzymes). These enzymes mediate S-acylation (palmitoylation) and are thus important in posttranslational modification [58]. Enzymatic S-acylation regulates the localization and function of different intracellular and membrane proteins [58], including cardiac ion channels and transporters, e.g., Nav1.5 [59]. The impact of altered palmitoylation of NAV1.5 on cardiac excitability was previously demonstrated in vitro [59]. However, thus far only Carboxypeptidase D, a carboxypeptidase with enzymatic function, was identified as a substrate of S-palmitoylation, and this S-palmitoylation impacts its cellular localization and half-life [60]. Further studies are thus necessary to clarify the potential interaction of Cpxm2 and Zdhhc2.

Another limitation of our study is related to the fact that for the definitive confirmation of a causative effect of Cpxm2 on the development of LVH in SHRSP rats, targeted knock-out of this gene in SHRSP rats is warranted [61]. Moreover, experiments in transgenic animals overexpressing Cpxm2 in the heart could also provide additional important information.

In summary, novel proteins that are expressed in the left ventricle of the heart and contribute to the transition from LVH to heart failure are of interest for the prevention and treatment of heart failure [62]. *Cpxm2* represents such a novel target, as it is upregulated in genetically hypertensive rat models, in response to DOCA-salt hypertension in mice, and in human patients with cardiac hypertrophy. *Cpxm2* deficiency in mice with sustained hypertension results in profound protection against cardiac damage and failure.

Although CPXM2 lacks enzymatic function and its molecular function is currently unclear, its expression and upregulation in both cardiomyocytes and cardiofibroblasts appears to be important. Moreover, its assignment to the small group of proteins that are expressed in both the matrisome and the t-tubule network of cardiomyocytes suggests that CPXM2 could play a role at this unique interface and possibly be involved in mechanosensitive pathways in the heart.

Data availability

The datasets generated and/or analyzed during the current study are available from the corresponding author on reasonable request.

Acknowledgements We acknowledge the contributions of Ilona Kamer, Claudia Plum and Karen Böhme for excellent laboratory assistance and Claudia Pallasch, Thomas Meyer, Bettina Bublath and Christiane Priebsch for excellent support in animal breeding. We thank Ute Ungethüm for excellent conduction of microarray analysis.

Funding This study was supported by the Deutsche Hochdruckliga (DHL) as Hypertensiologie Professur to Reinhold Kreutz and funded by the Deutsche Forschungsgemeinschaft (DFG, German Research Foundation) (Projektnummer 394046635—SFB 1365 and KR1152/3-1), DZHK (81×2100120) and Bundesministerium für Bildung und Forschung, Nationales Genomforschungsnetz, Herzkreislaufnetz in NGFNplus Grant 01GS0839 in Germany. Open Access funding enabled and organized by Projekt DEAL.

Compliance with ethical standards

Conflict of interest The authors declare no competing interests.

Publisher's note Springer Nature remains neutral with regard to jurisdictional claims in published maps and institutional affiliations.

References

1. Whelton PK, Carey RM, Aronow WS, Casey DE Jr, Collins KJ, Dennison Himmelfarb C, et al. 2017 ACC/AHA/AAPA/ABC/ACPM/AGS/APhA/ASH/ASPC/NMA/PCNA Guideline for the Prevention, Detection, Evaluation, and Management of High Blood Pressure in Adults: A Report of the American College of Cardiology/American Heart Association Task Force on Clinical Practice Guidelines. Hypertension. 2018;71:e13–e115.
2. Williams B, Mancia G, Spiering W, Agabiti Rosei E, Azizi M, Burnier M, et al. 2018 ESC/ESH Guidelines for the management of arterial hypertension. The Task Force for the management of arterial hypertension of the European Society of Cardiology and the European Society of Hypertension. J Hypertens. 2018;36:1953–2041.
3. Kjeldsen SE, von Lueder TG, Smiseth OA, Wachtell K, Mistry N, Westheim AS, et al. Medical Therapies for Heart Failure With Preserved Ejection Fraction. Hypertension. 2020;75:23–32.
4. Pfeffer MA, Shah AM, Borlaug BA. Heart failure with preserved ejection fraction in perspective. Circ Res. 2019;124:1598–617.
5. Lam CS, Donal E, Kraigher-Krainer E, Vasan RS. Epidemiology and clinical course of heart failure with preserved ejection fraction. Eur J Heart Fail. 2011;13:18–28.
6. Bella JN, Goring HH. Genetic epidemiology of left ventricular hypertrophy. Am J Cardiovasc Dis. 2012;2:267–78.
7. Newton-Cheh C. What can genetic studies of left ventricular mass tell us? Circ Cardiovasc Genet. 2011;4:581–4.
8. van der Harst P, van Setten J, Verweij N, Vogler G, Franke L, Maurano MT, et al. 52 genetic loci influencing myocardial mass. J Am Coll Cardiol. 2016;68:1435–48.
9. Atanur SS, Diaz AG, Maratou K, Sarkis A, Rotival M, Game L, et al. Genome sequencing reveals loci under artificial selection that underlie disease phenotypes in the laboratory rat. Cell 2013;154:691–703.
10. Curl CL, Danes VR, Bell JR, Raaijmakers AJA, Ip WTK, Chandramouli C, et al. Cardiomyocyte functional etiology in heart failure with preserved ejection fraction is distinctive-a new preclinical model. J Am Heart Assoc. 2018;7:e007451.
11. Innes BA, McLaughlin MG, Kapuscinski MK, Jacob HJ, Harrap SB. Independent genetic susceptibility to cardiac hypertrophy in inherited hypertension. Hypertension. 1998;31:741–6.
12. Lerman LO, Kurtz TW, Touyz RM, Ellison DH, Chade AR, Crowley SD, et al. Animal Models of Hypertension: A Scientific Statement From the American Heart Association. Hypertension. 2019;73:e87–e120.
13. Prestes PR, Marques FZ, Lopez-Campos G, Lewandowski P, Delbridge LMD, Charchar FJ, et al. Involvement of human monogenic cardiomyopathy genes in experimental polygenic cardiac hypertrophy. Physiol Genomics. 2018;50:680–7.
14. Tsujita Y, Iwai N, Tamaki S, Nakamura Y, Nishimura M, Kinoshita M. Genetic mapping of quantitative trait loci influencing left ventricular mass in rats. Am J Physiol Heart Circ Physiol. 2000;279:H2062–2067.
15. Nabika T, Ohara H, Kato N, Isomura M. The stroke-prone spontaneously hypertensive rat: still a useful model for post-GWAS genetic studies? Hypertens Res. 2012;35:477–84.
16. Rubattu S, Stanzione R, Volpe M. Mitochondrial dysfunction contributes to hypertensive target organ damage: lessons from an animal model of human disease. Oxid Med Cell Longev. 2016;2016:1067801.
17. Grabowski K, Koplin G, Aliu B, Schulte L, Schulz A, Kreutz R. Mapping and confirmation of a major left ventricular mass QTL on rat chromosome 1 by contrasting SHRSP and F344 rats. Physiol Genomics. 2013;45:827–33.
18. Plehm R, Barbosa ME, Bader M. Animal models for hypertension/blood pressure recording. Methods Mol Med. 2006;129:115–26.
19. Rothermund L, Pinto YM, Hocher B, Vetter R, Leggewie S, Kobetamehl P, et al. Cardiac endothelin system impairs left ventricular function in renin-dependent hypertension via decreased sarcoplasmic reticulum Ca(2+) uptake. Circulation. 2000;102:1582–8.
20. Rothermund L, Luckert S, Kossmehl P, Paul M, Kreutz R. Renal endothelin ET(A)/ET(B) receptor imbalance differentiates

salt-sensitive from salt-resistant spontaneous hypertension. Hypertension. 2001;37:275–80.
21. Primessnig U, Schonleitner P, Holl A, Pfeiffer S, Bracic T, Rau T, et al. Novel pathomechanisms of cardiomyocyte dysfunction in a model of heart failure with preserved ejection fraction. Eur J Heart Fail. 2016;18:987–97.
22. Pappritz K, Savvatis K, Koschel A, Miteva K, Tschope C, Van, et al. Cardiac (myo)fibroblasts modulate the migration of monocyte subsets. Sci Rep. 2018;8:5575.
23. Marwick TH, Gillebert TC, Aurigemma G, Chirinos J, Derumeaux G, Galderisi M, et al. Recommendations on the use of echocardiography in adult hypertension: a report from the European Association of Cardiovascular Imaging (EACVI) and the American Society of Echocardiography (ASE)†. Eur Heart J Cardiovasc Imaging. 2015;16:577–605.
24. Escher F, Kühl U, Lassner D, Stroux A, Gross U, Westermann D, et al. High perforin-positive cardiac cell infiltration and male sex predict adverse long-term mortality in patients with inflammatory cardiomyopathy. J Am Heart Assoc. 2017;6:e005352.
25. Lassner D, Siegismund CS, Kuhl U, Rohde M, Stroux A, Escher F, et al. CCR5del32 genotype in human enteroviral cardiomyopathy leads to spontaneous virus clearance and improved outcome compared to wildtype CCR5. J Transl Med. 2018;16:249.
26. Livak KJ, Schmittgen TD. Analysis of relative gene expression data using real-time quantitative PCR and the 2(-Delta Delta C(T)) Method. Methods. 2001;25:402–8.
27. systemsbio: Streamlined Analysis and Integration of Systems Biology Data. R package version 0.1.0. [computer program]. 2018.
28. Ritchie ME, Phipson B, Wu D, Hu Y, Law CW, Shi W, et al. limma powers differential expression analyses for RNA-sequencing and microarray studies. Nucleic Acids Res. 2015;43:e47.
29. Huang da W, Sherman BT, Lempicki RA. Systematic and integrative analysis of large gene lists using DAVID bioinformatics resources. Nat Protoc. 2009;4:44–57.
30. Xin X, Day R, Dong W, Lei Y, Fricker LD. Identification of mouse CPX-2, a novel member of the metallocarboxypeptidase gene family: cDNA cloning, mRNA distribution, and protein expression and characterization. DNA Cell Biol. 1998;17:897–909.
31. Reznik SE, Fricker LD. Carboxypeptidases from A to z: implications in embryonic development and Wnt binding. Cell Mol Life Sci. 2001;58:1790–804.
32. Nassar I, Schulz A, Bernardy C, Garrelds IM, Plehm R, Huber M, et al. A twofold genetic increase of ACE expression has no effect on the development of spontaneous hypertension. Am J Hypertens. 2008;21:200–5.
33. Cohn JN, Ferrari R, Sharpe N. Cardiac remodeling–concepts and clinical implications: a consensus paper from an international forum on cardiac remodeling. Behalf of an International Forum on Cardiac Remodeling. J Am Coll Cardiol. 2000;35:569–82.
34. Bacmeister L, Schwarzl M, Warnke S, Stoffers B, Blankenberg S, Westermann D, et al. Inflammation and fibrosis in murine models of heart failure. Basic Res Cardiol. 2019;114:19.
35. Basting T, Lazartigues E. DOCA-Salt Hypertension: an Update. Curr Hypertens Rep. 2017;19:32.
36. Lovelock JD, Monasky MM, Jeong EM, Lardin HA, Liu H, Patel BG, et al. Ranolazine improves cardiac diastolic dysfunction through modulation of myofilament calcium sensitivity. Circ Res. 2012;110:841–50.
37. Rothermund L, Vetter R, Dieterich M, Kossmehl P, Gogebakan O, Yagil C, et al. Endothelin-A receptor blockade prevents left ventricular hypertrophy and dysfunction in salt-sensitive experimental hypertension. Circulation. 2002;106:2305–8.
38. Sapio MR, Fricker LD. Carboxypeptidases in disease: insights from peptidomic studies. Proteom Clin Appl. 2014;8:327–37.
39. Fricker LD, Carboxypeptidases E and D. The Enzymes. In: Dalbey RE, Sigman DS (eds). Co- and Posttranslational Proteolysis of Proteins. Third ed. San Diego: Academic Press; 2002. Vol 22, pp. 421–52.
40. Chang EJ, Kwak HB, Kim H, Park JC, Lee ZH, Kim HH. Elucidation of CPX-1 involvement in RANKL-induced osteoclastogenesis by a proteomics approach. FEBS Lett. 2004;564:166–70.
41. Kim YH, Barclay JL, He J, Luo X, O'Neill HM, Keshvari S, et al. Identification of carboxypeptidase X (CPX)−1 as a positive regulator of adipogenesis. FASEB J. 2016;30:2528–40.
42. Kumar A, Bandapalli OR, Paramasivam N, Giangiobbe S, Diquigiovanni C, Bonora E, et al. Familial Cancer Variant Prioritization Pipeline version 2 (FCVPPv2) applied to a papillary thyroid cancer family. Sci Rep. 2018;8:11635.
43. Danzer E, Layne MD, Auber F, Shegu S, Kreiger P, Radu A, et al. Gastroschisis in mice lacking aortic carboxypeptidase-like protein is associated with a defect in neuromuscular development of the eviscerated intestine. Pediatr Res. 2010;68:23–28.
44. Tumelty KE, Smith BD, Nugent MA, Layne MD. Aortic carboxypeptidase-like protein (ACLP) enhances lung myofibroblast differentiation through transforming growth factor beta receptor-dependent and -independent pathways. J Biol Chem. 2014;289:2526–36.
45. Syx D, De Wandele I, Symoens S, De Rycke R, Hougrand O, Voermans N, et al. Bi-allelic AEBP1 mutations in two patients with Ehlers-Danlos syndrome. Hum Mol Genet. 2019;28:1853–64.
46. Gil-Varea E, Urcelay E, Vilarino-Guell C, Costa C, Midaglia L, Matesanz F, et al. Exome sequencing study in patients with multiple sclerosis reveals variants associated with disease course. J Neuroinflammation. 2018;15:265.
47. Niu G, Yang Y, Ren J, Song T, Hu Z, Chen L, et al. Overexpression of CPXM2 predicts an unfavorable prognosis and promotes the proliferation and migration of gastric cancer. Oncol Rep. 2019;42:1283–94.
48. Sabri A, Lai D, D'Silva A, Seeho S, Kaur J, Ng C, et al. Differential placental gene expression in term pregnancies affected by fetal growth restriction and macrosomia. Fetal Diagn Ther. 2014;36:173–80.
49. Somma G, Alger HM, McGuire RM, Kretlow JD, Ruiz FR, Yatsenko SA, et al. Head bobber: an insertional mutation causes inner ear defects, hyperactive circling, and deafness. J Assoc Res Otolaryngol. 2012;13:335–49.
50. Zhao X, Li R, Wang Q, Wu M, Wang Y. Overexpression of carboxypeptidase X M14 family member 2 predicts an unfavorable prognosis and promotes proliferation and migration of osteosarcoma. Diagn Pathol. 2019;14:118.
51. Dhahbi JM, Tsuchiya T, Kim HJ, Mote PL, Spindler SR. Gene expression and physiologic responses of the heart to the initiation and withdrawal of caloric restriction. J Gerontol A Biol Sci Med Sci. 2006;61:218–31.
52. Villoutreix BO, Miteva MA. Discoidin domains as emerging therapeutic targets. Trends Pharm Sci. 2016;37:641–59.
53. George M, Vijayakumar A, Dhanesh SB, James J, Shivakumar K. Molecular basis and functional significance of angiotensin II-induced increase in discoidin domain receptor 2 gene expression in cardiac fibroblasts. J Mol Cell Cardiol. 2016;90:59–69.
54. Goldsmith EC, Bradshaw AD, Zile MR, Spinale FG. Myocardial fibroblast-matrix interactions and potential therapeutic targets. J Mol Cell Cardiol. 2014;70:92–99.
55. Cowling RT, Yeo SJ, Kim IJ, Park JI, Gu Y, Dalton ND, et al. Discoidin domain receptor 2 germline gene deletion leads to altered heart structure and function in the mouse. Am J Physiol Heart Circ Physiol. 2014;307:H773–781.
56. Cheah JX, Nieuwenhuis TO, Halushka MK. An expanded proteome of cardiac t-tubules. Cardiovasc Pathol. 2019;42:15–20.

57. Saucerman JJ, Tan PM, Buchholz KS, McCulloch AD, Omens JH. Mechanical regulation of gene expression in cardiac myocytes and fibroblasts. Nat Rev Cardiol. 2019;16:361–78.
58. Chamberlain LH, Shipston MJ. The physiology of protein S-acylation. Physiol Rev. 2015;95:341–76.
59. Pei Z, Xiao Y, Meng J, Hudmon A, Cummins TR. Cardiac sodium channel palmitoylation regulates channel availability and myocyte excitability with implications for arrhythmia generation. Nat Commun. 2016;7:12035.
60. Kalinina EV, Fricker LD. Palmitoylation of carboxypeptidase D. Implications for intracellular trafficking. J Biol Chem. 2003; 278:9244–9.
61. Mahal Z, Fujikawa K, Matsuo H, Zahid HM, Koike M, Misumi M, et al. Effects of the Prdx2 depletion on blood pressure and life span in spontaneously hypertensive rats. Hypertens Res. 2019;42:610–7.
62. Kasiakogias A, Rosei EA, Camafort M, Ehret G, Faconti L, Ferreira JP, et al. Hypertension and heart failure with preserved ejection fraction: position paper by the European Society of Hypertension. J Hypertens. 2021;39:1522–45.
63. Eder P, Probst D, Rosker C, Poteser M, Wolinski H, Kohlwein SD, et al. Phospholipase C-dependent control of cardiac calcium homeostasis involves a TRPC3-NCX1 signaling complex. Cardiovasc Res. 2007;73:111–9.

International Journal of
Molecular Sciences

MDPI

Article

MiRNA-29b and miRNA-497 Modulate the Expression of Carboxypeptidase X Member 2, a Candidate Gene Associated with Left Ventricular Hypertrophy

Jana Subrova *, Karen Böhme, Allan Gillespie, Miriam Orphal, Claudia Plum, Reinhold Kreutz and Andreas Eisenreich

Institute of Clinical Pharmacology and Toxicology, Charité—Universitätsmedizin Berlin, Corporate Member of Freie Universität Berlin, Humboldt-Universität zu Berlin, and Berlin Institute of Health, 10117 Berlin, Germany; karen.boehme@charite.de (K.B.); allan.gillespie@charite.de (A.G.); miriam.orphal@charite.de (M.O.); claudia.plum@charite.de (C.P.); reinhold.kreutz@charite.de (R.K.); andreas.eisenreich@gmx.de (A.E.)
* Correspondence: jana.subrova@charite.de; Tel.: +49-30-450525112; Fax: +49-30-4507525112

Abstract: Left ventricular hypertrophy (LVH) is a major risk factor for adverse cardiovascular events. Recently, a novel candidate gene encoding the carboxypeptidase X member 2 (CPXM2) was found to be associated with hypertension-induced LVH. CPXM2 belongs to the M14 family of metallocarboxypeptidases, yet it lacks detectable enzyme activity, and its function remains unknown. Here, we investigated the impact of micro (mi)RNA-29b, miRNA-195, and miRNA-497 on the posttranscriptional expression control of CPXM2. Candidate miRNAs for CPXM2 expression control were identified in silico. CPXM2 expression in rat cardiomyocytes (H9C2) was characterized via real-time PCR, Western blotting, and immunofluorescence. Direct miRNA/target mRNA interaction was analysed by dual luciferase assay. CPXM2 was expressed in H9C2 and co-localised with z-disc associated protein PDZ and LIM domain 3 (Pdlim3). Transfection of H9C2 with miRNA-29b, miRNA-195, and miRNA-497 led to decreased levels of CPXM2 mRNA and protein, respectively. Results of dual luciferase assays revealed that miRNA-29b and miRNA-497, but not miRNA-195, directly regulated CPXM2 expression on a posttranscriptional level via binding to the 3′UTR of CPXM2 mRNA. We identified two miRNAs capable of the direct posttranscriptional expression control of CPXM2 expression in rat cardiomyocytes. This novel data may help to shed more light on the—so far—widely unexplored expression control of CPXM2 and its potential role in LVH.

Keywords: carboxypeptidase X member 2; microRNA; posttranscriptional; gene expression; left ventricular hypertrophy

Citation: Subrova, J.; Böhme, K.; Gillespie, A.; Orphal, M.; Plum, C.; Kreutz, R.; Eisenreich, A. MiRNA-29b and miRNA-497 Modulate the Expression of Carboxypeptidase X Member 2, a Candidate Gene Associated with Left Ventricular Hypertrophy. *Int. J. Mol. Sci.* **2022**, *23*, 2263. https://doi.org/10.3390/ijms23042263

Academic Editor: Gaetano Santulli

Received: 17 January 2022
Accepted: 14 February 2022
Published: 18 February 2022

1. Introduction

Cardiovascular diseases (CVDs) remain the most prevalent cause of morbidity and mortality worldwide [1–3]. High blood pressure is one of the principal risk factors for the development of CVDs, such as heart failure, coronary heart disease, atrial fibrillation, and stroke [4]. Although intensive research on the field of pathogenesis in cardiovascular system has been performed for decades, molecular mechanisms leading to CVDs in humans are still not entirely understood [5]. Yet, the knowledge about the molecular pathways involved in the development and progression of CVDs is essential in the search for more efficient targeted therapies.

Carboxypeptidase (CP) X member 2 (CPXM2) is a member of the M14 family and the N/E subfamily of metallocarboxypeptidases [6]. However, it does not show any detectable enzymatic activity. Recently, the gene encoding CPXM2 was found to be associated with the development of hypertension-induced left ventricular hypertrophy (LVH) in mice [7]. CPXM2 overexpression was also reported to promote proliferation, migration

and the epithelial to mesenchymal transition of osteosarcoma cells [8], as well as gastric cancer cells [9].

CPs represent a large group of enzymes involved in the C-terminal cleavage of different substrates, such as food proteins and neuropeptides [10]. The N/E subfamily contains three members which lack catalytic function. In addition to CPXM2, CP X member 1 (CPXM1) and aortic CP-like protein/adipocyte enhancer-binding protein 1 (ACLP/AEBP1) were found not to hydrolyse any of the tested CP substrates [6]. These findings are consistent with the fact that the CP domains of CPXM1, CPXM2, and AEBP1 lack different amino acid residues responsible for the catalytic function and/or substrate binding in active CPs [11].

CPXM2 was first discovered and described by Xin et al. in 1998. CPXM2 is expressed in various tissues, including brain, liver [6], inner ear [12] and heart [7]. Moreover, its sequence is evolutionarily conserved in different species, such as zebrafish, mice and humans (https://www.ncbi.nlm.nih.gov/gene/?term=cpxm2 (accessed on 14 January 2022)). This indicates that CPXM2 may play an important biological role. However, its distinct (patho-)physiological function is widely unknown.

High blood pressure is one of the most common causes of heart hypertrophy [13–15]. Additionally, LVH can result from athletic training [16] associated with physiologic higher plasma cardiac biomarkers, such as troponin I [17]. On the other hand, increased heart-wall thickness can also develop independent from high blood pressure due to primary heart diseases, e.g., hypertrophic cardiomyopathy [18] or cardiac amyloidosis [19,20]. The most prevalent causes of LVH are summarized in Figure 1. Mechanical stress evokes altered expression patterns in cardiac myocytes [21]. Various z-disc-associated proteins are involved in this process called mechanotransduction, such as PDZ and LIM domain 3 (Pdlim3; PDZ stands for postsynaptic density 95, discs large, and zonula occludens-1; LIM was originally described in the proteins LIN-11, Isl1m, and MEC-3), also known as actinin-associated LIM protein (ALP) [22].

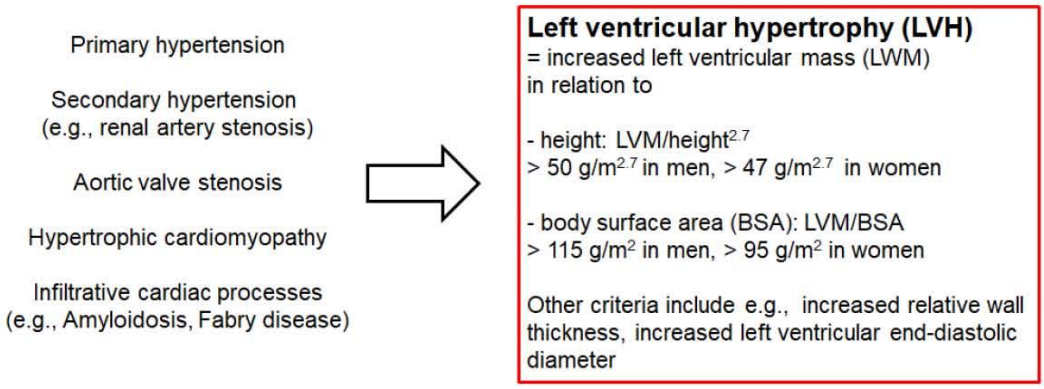

Figure 1. Different (patho-)physiologic conditions that can lead to left ventricular hypertrophy (LVH) in humans. Various CVDs as well as athletic training are associated with LVH. According to the American Society of Echocardiography and the European Association of Cardiovascular Imaging, LVH is defined as an increased left ventricular mass (LVM) in relation with height or body surface area. LVH can be determined via echocardiography or cardiac magnetic resonance imaging.

Micro (mi)RNAs are short (~22 nucleotides long), single-stranded, non-coding RNAs [23,24]. They act as posttranscriptional regulators of gene expression via binding to regulatory sequences in the 3′-untranslated region (3′UTR) of their corresponding target messenger (m)RNAs, thus leading to either repression of the translation or degradation of the target mRNA [25]. Various relevant processes involved in the development of CVDs, such as proliferation, apoptosis, inflammation, and fibrosis are influenced by miRNAs [26–31]. For example, miRNA (miR)-29b attenuated organ fibrosis in the cardiovascular system, and other tissues [32–36] via inhibiting the expression of collagens and other extracellular matrix proteins [37]. Members of the miR-15 family were also identified

to be involved in cardiac diseases [38–40]. Amongst other things, miR-15 family members mediated a protective effect against heart hypertrophy and fibrosis via the repression of the transforming growth factor β (TGFβ) pathway [41]. Moreover, miRNAs themselves can be downregulated by long non-coding RNAs (lncRNAs) [42]. Interactions on the lncRNA-miRNA axis seem to play an important role in the pathophysiology of CVDs and may imply novel targeted therapies in this field [43–45]. Additionally, miRNAs can serve as useful diagnostic markers for various diseases [46–49].

In this study, we identified miRNA candidates able to regulate the expression of CPXM2 on a posttranscriptional level. Here, we showed a significant reduction of CPXM2 mRNA and protein in rat cardiomyocytes after transfection with miRNA-29b, miRNA-497, and miRNA-195, respectively. With a dual luciferase reporter assay, we were able to confirm a direct interaction between miRNA-29b, and miRNA-497, respectively, with their in silico-predicted binding sides in the 3′UTR of the CPXM2 mRNA. Our data provide new insights into the expression control of CPXM2 in the context of its potential functional role in cardiovascular biology.

2. Results

2.1. CPXM2 Is Expressed in Rat Cardiac Cells

Immunofluorescence analysis revealed that CPXM2 was expressed in H9C2 rat cardiomyocytes (Figure 2A–C). In H9C2 cells, CPXM2 was co-localized with the z-disc-associated protein Pdlim3. Western blot analysis confirmed the presence of CPXM2 protein in H9C2 (Figure 2D).

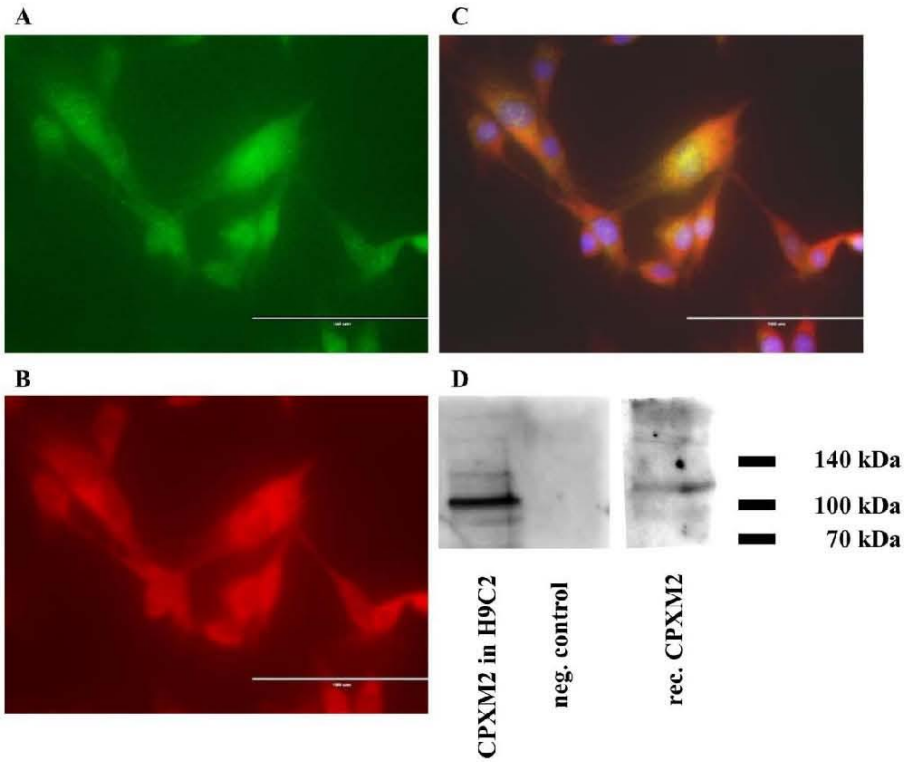

Figure 2. Expression of CPXM2 and Pdlim3 in rat cardiomyocytes. H9C2 cells were fixed and double-labelled for confocal indirect immunofluorescence microscopy with the polyclonal (**A**) anti-CPXM2 and (**B**) anti-Pdlim3 antibodies. In the overlay image (**C**) intracellular co-localisation of CPXM2 and Pdlim3 in rat cardiomyocytes is depicted. Nuclear DNA was stained with DAPI (shown in blue). In (**D**) the CPXM2 protein expression in H9C2 as well as a positive control (human recombinant CPXM2) and negative control (empty well) are shown. Bar = 100 µm.

2.2. *Identification of miR-29b, mir-195, and miR-497 as Candidates for Posttranscriptional CPXM2 Expression Control*

Using several independent miRNA databases, approximately 20 different miRNAs were predicted to potentially bind to the 3′UTR of CPXM2 (data not shown). For three of them, miR-29b, miR-195, and miR-497, structural in silico analysis of the miRNA/target mRNA interaction indicated a possible formation of regulatory or stabilizing structures [24]. MiR-29b and mit-497 showed two important attributes necessary for the building of a stable miRNA/target mRNA complex: a perfect complementarity of miRNA bases 2–8 (seed region) with the corresponding mRNA sequences and the existence of a central bulge in the miRNA/target mRNA complexes (Figure 3A,B). The miR-195/CPXM2 3′UTR duplex exhibited only the presence of a central bulge, but the seed region of miR-195 was not perfectly complementary to the corresponding mRNA sequence (Figure 3C).

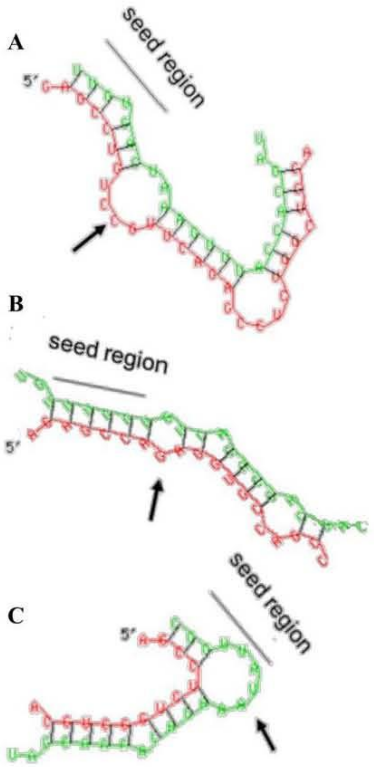

Figure 3. Structural in silico analysis of the miRNA/target mRNA interaction. Computational models of miRNA/mRNA interaction between (**A**) miR-29b, (**B**) miR-497, and (**C**) miR-195, respectively, with a corresponding sequence in the 3′UTR of CPXM2 mRNA. (green) miRNA; (red) CPXM2 mRNA 3′UTR sequence; (seed region) miRNA nucleotides 2–8; (arrow) central bulge.

2.3. *MiR-29b, mir-195, and miR-497 Suppressed the Expression of CPXM2*

To determine whether the miRNA candidates acted as posttranscriptional regulators of CPXM2 expression in cardiac cells, we transfected H9C2 with miR-29b, miR-195, miR-497, and negative control miRNA mimics, respectively. Treatment of cells with all three miRNA candidates significantly reduced the CPXM2 mRNA expression after 48 h (Figure 4A). A comparable effect was also found on protein level 48 h after transfection. Compared to the controls, CPXM2 protein expression was significantly reduced in H9C2 by miR-29b, miR-195, and miR-497, respectively (Figure 4B).

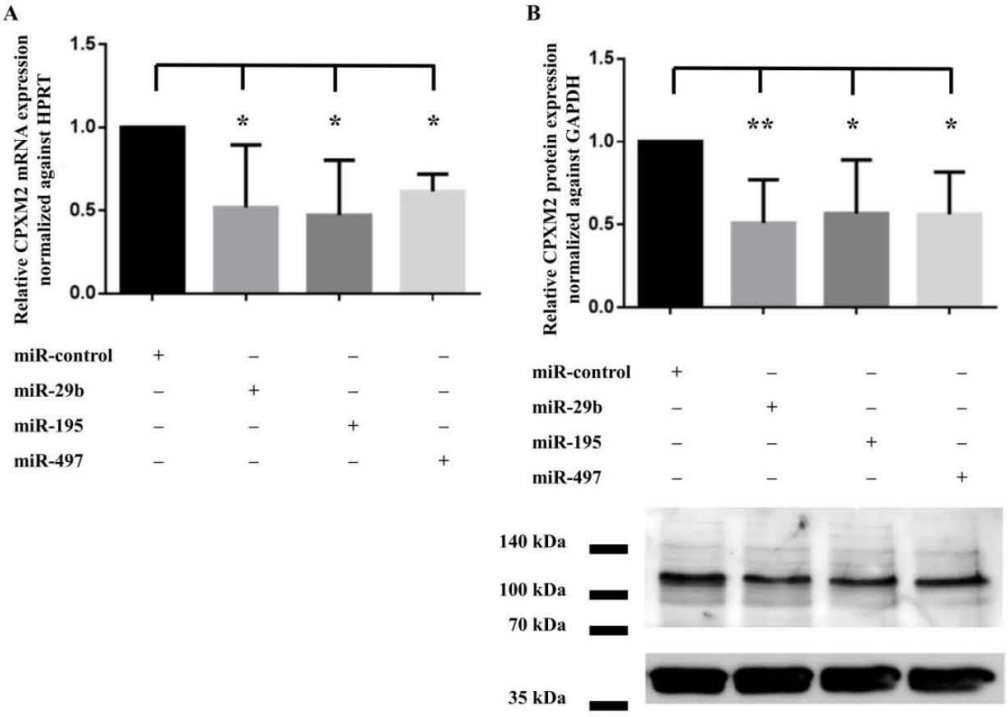

Figure 4. Impact of miR-29b, miR-195, and miR-497 on CPXM2 expression in H9C2 cells. Shown is the relative reduction of CPXM2 (**A**) mRNA and (**B**) protein expression in H9C2 48 h after transfection with miR-29b, miR-195, miR-497, or a negative control miRNA mimics (miR-control), respectively. CPXM2 mRNA expression was normalized against HPRT. CPXM2 protein expression was normalized against GAPDH. Data were presented as relative (x-fold) expression change. (*) $p < 0.05$; (**) $p < 0.01$; $n \geq 3$.

2.4. MiR-29b, and miR-497 Inhibit CPXM2 Expression through Direct Binding to Regulatory Sequences in the 3′UTR of CPXM2 mRNA

Dual luciferase reporter assays were performed to analyse whether the inhibitory impact of the miRNA candidates on CPXM2 was mediated by direct interaction with the 3′UTR of CPXM2 mRNA. Co-transfection of H9C2 with miR-29b or miR-497, respectively, and luciferase reporter vector containing the 3′UTR of CPXM2 led to a significant reduction of luciferase activity, compared to cells treated with negative control miRNA mimics (Figure 5A). For miR-195, no significant effect on luciferase activity was detected (Figure 5A).

To verify that the effect of candidate miRNAs on the luciferase activity was due to direct binding to the predicted sides in the CPXM2 3′UTR, we mutated the corresponding binding sides and repeated the experiment with the mutated vectors. Mutation of predicted binding sides completely abolished the inhibitory impact of miR-29b and miR-497 on luciferase activity in this experimental setting (Figure 5B).

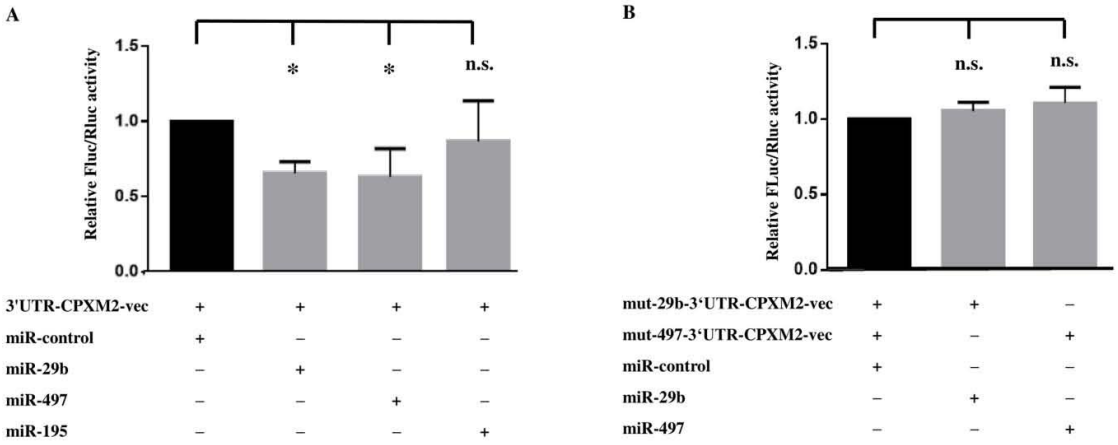

Figure 5. Dual luciferase reporter assay in H9C2. (**A**) Shown is the influence of miR-29b, miR-497, and miR-195, respectively, on the relative firefly luciferase activity of the miRNA 3′UTR target clone pEZX-MT06, containing the 3′UTR of CPXM2 (3′UTR-CPXM2-vec) 48 h after transfection. (**B**) Depicts the impact of miR-29b and miR-497 on the relative firefly luciferase activity, respectively, containing the 3′UTR of CPXM2 with mutated binding sides for miR-29b (mut-29b-3′UTR-CPXM2-vec), or miR-497 (mut-497-3′UTR-CPXM2-vec), respectively, 48 h after transfection. Firefly luciferase activity was normalized against renilla luciferase activity. (*) $p < 0.05$; (n.s.) no significant difference; $n \geq 3$; FLuc, firefly luciferase activity; RLuc, renilla luciferase activity; miR-control, negative control miRNA mimics.

3. Discussion

Although CPXM2 was first described more than 20 years ago [6], there is still little evidence about its expression control and biological role. In the present study, we determined its expression and localization in H9C2 rat cardiomyocytes, representing a relevant in vitro model. Moreover, we characterized the impact of three candidate miRNAs on the posttranscriptional control of CPXM2 expression in H9C2 cells. Concerning the evolutionary conservation of CPXM2 among different species, our findings should be applicable to human cardiomyocytes as well. To verify this, future studies should be carried out.

3.1. CPXM2 Is Expressed in Rat Cardiomyocytes and Co-Localized with Pdlim3

Immunofluorescence and Western blot analysis showed that CPXM2 was expressed in rat cardiomyocytes. This is consistent with the findings of Grabowski et al. who explored CPXM2 in the cardiac tissue of rats, mice, and humans [7,50]. Furthermore, we demonstrated the co-localisation of CPXM2 with Pdlim3 in H9C2 (Figure 2A–C). Pdlim3 is a z-disc protein which plays an important role in signal transduction, cell proliferation and cytoskeleton assembly in cardiac myocytes [51,52]. Lodder et al. associated elevated Pdlim3 levels with increased collagen deposition in the heart, a process involved in fibrosis in the context of cardiac disease [53]. Considering its co-localisation with Pdlim3, CPXM2 could potentially be involved in Pdlim3-mediated effects during the development of heart hypertrophy and fibrosis.

CPXM2, similar to two other related proteins sharing a high sequence homology with CPXM2 (CPXM1 and AEBP1) contains a discoidin domain, which is not present in any other metallocarboxypeptidase family member [10,11]. Discoidin motive can be found in many eukaryotic and prokaryotic proteins. It usually serves as a binding domain for different ligands, such as growth factors, galactose or collagens [54]. Both CPXM1 and AEBP1 are able to bind collagen [11,55]. Therefore, it is conceivable that CPXM2 may also interact with collagen, which—in turn—may affect cardiac fibrosis. However, further experiments are needed to test the ability of CPXM2 to bind collagen and to examine the possible involvement of CPXM2 in the process of cardiac fibrosis.

3.2. CPXM2 Expression Is Directly Regulated via miR-29b and via miR-497

MiRNAs influence many cellular functions via suppressing the generation of their corresponding target proteins on a posttranscriptional level [56]. MiRNAs have been associated with the pathogenesis of several cardiovascular pathologies, such as heart hypertrophy and fibrosis [36,57–61]. Here, we showed for the first time that miR-29b, as well as miR-497, reduced CPXM2 expression in H9C2 through its specific binding to the 3′UTR of CPXM2 mRNA.

Other groups reported elevated miRNA-29b levels to be associated with antifibrotic effects in the heart and other tissues [32,34,62–65]. For example, Monaghan et al. showed that local delivery of miR-29b into heart tissue shortly after myocardial infarction positively influenced postischemic cardiac remodelling in mice [32]. Zhang et al. demonstrated that miR-29b overexpression prevented angiotensin II-induced cardiac fibrosis by targeting the TGFβ pathway [65]. Qin et al. also found miR-29b to be involved in TGFβ signalling. MiR-29 reduced TGFβ-mediated renal fibrosis in mice with obstructive nephropathy [34].

The other miRNA candidate from this study, miR-497, was also shown to play an important role in the development of CVDs in previous studies [39,60]. Xiao et al. described in 2016 that treatment of primary mouse cardiomyocytes with angiotensin II led to lowered miR-497 levels in an in vitro model of cardiac hypertrophy [60]. Moreover, miR-497 overexpression led to a decrease in various hypertrophy markers, such as cell area and atrial natriuretic peptides.

Together, these studies indicate a potential role of miR-29b and miR-497 in fibrosis, cellular remodelling, and in the development of heart hypertrophy, which may be potentially mediated via modulating CPXM2 expression (Figure 6). However, further studies should be performed to explore the molecular pathways in which CPXM2 may be involved to better understand its biological function. Deeper knowledge about the pathophysiological role of CPXM2 in the development of cardiac hypertrophy and fibrosis could help us to implement novel targeted therapies for these conditions. MiRNAs, in general, have been shown to act as potential therapeutic agents [66,67]. For example, Ban et al. demonstrated miRNA-497 to accelerate wound healing in diabetic mice after local injection [68]. Thus, our findings could contribute to the development of future miRNA-based therapeutics for hypertension-induced CVDs.

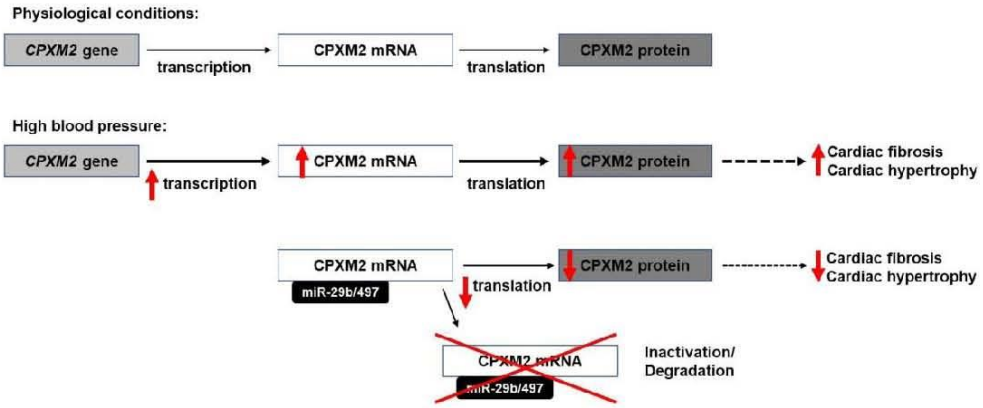

Figure 6. Possible effects of CPXM2 expression regulation via miRNA-29b and miRNA-497. According to Grabowski at al., CPXM2 is overexpressed under high blood pressure conditions. miRNA-mediated CPXM2 downregulation may reduce cardiac hypertrophy and fibrosis. Red arrow indicates an increase (↑) or a decrease (↓).

In addition to the direct effects of miR-29b and miR-497, we also found a significant inhibitory effect of miR-195 on the CPXM2 expression in H9C2. However, in contrast to the other tested miRNA candidates, miR-195 did not reduce luciferase activity, indicating no direct interaction of miR-195 with the CPXM2 mRNA (Figure 5A). This finding is in line with

the lack of perfect base pairing between the seed region of miR-195 and the corresponding sequence in the CPXM2 3′UTR revealed by our in silico analysis (Figure 3C). Possibly, miR-195 reduced the CPXM2 expression via indirect effects. Zhang et al. show miR-195 to be involved in the TGFβ signalling pathway, thus attenuating cardiac hypertrophy [69]. It may be possible that miR-195 influences the CPXM2 expression via the TGFβ signalling pathway. However, further research would be needed to verify this hypothesis.

In addition, more experiments should be carried out to better understand the role of CPXM2 in cardiac tissue. Until now, we were not able to show a functional influence of miRNA-induced CPXM2 downregulation on cell signalling in H9C2 cells. Our pilot studies (data not shown) did not reveal a significant impact of the tested miRNA candidates via the transfection of H9C2 on the phosphorylation state of factors involved in the phosphatidylinositol 3-kinase/protein kinase B/mammalian target of rapamycin (PI3K/Akt/mTOR) pathway, which could indicate a potential influence of CPXM2 on cell survival and proliferation [70]. Further research is necessary to examine the involvement of CPXM2 on cell signalling or the other biological effects of CPXM2 in cardiomyocytes. Such analyses are planned for future studies.

4. Materials and Methods

4.1. Cell Culture

Rat cardiomyocytes (H9C2) were cultured in Dulbecco's Modified Eagle Medium (DMEM) with 10% foetal bovine serum (FBS), and 1% penicillin/streptomycin, all purchased from Biochrom GmbH, Berlin, Germany. H9C2 were kept at 37 °C and in a humidified 5% CO_2 atmosphere. Before transfection, cells were starved with FBS-free DMEM for at least 12 h. Transfection of H9C2 was performed using 200 nM miRNA-mimics for miR-29b, miR-195, miR-497, and nonsense miRNA control (miR-control), all provided by Sigma-Aldrich Chemie GmbH by Merck, Munich, Germany. Lipofectamine®2000 was supplied by Thermo Fisher Scientific, Carlsbad, CA, USA. Transfection efficiency, tested via fluorescence-activated cell sorting 6 h after transfection with 200 nM Dy547 transfection control (Dharmacon, Lafayette, CO, USA), was 62% in H9C2.

4.2. In Silico Analysis

Potential miRNA candidates capable of regulating the CPXM2 expression were identified using the miRNA databases TargetScan (http://www.TargetScan.org), miRDB (http://miRDB.org), and microRNA.org—Targets and Expression (http://www.microRNA.org), all accessed on 18 April 2016. Structural in silico analysis of the miRNA/mRNA interaction was performed using the RNAhybrid 2.2 database (https://bibiserv.cebitec.uni-bielefeld.de/rnahybrid (accessed on 20 April 2016)).

4.3. Immunofluorescence Staining

For immunofluorescence analysis, H9C2 cells were fixated with 4% formaldehyde and permeabilized with 0.5% Triton X-100 for 10 min. Three washing steps with 1× phosphate-buffered saline (PBS) were performed to remove residual formaldehyde. To prevent unspecific binding, cells were blocked for 20 min at room temperature in PBS with 5% FBS and 0.1% Triton X100. Samples were then directly incubated with polyclonal rabbit anti-rat CPXM2 antibodies (Thermo Fisher, Carlsbad, CA, USA) 1:100 for 1 h at room temperature. For detection, after three washings steps in 1× PBS, fluorescein isothiocyanate (FITC)-labelled goat anti-rabbit antibodies (#12-507, Millipore by Merck, Darmstadt, Germany) were used in a 1:200 dilution for 1 h at room temperature in the dark. Next, after two washings steps in 1× PBS, samples were incubated with polyclonal ALEXA FLUOR® 594 conjugated rabbit anti-rat Pdlim3 antibodies (#bs-2928R-A594, Bioss, Woburn, MA, USA) in a 1:200 dilution for 1 h at room temperature in the dark. Nuclear DNA was stained with 4′,6-Diamidino-2-Phenylindole (DAPI, #D1306, Thermo Fisher, Carlsbad, CA, USA), 1:5000, for 10 min at room temperature in the dark. Immunofluorescence was detected with a

confocal microscope (Leica TCS SPE, Wetzlar, Germany) and analysed by the EVOS® FL Auto Imaging System (Thermo Fisher, Carlsbad, CA, USA).

4.4. Quantitative Real-Time Polymerase Chain Reaction (RT-qPCR)

Total RNA was isolated 48 h after transfection via the universal RNA purification kit (Roboklon GmbH, #E3598-02, Berlin, Germany). Then, 1 µg of isolated RNA was reverse transcribed using the high-capacity cDNA reverse transcription kit (Thermo Fisher Scientific, #4368814, Carlsbad, CA, USA) under conditions: 65 °C, 5 min; 25 °C, 10 min; 37 °C, 120 min; 85 °C, 5 min. Subsequent, RT-qPCR was performed by using a 7500 Fast Real-Time PCR System (Thermo Fisher Scientific, Carlsbad, CA, USA) and the Fast SYBR® Green Master Mix (Applied Biosystems, Darmstadt, Germany) for measurement of CPXM2 and hypoxanthine phosphoribosyltransferase (HPRT), following the manufacturer's protocol. Primers CPXM2-f/CPXM2-r (CATCCCTGAGTGGTTTCTGTCTG/TGCTACAACCAGCTCACCCC) and HPRT-f/HPRT-r (CTCATGGACTGATTATGGACAGGACT/TCCAGCAGGTCAGCAA AGAAC) were used. PCR temperature conditions: 95 °C, 20 s; 50 cycles 95 °C, 3 s; 60 °C, 30 s. Relative quantification was performed using the ΔΔ-cq method [71].

4.5. Western Blotting

Proteins were isolated from H9C2 48 h after transfection. Western blot analyses of protein samples were carried out as described before [72]. In brief, protein samples were separated by sodium dodecyl sulfate polyacrylamide gel electrophoresis (SDS-PAGE) and transferred to polyvinylidene difluoride (PVDF) membrane (Carl Roth GmbH, Karlsruhe, Germany). For detection, specific rabbit anti-rat antibodies against CPXM2 (Thermo Fisher, Carlsbad, CA, USA) 1:300, and mouse anti-rat antibodies against glyceraldehyde 3-phosphate dehydrogenase (GAPDH, Calbiochem by Merck, Darmstadt, Germany) 1:500 were used (incubation overnight at 4 °C). Subsequently, the samples were incubated with corresponding secondary goat anti-rabbit antibodies (Sc-2004, Sigma-Aldrich Chemie GmbH by Merck, Munich, Germany) in a 1:5000 dilution and goat anti-mouse antibodies (# A4416-1ML, Sigma-Aldrich Chemie GmbH by Merck, Munich, Germany) in a 1:10000 dilution for 1 h at room temperature in the dark. Human recombinant CPXM2 protein (Abnova, Taipei, Taiwan) was used as a positive control. Blots were visualized and quantified by using FUSION FX7 (Peqlab Biotechnologie GmbH, Erlangen, Deutschland). Western blot results were quantified via Gel-Pro Analyzer software version 4.0.00.001 (Media Cybernetics, Bethesda, MD, USA).

4.6. Dual Luciferase Reporter Assay

Dual luciferase reporter assays were preformed using a miRNA 3′UTR target clone pEZX-MT06, containing the 3′UTR of CPXM2 (# HmiT002050-MT06) and the negative control vector (# CmiT000001-MT01), both supplied by GeneCopoeia, Rockville, MD, USA. Furthermore, two 3′UTR clones with a mutated binding side for miR-29b, or miR-497, respectively, were prepared using the Q5® Site-Directed Mutagenesis Kit (New England BioLabs, Ipswich, MA, USA) according to the manufacturer's protocol. H9C2 were co-transfected with 200 nM miR-29b, miR-195, or miR-497 mimics, and 200 ng of the luciferase reporter vector (wild type or mutated vectors, respectively) or the empty control vector in 96-well plates in total volume 100 µL of DMEM. Then, 48 h after transfection the luciferase reporter assay (Dual-Glo® Luciferase Assay System, Promega, Madison, WI, USA) was performed, following the manufacturer's instructions.

4.7. Statistical Analysis

All data were expressed as mean ± SEM. Data were analysed by Student's *t*-test or one-way ANOVA, as appropriate. Statistical analyses were performed using GraphPad Prism v4.03 (GraphPad Software, Inc., La Jolla, CA, USA). A probability value (p) ≤ 0.05 was regarded as significant.

5. Conclusions

In summary, we showed for the first time that CPXM2 is expressed in rat cardiomyocytic cells. Moreover, we demonstrated miR-29b and miR-497 to regulate CPXM2 expression on a posttranscriptional level. This was mediated via the direct interaction of these miRNAs with the regulatory elements within the 3′UTR of CPXM2 mRNA. These novel findings may help to shed more light on the—so far—widely unexplored expression control of CPXM2 and may help to further characterize the functional role of this factor in the context of arterial hypertension-induced heart hypertrophy and cardiac fibrosis. Understanding of the pathophysiological function of CPXM2 in cardiac tissue could lead to development of future targeted therapies for CVDs.

Author Contributions: Conceptualization, J.S. and A.E.; formal analysis, J.S. and A.E.; funding acquisition, R.K.; investigation, J.S., K.B., A.G., M.O., C.P. and A.E.; methodology, K.B., C.P. and A.E.; resources, R.K.; supervision, R.K. and A.E.; writing—original draft, J.S.; writing—review and editing, K.B., R.K. and A.E. All authors have read and agreed to the published version of the manuscript.

Funding: This study was supported by the Deutsche Hochdruckliga (DHL) as Hypertensiologie Professur to Reinhold Kreutz and funded by the Deutsche Forschungsgemeinschaft (DFG, German Research Foundation) (project number 394046635—SFB 1365 and KR1152/3-1), DZHK (81X2100120) and Bundesministerium für Bildung und Forschung, Nationales Genomforschungsnetz, Herzkreislaufnetz in NGFN plus Grant 01GS0839 in Germany. The article processing charges were paid from the Open Access Fund of the Charité Library.

Institutional Review Board Statement: Not applicable.

Informed Consent Statement: Not applicable.

Data Availability Statement: The datasets generated and/or analysed during the current study are available from the corresponding author on reasonable request.

Acknowledgments: We thank Anja Brehm, Petra Karsten, and Sarah Podlich for technical and experimental support.

Conflicts of Interest: The authors declare that there are no conflict of interest.

References

1. Burden of Disease Study 2013. *Lancet* **2015**, *385*, 117–171.
2. Xu, J.; Murphy, S.L.; Kockanek, K.D.; Arias, E. Mortality in the United States, 2018. *NCHS Data Brief.* **2020**, *355*, 1–8.
3. Aryan, L.; Younessi, D.; Zargari, M.; Banerjee, S.; Agopian, J.; Rahman, S.; Borna, R.; Ruffenach, G.; Umar, S.; Eghbali, M. The Role of Estrogen Receptors in Cardiovascular Disease. *Int. J. Mol. Sci.* **2020**, *21*, 4314. [CrossRef] [PubMed]
4. Fuchs, F.D.; Whelton, P.K. High Blood Pressure and Cardiovascular Disease. *Hypertension* **2020**, *75*, 285–292. [CrossRef]
5. Brown, S.K.; Sheikh, A.M.; Guzik, T.J. Cardiovascular Research at the frontier of biomedical science. *Cardiovasc. Res.* **2020**, *116*, e83–e86. [CrossRef]
6. Xin, X.; Day, R.; Day, R.; Dong, W.; Lei, Y.; Fricker, L.D. Identification of Mouse CPX-2, a Novel Member of the Metallocarboxypeptidase Gene Family: cDNA Cloning, mRNA Distribution, and Protein Expression and Characterization. *DNA Cell Biol.* **1998**, *17*, 897–909. [CrossRef]
7. Grabowski, K.; Herlan, L.; Eisenreich, A.; Schulz, A.; Müller, D.N.; Plehm, R.; Bader, M.; Kreutz, R. [OP.8C.01] A novel candidate gene identified in stroke-prone spontaneously hypertensive rats has a major impact on adverse left ventricular remodeling in salt-induced hypertension. *J. Hypertens.* **2016**, *34*, e102. [CrossRef]
8. Zhao, X.; Li, R.; Li, R.; Wang, Q.; Wu, M.; Wang, Y. Overexpression of carboxypeptidase X M14 family member 2 predicts an unfavorable prognosis and promotes proliferation and migration of osteosarcoma. *Diagn Pathol.* **2019**, *14*, 118. [CrossRef]
9. Niu, G.; Yang, Y.; Ren, J.; Song, T.; Hu, Z.; Chen, L.; Hong, R.; Xia, J.; Ke, C.; Wang, X. Overexpression of CPXM2 Predicts an Unfavorable Prognosis and Promotes the Proliferation and Migration of Gastric Cancer. *Oncol. Rep.* **2019**, *42*, 1283–1294. [CrossRef]
10. Reznik, S.E.; Fricker, L.D. Carboxypeptidases from A to Z: Implications in embryonic development and Wnt binding. *Cell Mol. Life Sci.* **2001**, *58*, 1790–1804. [CrossRef]
11. Kim, Y.H.; O'Neill, H.M.; Whitehead, J.P. Carboxypeptidase X-1 (CPX-1) is a secreted collagen-binding glycoprotein. *Biochem. Biophys. Res. Commun.* **2015**, *468*, 894–899. [CrossRef]

12. Somma, G.; Alger, H.M.; McGuire, R.M.; Kretlow, J.D.; Ruiz, F.R.; Yatsenko, S.A.; Stankiewicz, P.; Harrison, W.; Funk, E.; Bergamaschi, A.; et al. Head bobber: An insertional mutation causes inner ear defects, hyperactive circling, and deafness. *J. Assoc. Res. Otolaryngol.* **2012**, *13*, 335–349. [CrossRef]
13. Grabowski, K.; Riemenschneider, M.; Schulte, L.; Witten, A.; Schulz, A.; Stoll, M.; Kreutz, R. Fetal-adult cardiac transcriptome analysis in rats with contrasting left ventricular mass reveals new candidates for cardiac hypertrophy. *PLoS ONE* **2015**, *10*, e0116807. [CrossRef]
14. Yildiz, M.; Oktay, A.A.; Stewart, M.H.; Milani, R.V.; Ventura, H.O.; Lavie, C.J. Left ventricular hypertrophy and hypertension. *Prog. Cardiovasc. Dis.* **2020**, *63*, 10–21. [CrossRef] [PubMed]
15. Bornstein, A.B.; Rao, S.S.; Marwaha, K. *Left Ventricular Hypertrophy*; StatPearls Publishing: Orlando, FL, USA, 2022.
16. Pavlik, G.; Kováts, T.; Kneffel, Z.; Komka, Z.; Radák, Z.; Tóth, M.; Nemcsik, J. Characteristics of the athlete's heart in aged hypertensive and normotensive subjects. *J. Sports Med. Phys. Fit.* **2021**, *21*, 126994. [CrossRef] [PubMed]
17. Mascia, G.; Pescetelli, F.; Baldari, A.; Gatto, P.; Seitun, S.; Sartori, P.; Pieroni, M.; Calò, L.; Della Bona, R.; Porto, I. Interpretation of elevated high-sensitivity cardiac troponin I in elite soccer players previously infected by severe acute respiratory syndrome coronavirus 2. *Int. J. Cardiol.* **2021**, *326*, 248–251. [CrossRef] [PubMed]
18. Mascia, G.; Olivotto, I.; Brugada, J.; Arbelo, E.; Di Donna, P.; Della Bona, R.; Canepa, M.; Porto, I. Sport practice in hypertrophic cardiomyopathy: Running to stand still? *Int. J. Cardiol.* **2021**, *345*, 77–82. [CrossRef]
19. Maurizi, N.; Rella, V.; Fumagalli, C.; Salerno, S.; Castelletti, S.; Dagradi, F.; Torchio, M.; Marceca, A.; Meda, M.; Gasparini, M.; et al. Prevalence of cardiac amyloidosis among adult patients referred to tertiary centres with an initial diagnosis of hypertrophic cardiomyopathy. *Int. J. Cardiol.* **2020**, *300*, 191–195. [CrossRef]
20. Lioncino, M.; Monda, E.; Palmiero, G.; Caiazza, M.; Vetrano, E.; Rubino, M.; Esposito, A.; Salerno, G.; Dongiglio, F.; D'Onofrio, B.; et al. Cardiovascular Involvement in Transthyretin Cardiac Amyloidosis. *Heart Fail. Clin.* **2022**, *1*, 73–87. [CrossRef]
21. Knöll, R.; Hoshijima, M.; Chien, K. Cardiac mechanotransduction and implications for heart disease. *J. Mol. Med.* **2003**, *81*, 750–756. [CrossRef]
22. Frank, D.; Frey, N. Cardiac Z-disc Signaling Network. *J. Biol. Chem.* **2011**, *286*, 9897–9904. [CrossRef]
23. Blahna, M.T.; Hata, A. Regulation of miRNA biogenesis as an integrated component of growth factor signaling. *Curr. Opin. Cell Biol.* **2013**, *25*, 233–240. [CrossRef] [PubMed]
24. Eisenreich, A.; Leppert, U. The impact of microRNAs on the regulation of tissue factor biology. *Trends Cardiovasc. Med.* **2014**, *24*, 128–132. [CrossRef] [PubMed]
25. Van Rooij, E. The Art of MicroRNA Research. *Circ. Res.* **2011**, *108*, 219–234. [CrossRef] [PubMed]
26. Olson, E.N. MicroRNAs as therapeutic targets and biomarkers of cardiovascular disease. *Sci. Transl. Med.* **2014**, *6*, 239ps233. [CrossRef]
27. Eisenreich, A.; Rauch, U. Regulation of the Tissue Factor Isoform Expression and Thrombogenicity of HMEC-1 by miR-126 and miR-19a. *Cell Biol. Res. Ther.* **2013**, *2*, 124.
28. Lee, J.; Kang, H. Hypoxia Promotes Vascular Smooth Muscle Cell Proliferation through microRNA-Mediated Suppression of Cyclin-Dependent Kinase Inhibitors. *Cells* **2019**, *8*, 802. [CrossRef]
29. Li, Z.; Yi, N.; Chen, R.; Meng, Y.; Wang, Y.; Liu, H.; Cao, W.; Hu, Y.; Gu, Y.; Tong, C.; et al. miR-29b-3p protects cardiomyocytes against endotoxin-induced apoptosis and inflammatory response through targeting FOXO3A. *Cell. Signal.* **2020**, *74*, 109716. [CrossRef]
30. Sun, D.G.; Tian, S.; Zhang, L.; Hu, Y.; Guan, C.Y.; Ma, X.; Xia, H.F. The miRNA-29b Is Downregulated in Placenta During Gestational Diabetes Mellitus and May Alter Placenta Development by Regulating Trophoblast Migration and Invasion Through a HIF3A-Dependent Mechanism. *Front. Endocrinol.* **2020**, *11*, 169. [CrossRef]
31. Esteves, J.V.; Yonamine, C.Y.; Pinto-Junior, D.C.; Gerlinger-Romero, F.; Enguita, F.J.; Machado, U.F. Diabetes Modulates MicroRNAs 29b-3p, 29c-3p, 199a-5p and 532-3p Expression in Muscle: Possible Role in GLUT4 and HK2 Repression. *Front. Endocrinol.* **2018**, *9*, 536. [CrossRef]
32. Monaghan, M.G.; Holeiter, M.; Brauchle, E.; Layland, S.L.; Lu, Y.; Deb, A.; Pandit, A.; Nsair, A.; Schenke-Layland, K. Exogenous miR-29B Delivery Through a Hyaluronan-Based Injectable System Yields Functional Maintenance of the Infarcted Myocardium. *Tissue Eng. Part A* **2018**, *24*, 57–67. [CrossRef]
33. Xiao, J.; Meng, X.M.; Huang, X.R.; Chung, A.C.; Feng, Y.L.; Hui, D.S.; Yu, C.M.; Sung, J.J.; Lan, H.Y. miR-29 inhibits bleomycin-induced pulmonary fibrosis in mice. *Mol. Ther.* **2012**, *20*, 1251–1260. [CrossRef]
34. Qin, W.; Chung, A.C.K.; Huang, X.R.; Meng, X.M.; Hui, D.S.C.; Yu, C.M.; Sung, J.J.Y.; Lan, H.Y. TGF-β/Smad3 signaling promotes renal fibrosis by inhibiting miR-29. *J. Am. Soc. Nephrol.* **2011**, *22*, 1462–1474. [CrossRef] [PubMed]
35. Van Rooij, E.; Sutherland, L.B.; Thatcher, J.E.; DiMaio, J.M.; Naseem, R.H.; Marshall, W.S.; Hill, J.A.; Olson, E.N. Dysregulation of microRNAs after myocardial infarction reveals a role of miR-29 in cardiac fibrosis. *Proc. Natl. Acad. Sci. USA* **2008**, *105*, 13027–13032. [CrossRef]
36. García, R.; Salido-Medina, A.B.; Gil, A.; Merino, D.; Gómez, J.; Villar, A.V.; González-Vílchez, F.; Hurlé, M.A.; Nistal, J.F. Sex-Specific Regulation of miR-29b in the Myocardium Under Pressure Overload is Associated with Differential Molecular, Structural and Functional Remodeling Patterns in Mice and Patients with Aortic Stenosis. *Cells* **2020**, *9*, 833. [CrossRef]

37. Abonnenc, M.; Nabeebaccus, A.A.; Mayr, U.; Barallobre-Barreiro, J.; Dong, X.; Cuello, F.; Sur, S.; Drozdov, I.; Langley, S.R.; Lu, R.; et al. Extracellular matrix secretion by cardiac fibroblasts: Role of microRNA-29b and microRNA-30c. *Circ. Res.* **2013**, *113*, 1138–1147. [CrossRef] [PubMed]
38. Zhang, X.; Ji, R.; Liao, X.; Castillero, E.; Kennel, P.J.; Brunjes, D.L.; Franz, M.; Möbius-Winkler, S.; Drosatos, K.; George, I.; et al. MicroRNA-195 Regulates Metabolism in Failing Myocardium Via Alterations in Sirtuin 3 Expression and Mitochondrial Protein Acetylation. *Circulation* **2018**, *137*, 2052–2067. [CrossRef]
39. Li, X.; Zeng, Z.; Li, Q.; Xu, Q.; Xie, J.; Hao, H.; Luo, G.; Liao, W.; Bin, J.; Huang, X.; et al. Inhibition of microRNA-497 ameliorates anoxia/reoxygenation injury in cardiomyocytes by suppressing cell apoptosis and enhancing autophagy. *Oncotarget* **2015**, *6*, 18829–18844. [CrossRef]
40. Porrello, E.R.; Mahmoud, A.I.; Simpson, E.; Johnson, B.A.; Grinsfelder, D.; Canseco, D.; Mammen, P.P.; Rothermel, B.A.; Olson, E.N.; Sadek, H.A. Regulation of neonatal and adult mammalian heart regeneration by the miR-15 family. *Proc. Natl. Acad. Sci. USA* **2013**, *110*, 187–192. [CrossRef] [PubMed]
41. Tijsen, A.J.; van der Made, I.; van den Hoogenhof, M.M.; Wijnen, W.J.; van Deel, E.D.; de Groot, N.E.; Alekseev, S.; Fluiter, K.; Schroen, B.; Goumans, M.J.; et al. The microRNA-15 family inhibits the TGFβ-pathway in the heart. *Cardiovasc. Res.* **2014**, *104*, 61–71. [CrossRef]
42. Mirzaei, S.; Zarrabi, A.; Hashemi, F.; Zabolian, A.; Saleki, H.; Ranjbar, A.; Seyed Saleh, S.H.; Bagherian, M.; Sharifzadeh, S.O.; Hushmandi, K.; et al. Regulation of Nuclear Factor-KappaB (NF-κB) signaling pathway by non-coding RNAs in cancer: Inhibiting or promoting carcinogenesis? *Cancer Lett.* **2021**, *509*, 63–80. [CrossRef] [PubMed]
43. Braga, L.; Ali, H.; Secco, I.; Giacca, M. Non-coding RNA therapeutics for cardiac regeneration. *Cardiovasc. Res.* **2021**, *117*, 674–693. [CrossRef]
44. Yan, Y.; Song, D.; Song, X.; Song, C. The role of lncRNA MALAT1 in cardiovascular disease. *IUBMB Life* **2020**, *72*, 334–342. [CrossRef] [PubMed]
45. Cheng, X.W.; Chen, Z.F.; Wan, Y.F.; Zhou, Q.; Wang, H.; Zhu, H.Q. Long Non-coding RNA H19 Suppression Protects the Endothelium Against Hyperglycemic-Induced Inflammation via Inhibiting Expression of miR-29b Target Gene Vascular Endothelial Growth Factor a Through Activation of the Protein Kinase B/Endothelial Nitric Oxide Synthase Pathway. *Front. Cell. Dev. Biol.* **2019**, *7*, 263. [PubMed]
46. Galeano-Otero, I.; Del Toro, R.; Guisado, A.; Díaz, I.; Mayoral-González, I.; Guerrero-Márquez, F.; Gutiérrez-Carretero, E.; Casquero-Domínguez, S.; Díaz-de la Llera, L.; Barón-Esquivias, G.; et al. Circulating miR-320a as a Predictive Biomarker for Left Ventricular Remodelling in STEMI Patients Undergoing Primary Percutaneous Coronary Intervention. *J. Clin. Med.* **2020**, *9*, 1051. [CrossRef]
47. Samandari, N.; Mirza, A.H.; Kaur, S.; Hougaard, P.; Nielsen, L.B.; Fredheim, S.; Mortensen, H.B.; Pociot, F. Influence of Disease Duration on Circulating Levels of miRNAs in Children and Adolescents with New Onset Type 1 Diabetes. *Noncoding RNA* **2018**, *4*, 35. [CrossRef]
48. Özdirik, B.; Stueven, A.K.; Mohr, R.; Geisler, L.; Wree, A.; Knorr, J.; Demir, M.; Vucur, M.; Loosen, S.H.; Benz, F.; et al. Analysis of miR-29 Serum Levels in Patients with Neuroendocrine Tumors-Results from an Exploratory Study. *J. Clin. Med.* **2020**, *9*, 2881. [CrossRef]
49. Marttila, S.; Rovio, S.; Mishra, P.P.; Seppälä, I.; Lyytikäinen, L.P.; Juonala, M.; Waldenberger, M.; Oksala, N.; Ala-Korpela, M.; Harville, E.; et al. Adulthood blood levels of hsa-miR-29b-3p associate with preterm birth and adult metabolic and cognitive health. *Sci. Rep.* **2021**, *11*, 9203. [CrossRef] [PubMed]
50. Grabowski, K.; Herlan, L.; Witten, A.; Qadri, F.; Eisenreich, A.; Lindner, D.; Schädlich, M.; Schulz, A.; Subrova, J.; Mhatre, K.N.; et al. Cpxm2 as a novel candidate for cardiac hypertrophy and failure in hypertension. *Hypertens. Res.* **2021**, *45*, 292–307. [CrossRef]
51. Dixon, D.M.; Choi, J.; El-Ghazali, A.; Park, S.Y.; Roos, K.P.; Jordan, M.C.; Fishbein, M.C.; Comai, L.; Reddy, S. Loss of muscleblind-like 1 results in cardiac pathology and persistence of embryonic splice isoforms. *Sci. Rep.* **2015**, *5*, 9042. [CrossRef]
52. Xue, K.; Wang, Y.; Hou, Y.; Wang, Y.; Zhong, T.; Li, L.; Zhang, H.; Wang, L. Molecular characterization and expression patterns of the actinin-associated LIM protein (ALP) subfamily genes in porcine skeletal muscle. *Gene* **2014**, *539*, 111–116. [CrossRef] [PubMed]
53. Lodder, E.M.; Scicluna, B.P.; Beekman, L.; Arends, D.; Moerland, P.D.; Tanck, M.W.; Adriaens, M.E.; Bezzina, C.R. Integrative genomic approach identifies multiple genes involved in cardiac collagen deposition. *Circ. Cardiovasc. Genet.* **2014**, *7*, 790–798. [CrossRef] [PubMed]
54. Kiedzierska, A.; Smietana, K.; Czepczynska, H.; Otlewski, J. Structural similarities and functional diversity of eukaryotic discoidin-like domains. *Biochim. Biophys.* **2007**, *1774*, 1069–1078. [CrossRef] [PubMed]
55. Schissel, S.L.; Dunsmore, S.E.; Liu, X.; Shine, R.W.; Perrella, M.A.; Layne, M.D. Aortic Carboxypeptidase-Like Protein Is Expressed in Fibrotic Human Lung and its Absence Protects against Bleomycin-Induced Lung Fibrosis. *Am. J. Pathol.* **2009**, *174*, 818–828. [CrossRef] [PubMed]
56. Eisenreich, A. Regulation of Vascular Function on Posttranscriptional Level. *Thrombosis* **2013**, *2013*, 3452. [CrossRef]
57. Chiang, M.H.; Liang, C.J.; Lin, L.C.; Yang, Y.F.; Huang, C.C.; Chen, Y.H.; Kao, H.L.; Chen, Y.C.; Ke, S.R.; Lee, C.W.; et al. miR-26a attenuates cardiac apoptosis and fibrosis by targeting ataxia-telangiectasia mutated in myocardial infarction. *J. Cell. Physiol.* **2020**, *235*, 6085–6102. [CrossRef]

58. Huang, Y.; Tang, S.; Huang, C.; Chen, J.; Li, J.; Cai, A.; Feng, Y. Circulating miRNA29 family expression levels in patients with essential hypertension as potential markers for left ventricular hypertrophy. *Clin. Exp. Hypertens.* **2017**, *39*, 119–125. [CrossRef]
59. Panizo, S.; Carrillo-López, N.; Naves-Díaz, M.; Solache-Berrocal, G.; Martínez-Arias, L.; Rodrigues-Díez, R.R.; Fernández-Vázquez, A.; Martínez-Salgado, C.; Ruiz-Ortega, M.; Dusso, A.; et al. Regulation of miR-29b and miR-30c by vitamin D receptor activators contributes to attenuate uraemia-induced cardiac fibrosis. *Nephrol. Dial. Transpl.* **2017**, *32*, 1831–1840. [CrossRef]
60. Xiao, Y.; Zhang, X.; Fan, S.; Cui, G.; Shen, Z. MicroRNA-497 Inhibits Cardiac Hypertrophy by Targeting Sirt4. *PLoS ONE* **2016**, *11*, e0168078. [CrossRef]
61. Wan, X.; Chen, S.; Fang, Y.; Zuo, W.; Cui, J.; Xie, S. Mesenchymal stem cell-derived extracellular vesicles suppress the fibroblast proliferation by downregulating FZD6 expression in fibroblasts via micrRNA-29b-3p in idiopathic pulmonary fibrosis. *J. Cell Physiol.* **2020**, *235*, 8613–8625. [CrossRef]
62. Widlansky, M.E.; Jensen, D.M.; Wang, J.; Liu, Y.; Geurts, A.M.; Kriegel, A.J.; Liu, P.; Ying, R.; Zhang, G.; Casati, M.; et al. miR-29 contributes to normal endothelial function and can restore it in cardiometabolic disorders. *EMBO Mol. Med.* **2018**, *10*, e8046. [CrossRef] [PubMed]
63. Yamada, Y.; Takanashi, M.; Sudo, K.; Ueda, S.; Ohno, S.I.; Kuroda, M. Novel form of miR-29b suppresses bleomycin-induced pulmonary fibrosis. *PLoS ONE* **2017**, *12*, e0171957. [CrossRef] [PubMed]
64. Yang, F.; Li, P.; Li, H.; Shi, Q.; Li, S.; Zhao, L. microRNA-29b Mediates the Antifibrotic Effect of Tanshinone IIA in Postinfarct Cardiac Remodeling. *J. Cardiovasc. Pharmacol.* **2015**, *65*, 456–464. [CrossRef] [PubMed]
65. Zhang, Y.; Huang, X.R.; Wei, L.H.; Chung, A.C.; Yu, C.M.; Lan, H.Y. miR-29b as a therapeutic agent for angiotensin II-induced cardiac fibrosis by targeting TGF-β/Smad3 signaling. *Mol. Ther.* **2014**, *22*, 974–985. [CrossRef] [PubMed]
66. Horita, M.; Farquharson, C.; Stephen, L.A. The role of miR-29 family in disease. *J. Cell. Biochem.* **2021**, *122*, 696–715. [CrossRef]
67. Saliminejad, K.; Khorram Khorshid, H.R.; Soleymani Fard, S.; Ghaffari, S.H. An overview of microRNAs: Biology, functions, therapeutics, and analysis methods. *J. Cell. Physiol.* **2019**, *234*, 5451–5465. [CrossRef] [PubMed]
68. Ban, E.; Jeong, S.; Park, M.; Kwon, H.; Park, J.; Song, E.J.; Kim, A. Accelerated wound healing in diabetic mice by miRNA-497 and its anti-inflammatory activity. *Biomed. Pharmacother.* **2020**, *121*, 109613. [CrossRef] [PubMed]
69. Zhang, X.; Liu, Y.; Han, Q. Puerarin Attenuates Cardiac Hypertrophy Partly Through Increasing Mir-15b/195 Expression and Suppressing Non-Canonical Transforming Growth Factor Beta (Tgfβ) Signal Pathway. *Med. Sci. Monit.* **2016**, *22*, 1516–1523. [CrossRef]
70. Magaye, R.R.; Savira, F.; Hua, Y.; Xiong, X.; Huang, L.; Reid, C.; Flynn, B.L.; Kaye, D.; Liew, D.; Wang, B.H. Attenuating PI3K/Akt-mTOR pathway reduces dihydrosphingosine 1 phosphate mediated collagen synthesis and hypertrophy in primary cardiac cells. *Int. J. Biochem. Cell Biol.* **2021**, *134*, 105952. [CrossRef]
71. Livak, K.J.; Schmittgen, T.D. Analysis of relative gene expression data using real-time quantitative PCR and the 2(-Delta Delta C(T)) Method. *Methods* **2001**, *25*, 402–408. [CrossRef]
72. Eisenreich, A.; Langer, S.; Herlan, L.; Kreutz, R. Regulation of podoplanin expression bymicroRNA-29b associateswith its antiapoptotic effect in angiotensin II-induced injury of human podocytes. *J. Hypertens.* **2016**, *34*, 323–331. [CrossRef] [PubMed]

Kidney and Blood Pressure Research

Kidney Blood Press Res 2020;45:850–862
DOI: 10.1159/000508477
Received: February 14, 2020
Accepted: May 6, 2020
Published online: October 20, 2020

Research Article

TMEM63C, a Potential Novel Target for Albuminuria Development, Is Regulated by MicroRNA-564 and Transforming Growth Factor beta in Human Renal Cells

Miriam Orphal Allan Gillespie Karen Böhme Jana Subrova
Andreas Eisenreich Reinhold Kreutz

Charité-Universitätsmedizin Berlin, Corporate Member of Freie Universität Berlin, Humboldt-Universität zu Berlin, and Berlin Institute of Health, Institute of Clinical Pharmacology and Toxicology, Berlin, Germany

Keywords
Transmembrane protein 63C · MicroRNA · Podocyte · Transforming growth factor beta · Epithelial-mesenchymal transition

Abstract
Introduction: Transmembrane protein (TMEM) 63C is a member of the TMEM gene family and was recently linked to glomerular filtration barrier function and albuminuria. Its molecular function and expression regulation are largely unknown. ***Objective:*** In this study, we set out to characterize the regulating impact of microRNAs (miRNAs) such as miRNA-564 (miR-564) on TMEM63C expression in renal cells. Also, we examined the influence of transforming growth factor beta (TGF-ß) on TMEM63C expression and the potential impact of TMEM63C inhibition on epithelial-mesenchymal transition (EMT) in renal cells and on cell viability in human embryonic kidney 293 cells (HEK 293). ***Methods:*** Expression analyses were done using real-time PCR and Western blot. Dual luciferase assay was performed to determine the miRNA-mediated expression control. Cell viability was assessed via trypan blue exclusion staining. ***Results and Conclusions:*** MiR-564 reduced TMEM63C expression in HEK 293 and human podocytes (hPC). The treatment of renal cells with TGF-ß led to an increased expression of TMEM63C. Moreover, a reduced TMEM63C expression was associated with a changed ratio of EMT marker proteins such as α-smooth muscle actin versus E-cadherin in HEK 293 and

Andreas Eisenreich and Reinhold Kreutz contributed equally.

Reinhold Kreutz
Department for Toxicology and Pharmacology, Charité University Berlin
Charitéplatz 1
DE–10117 Berlin (Germany)
reinhold.kreutz@charite.de

Kidney and Blood Pressure Research

Kidney Blood Press Res 2020;45:850–862
DOI: 10.1159/000508477

decreased nephrin expression in hPC. In addition, cell viability was reduced upon inhibition of TMEM63C expression in HEK 293. This study demonstrates first mechanisms involved in TMEM63C expression regulation and a link to EMT in renal cells.

Introduction

Podocytes are terminally differentiated and highly specialized glomerular cells with a great importance for the glomerular filtration barrier (GFB) [1]. In this context, nephrin is known as an essential structural protein of the slit diaphragm and is considerably involved in the preservation of glomerular function as well as podocyte viability [2]. The injury or loss of podocytes leads to albuminuria and plays a pivotal role in several glomerular diseases including diabetic and non-diabetic kidney diseases [3, 4]. While albuminuria itself represents a marker of renal damage, it also has a direct pathogenic effect on renal tissue [5, 6]. Therefore, albuminuria is discussed as suitable therapeutic target for intervention to slow the progression of CKD [5].

Recently, a study identified transmembrane protein (TMEM) 63C as a novel candidate for albuminuria development [7]. TMEM63C, a member of the TMEM gene family, is expressed in the kidney, but also in many other tissues such as the cerebral cortex and endocrine tissues [7]. Schulz et al. [7] showed a loss of TMEM63C expression in podocytes of patients with focal segmental glomerulosclerosis. In addition, functional studies in zebra fish models suggested that TMEM63C could play an important role in GFB function [7]. Nevertheless, the biological function of TMEM63C and its expression regulation are widely unknown.

MicroRNAs (miRNAs) are short, non-coding RNAs consisting of 20–22 nucleotides, which are known to be influential regulators of post-transcriptional gene expression [8]. The regulation and function of miRNAs are subject of current research. In this context, previous studies described a major influence of miRNAs on kidney diseases [8–10]. For example, miRNA-21 (miR-21), miR-29, and miR-192 were found to play a pathophysiological role in renal fibrosis induced by transforming growth factor beta (TGF-β) [10]. Furthermore, the regulating effect of miRNAs becomes more important in cancer research. In this regard, the impact of several miRNAs, such as miR-21, miR-22, and miR-566, were described in the pathogenesis of renal cell cancer [11–13].

This study sets out to characterize the post-transcriptional regulation of TMEM63C expression by miRNAs including miR-30b and miR-564 in renal cells. Moreover, we analyzed the impact of small interfering RNA (siRNA)-mediated TMEM63C inhibition on cell viability. In addition, the effect of TGF-β on TMEM63C regulation and the impact of TMEM63C deficiency on epithelial-mesenchymal transition (EMT) were analyzed in cell culture studies.

Methods

Cell Culture

Human podocytes (hPC; supplied by Dr. M. Saleem, University of Bristol, Bristol, UK) were cultured and differentiated as described previously [14]. For our investigations, we not only used hPC, but also human embryonic kidney 293 cells (HEK 293) due to its high transfection efficiency and as suitable model to study epithelial characteristics in kidney cells. HEK 293 (a kind gift of Prof. Dr. H. Fechner, Technical University of Berlin, Berlin, Germany) were cultured in DMEM enriched with 10% fetal bovine serum and 1% penicillin/streptomycin – all provided by Biochrom GmbH, Berlin, Germany. HEK 293 were grown in a humidified incu-

Kidney and Blood Pressure Research

Kidney Blood Press Res 2020;45:850–862
DOI: 10.1159/000508477

Table 1. The primer sequences of real-time PCR

Gene	Primer sequences (5′–>3′)
TMEM63C	
Forward	CAAGCGTGTCCGTAAGGATT
Reverse	ACAATTGGGTTCTGCAGCTT
GAPDH	
Forward	GAGTCAACGGATTTGGTCGT
Reverse	GATCTCGCTCCTGGAAGATG
Nephrin	
Forward	ATCCTCTCCATCCTGGTTCC
Reverse	GTCCTGGAGGGAACAGAACA
E-cadherin	
Forward	ACATTTCCCAACTCCTCTCC
Reverse	TCTGTCACCTTCAGCCATC
α-SMA	
Forward	CGAAGCACAGAGCAAAAGAG
Reverse	AGGCATAGAGAGACAGCACCG

bator at 37°C and with 5% CO_2. Before transfection, HEK 293 and hPC were starved in fetal bovine serum-free DMEM or RPMI 1640, respectively. 200 nM of miR-30b, miR-564, or negative control (miRControl) miRNA mimic was used for miRNA transfection. For siRNA transfection, 200 nM of TMEM63C siRNAs (siTMEM63C) or scrambled control siRNAs (siControl) were deployed. Transfection was done by using Lipofectamine™ 2000 (Invitrogen GmbH, Karlsruhe, Germany). The inhibitory effect of siTMEM63C was examined on mRNA and protein levels. For stimulation, hPC and HEK 293 were treated with 5 and 10 ng/mL TGF-β (eBioscience; Thermo Fisher Scientific GmbH, Waltham, MA, USA), respectively, for 48 h. Transfection efficiency, determined by Dy547 transfection control (200 nmol/L; Fisher Scientific – Germany GmbH, Schwerte, Germany), was determined to be 25% in hPC [14] and 62% in HEK 293.

Real-Time PCR

Analyses of mRNA expression were performed as described previously [14]. Specific TaqMan® Gene Expression Assays (Life Technologies GmbH, Darmstadt, Germany) were utilized for determination of TMEM63C, nephrin, α-smooth muscle actin (α-SMA), E-cadherin, and glyceraldehyde-3-phosphate dehydrogenase expression, following the manufacturer's instructions. Real-time PCR was accomplished by means of 7500 Fast Real-time PCR System (Applied Biosystems, Carlsbad, CA, USA) using the following conditions: 50°C, 2 min; 95°C, 20 s; 45 cycles 95°C, 3 s; 60°C, 30 s. The PCR primers used are shown in Table 1.

Western Blotting

Western blot analyses were done as described previously [15]. Specific antibodies against TMEM63C (Sigma-Aldrich Chemie GmbH, Munich, Germany) and glyceraldehyde-3-phosphate dehydrogenase (Calbiochem, Darmstadt, Germany) were used for detection. Blots were visualized and quantified by using FUSION FX7 (Peqlab Biotechnologie GmbH, Erlangen, Deutschland) and Gel-Pro Analyser software version 4.0.00.001 (Media Cybernetics, Bethesda, MD, USA).

Dual Luciferase Activity Assay

For determination of dual luciferase activity, 2×10^4 HEK 293 were treated with miR-30b, miR-564, or miRControl in 96-well plates. Cells were co-transfected with aforementioned

Kidney and Blood Pressure Research

Kidney Blood Press Res 2020;45:850–862
DOI: 10.1159/000508477

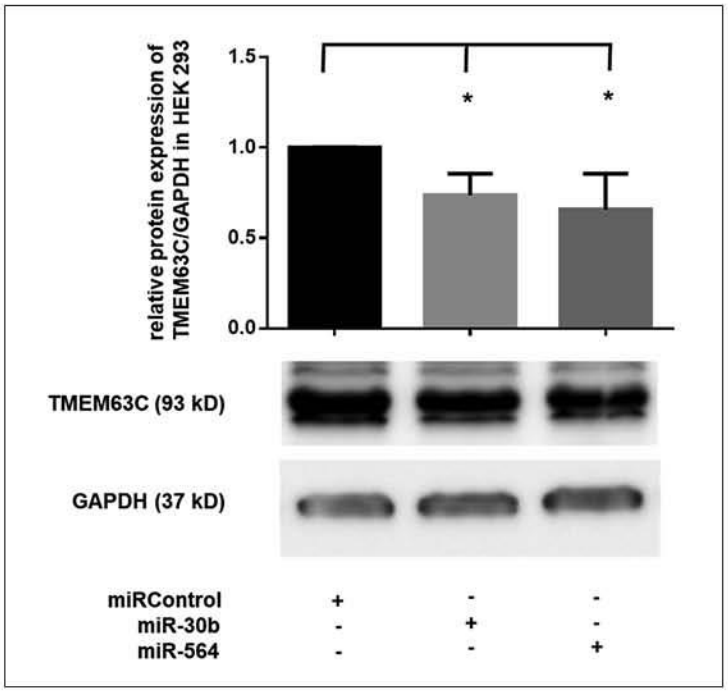

Fig. 1. The impact of miR-30b and miR-564 on TMEM63C protein expression in HEK 293. The protein expression of TMEM63C in HEK 293 transfected with miR-30b, miR-564, or a negative control miRNA mimic (miRControl) is depicted. The expression was analyzed after 48 h. GAPDH was used for normalization. Shown is the mean ± SEM of at least 3 independent experiments. (*) $p < 0.05$. miR, miRNA; TMEM63C, transmembrane protein 63C; HEK 293, human embryonic kidney cells 293; GAPDH, glyceraldehyde-3-phosphate dehydrogenase.

miRNAs and 200 ng/mL dual luciferase reporter vector (3′UTR-TMEM63C vec) containing the 3′-untranslated region (3′UTR) of TMEM63C, a reporter vector (3′UTR-TMEM63C-mut vec) containing a mutated miRNA binding site in the 3′UTR of TMEM63C or a negative control vector (control vec), respectively (provided by GeneCopoeia, Inc., Rockville, MD, USA). After 24 h, dual luciferase activity was analyzed by using a luciferase reporter assay (Promega GmbH, Mannheim, Germany) following the manufacturer's protocol.

Cell Viability Assay

Cell viability was determined by a trypan blue staining assay. In brief, HEK 293 were seeded in 12-well plates and transfected with 200 nM siTMEM63C or siControl, as described previously. After 48 h, cells were removed from the wells using trypsin-EDTA and subsequently resuspended in fresh DMEM. 10 µL of cell suspension was mixed with 90 µL of trypan blue solution (Biochrom GmbH, Berlin, Germany). Eventually, living and trypan blue-stained dead cells were counted using a C-Chip Neubauer improved hemocytometer chamber (Carl Roth GmbH & Co. KG., Karlsruhe, Germany).

Statistical Analysis

All results were represented as mean ± standard error the mean (SEM) and analyzed by Student's *t* test or one-way ANOVA. A probability value (p) <0.05 was deemed as significant.

Results

Impact of Different miRNAs on TMEM63C Expression in HEK 293

First, we performed in silico analysis to identify potential miRNAs modulating TMEM63C expression on post-transcriptional level. In our analysis, we searched relevant databases, such as TargetScanHuman 7.1 (www.targetscan.org), miRDB (www.mirdb.org), and Diana

Kidney and Blood Pressure Research

Kidney Blood Press Res 2020;45:850–862

DOI: 10.1159/000508477

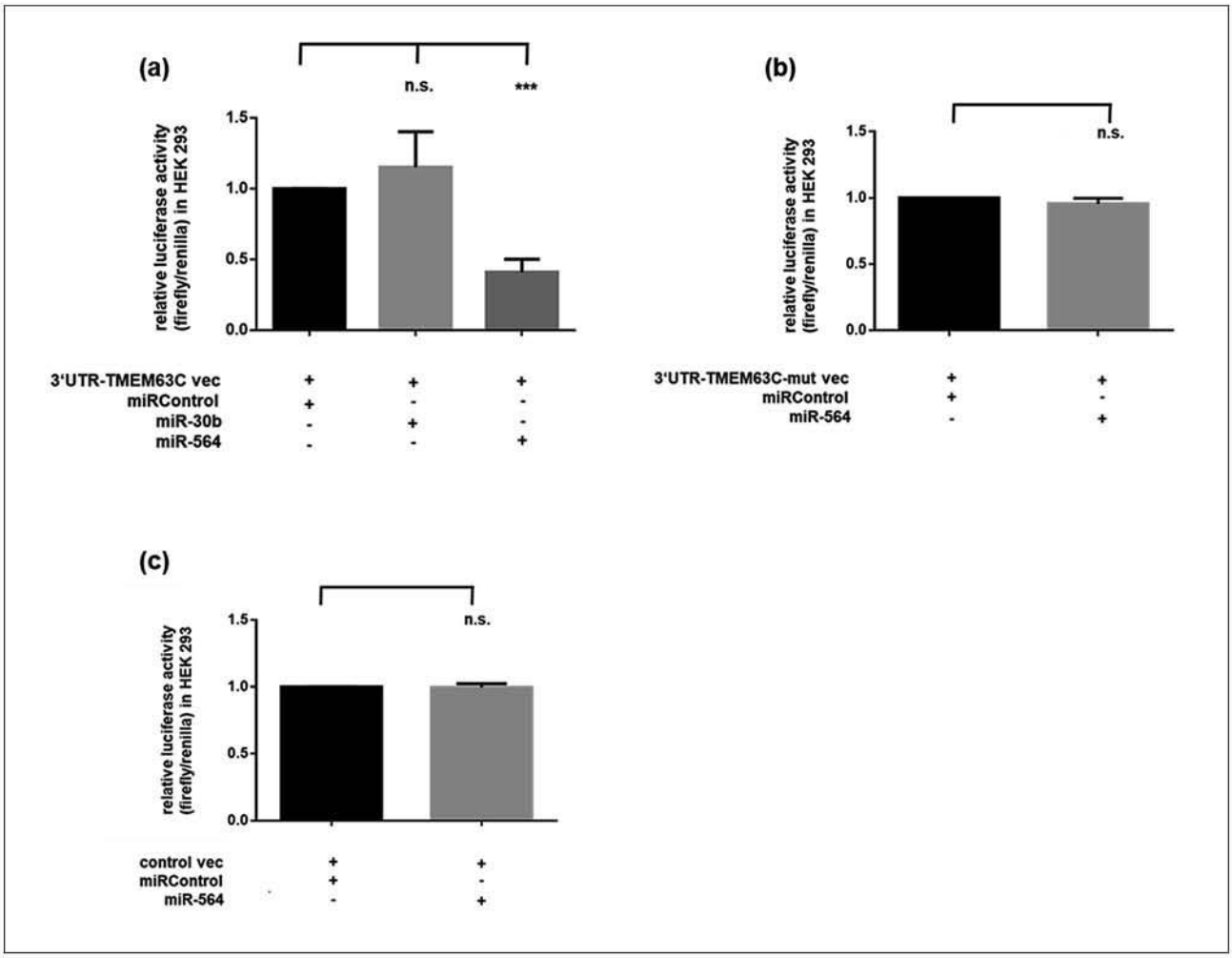

Fig. 2. The influence of miR-30b and miR-564 on luciferase activity in HEK 293. Shown is the luciferase activity in HEK 293 transfected with (**a**) luciferase reporter construct containing 3′UTR of TMEM63C (3′UTR-TMEM63C vec) and co-transfected with miR-30b, miR-564, or a negative control miRNA mimic (miRControl). For control, HEK 293 were co-transfected with (**b**) control vector (3′UTR-TMEM63C-mut vec), containing a mutated miRNA binding site in the 3′UTR of TMEM63C, and (**c**) a non-functional control vector (control vec), respectively. Firefly luciferase activity was determined 24 h after transfection and normalized against renilla luciferase activity. In **a**, **b**, **c**, the mean ± SEM of at least 3 independent experiments is shown. (***) $p < 0.001$. n.s., no significant difference; miR, miRNA; HEK 293, human embryonic kidney cells 293; 3′UTR, 3′-untranslated region; TMEM63C, transmembrane protein 63C.

Tools (www.diana.imis.athena-innovation.gr). All of the abovementioned prediction tools revealed miR-30b and miR-564 as potential candidates for TMEM63C expression regulation via binding to the 3′UTR of TMEM63C mRNA. To examine the effect of the potential miRNA candidates on TMEM63C expression, we used respective miRNA mimics in our experiments. Next, we determined the influence of the aforementioned miRNAs on protein expression of TMEM63C in HEK 293. In our experiments, miR-30b and miR-564 led to a decreased protein generation of TMEM63C after 48 h (Fig. 1).

Kidney and Blood Pressure Research

Kidney Blood Press Res 2020;45:850–862

DOI: 10.1159/000508477

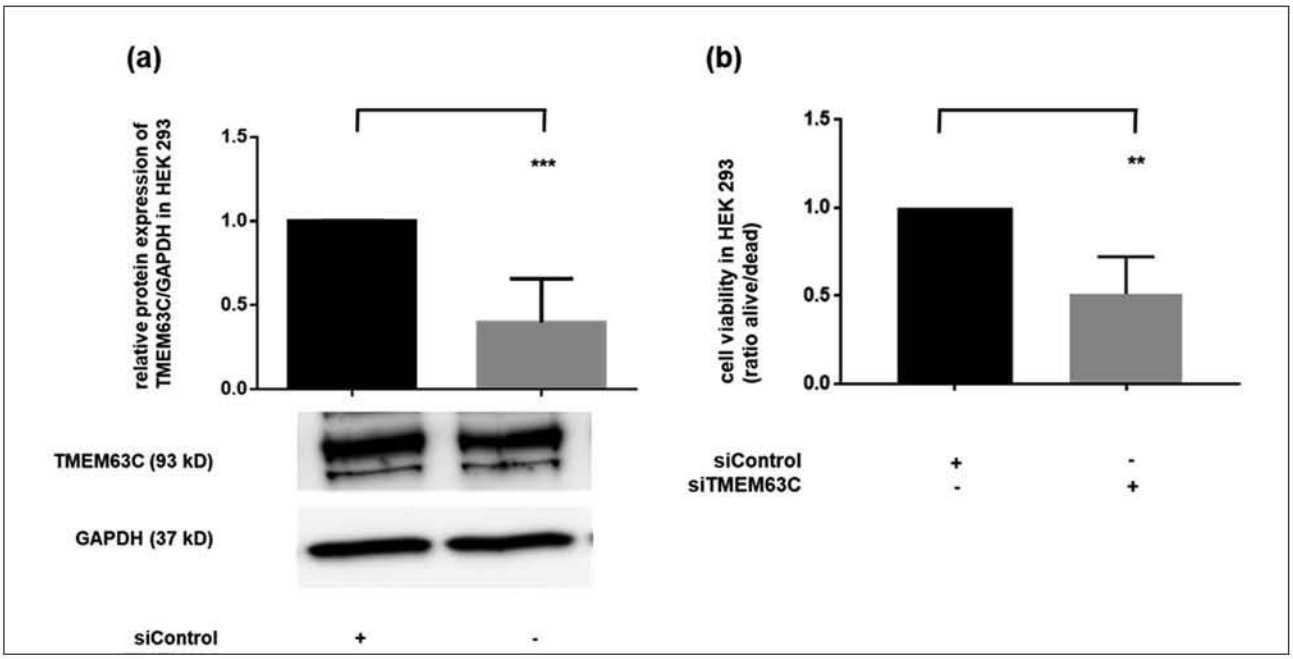

Fig. 3. The impact of TMEM63C inhibition on cell viability in HEK 293. HEK 293 were treated with specific siRNAs against TMEM63C (siTMEM63C) or scrambled control siRNAs (siControl) for 48 h. Shown is the (**a**) protein expression of TMEM63C and the (**b**) cell viability of HEK 293. The mean ± SEM of at least 3 independent experiments is represented. (**) $p < 0.01$; (***) $p < 0.001$. TMEM63C, transmembrane protein 63C; HEK 293, human embryonic kidney cells 293; siRNA, small interfering RNA.

Relative Luciferase Activity Measurement in HEK 293

Compared to controls, co-transfection of cells with the TMEM63C reporter vector and miR-564 led to a reduced luciferase activity, whereas co-transfection with a TMEM63C reporter vector including a mutated 3′UTR binding site and miR-564 exhibited no significant difference in luciferase activity (Fig. 2a, b). In contrast, co-treatment of HEK 293 with the reporter construct and miR-30b had no significant impact on luciferase activity in relation to controls (Fig. 2a).

Cell Viability of HEK 293 Was Decreased by siRNA-Mediated Inhibition of TMEM63C

After 48 h, we observed a significant reduction of TMEM63C protein expression in siTMEM63C-treated cells (Fig. 3a). Compared to controls, cell viability was also significantly reduced in siTMEM63C-transfected HEK 293 after 48 h (Fig. 3b).

TGF-β Stimulation Increased TMEM63C Protein Expression in HEK 293

We analyzed the impact of TGF-β stimulation on TMEM63C expression in HEK 293 after 48 h. Compared to controls, treatment of the cells with TGF-β increased TMEM63C expression on protein level in a concentration-dependent manner (Fig. 4).

The Ratio of α-SMA versus E-Cadherin Was Affected by TMEM63C Expression

To investigate the impact of TMEM63C on EMT, we transfected HEK 293 with specific siRNAs against TMEM63C for 48 h and analyzed the ratio of α-SMA versus E-cadherin mRNA expression. Compared to controls, the ratio of α-SMA versus E-cadherin increased significantly in siTMEM63C-treated cells (Fig. 5).

Kidney and Blood Pressure Research

Kidney Blood Press Res 2020;45:850–862
DOI: 10.1159/000508477

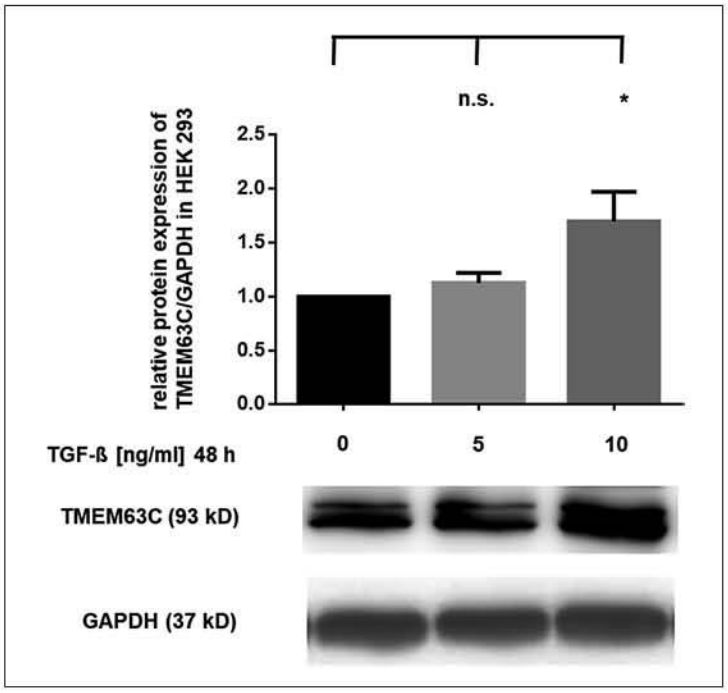

Fig. 4. The effect of TGF-β stimulation on TMEM63C protein expression in HEK 293. HEK 293 were stimulated with 5 or 10 ng/mL TGF-β for 48 h. TMEM63C was normalized against GAPDH. The mean ± SEM of at least 3 independent experiments is shown. (*) $p < 0.05$. n.s., no significant difference; TGF-β, transforming growth factor beta; TMEM63C, transmembrane protein 63C; HEK 293, human embryonic kidney cells 293; GAPDH, glyceraldehyde-3-phosphate dehydrogenase.

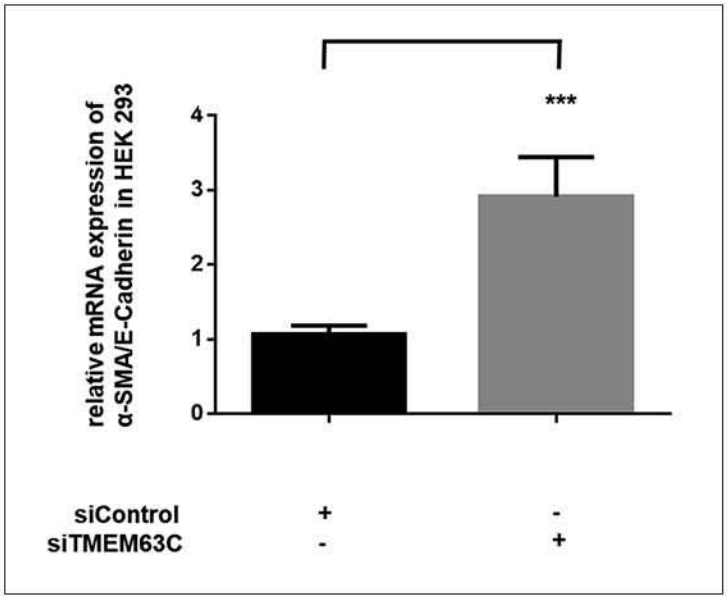

Fig. 5. The effect of TMEM63C inhibition on α-SMA versus E-cadherin. HEK 293 were transfected with inhibitory siRNAs against TMEM63C (siTMEM63C) or nonsense control siRNAs (siControl) for 48 h. Shown is the ratio of mRNA expression of α-SMA versus E-cadherin normalized against GAPDH. The mean ± SEM of at least 3 independent experiments is represented. (***) $p < 0.001$. TMEM63C, transmembrane protein 63C; α-SMA, α-smooth muscle actin; HEK 293, human embryonic kidney cells 293; siRNA, small interfering RNA.

MiR-564 Decreased TMEM63C Expression in hPC

In addition to the experiments in HEK 293, we analyzed the impact of miR-564 on TMEM63C expression in hPC. Compared to controls, TMEM63C mRNA expression was significantly reduced in miR-564-transfected cells after 48 h (Fig. 6).

TGF-β Stimulation Increased TMEM63C Protein Expression in hPC

Subsequently, we investigated the impact of TGF-β on TMEM63C expression in hPC. Compared to controls, the treatment of the cells with 5 or 10 ng/mL TGF-β for 48 h increased TMEM63C expression on protein level in a concentration-dependent manner (Fig. 7).

Kidney and Blood Pressure Research

Kidney Blood Press Res 2020;45:850–862

DOI: 10.1159/000508477

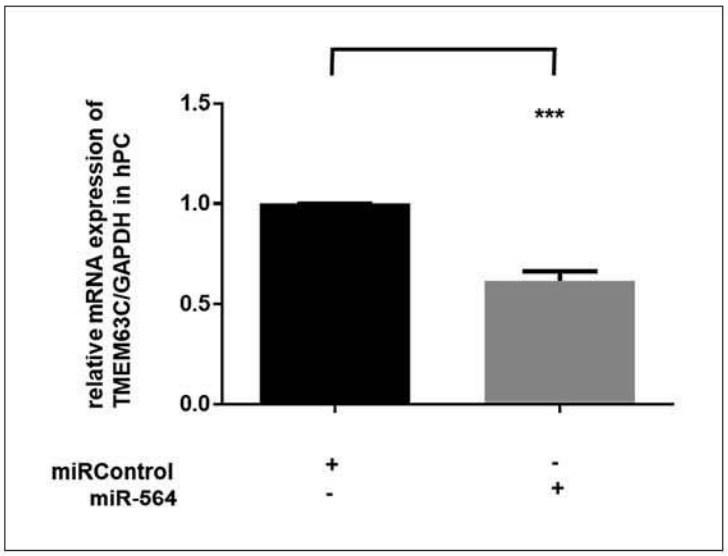

Fig. 6. The effect of miR-564 on TMEM63C mRNA expression in hPC. Shown is the expression of TMEM63C mRNA in hPC. Cells were transfected with miR-564 or a negative control miRNA mimic (miRControl). The expression was analyzed after 48 h. GAPDH was used for normalization. The mean ± SEM of at least 3 independent experiments is shown. (***) $p < 0.001$. miR, miRNA; TMEM63C, transmembrane protein 63C; hPC, human podocytes; GAPDH, glyceraldehyde-3-phosphate dehydrogenase.

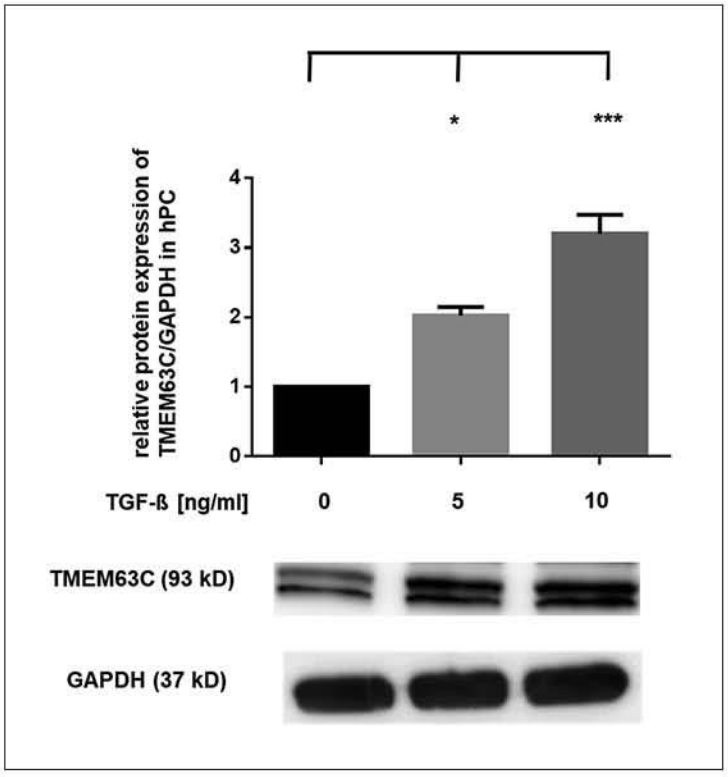

Fig. 7. The effect of TGF-β stimulation on TMEM63C protein expression in hPC. hPC were stimulated with 5 and 10 ng/mL TGF-β for 48 h, respectively. TMEM63C was normalized against GAPDH. The mean ± SEM of at least 3 independent experiments is shown. (*) $p < 0.05$; (***) $p < 0.001$. TGF-β, transforming growth factor beta; TMEM63C, transmembrane protein 63C; hPC, human podocytes; GAPDH, glyceraldehyde-3-phosphate dehydrogenase.

Expression of Nephrin Was Reduced by siRNA-Mediated Inhibition of TMEM63C in hPC

Moreover, we studied the impact of TMEM63C expression on nephrin generation in hPC. Transfection of cells with TMEM63C-specific siRNAs led to a significant reduction of TMEM63C mRNA expression in hPC (Fig. 8a). Compared to controls, siRNA-mediated downregulation of TMEM63C was additionally associated with a significant decrease in nephrin expression on mRNA level after 48 h (Fig. 8b).

Kidney and Blood Pressure Research

Kidney Blood Press Res 2020;45:850–862

DOI: 10.1159/000508477

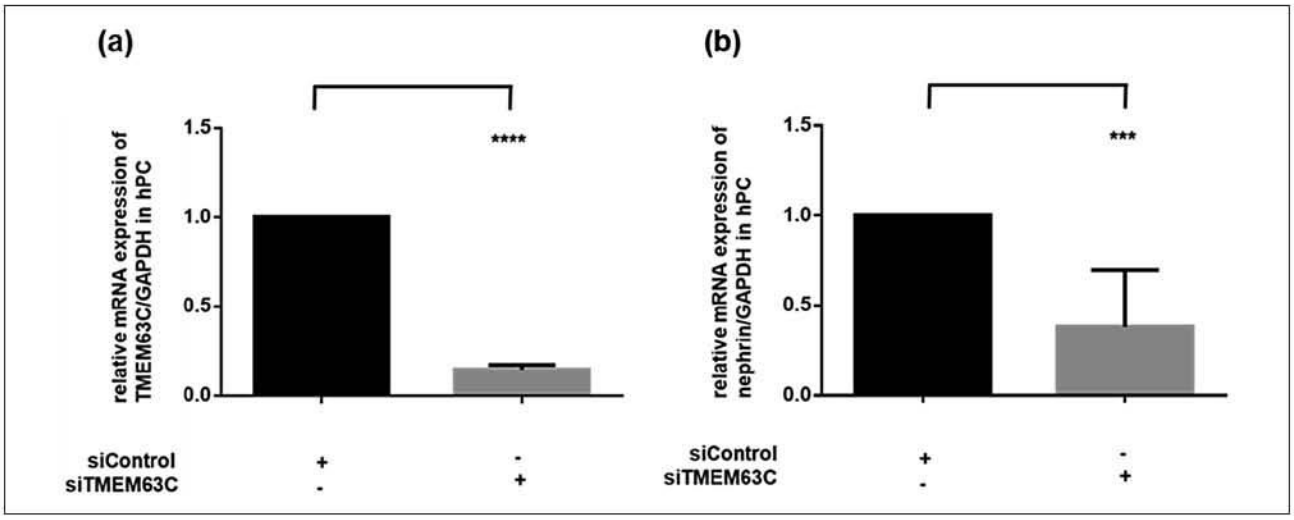

Fig. 8. TMEM63C and nephrin expression in siTMEM63C-treated hPC. hPC were transfected with inhibitory siRNAs against TMEM63C (siTMEM63C) or nonsense control siRNAs (siControl) for 48 h. Shown is the mRNA expression of (**a**) TMEM63C and (**b**) nephrin. The mean ± SEM of at least 3 independent experiments is represented. (***) $p < 0.001$; (****) $p < 0.0001$. TMEM63C, transmembrane protein 63C; hPC, human podocytes; siRNA, small interfering RNA.

Discussion

In this study, we identified TMEM63C as a direct target of miR-564. Furthermore, we showed an association between TMEM63C deficiency and reduced cell viability. Moreover, TMEM63C expression was found to be modulated by TGF-β stimulation in kidney cells. In addition to previous data [7], our data indicate that TMEM63C could be involved not only in GFB function but also in EMT.

Post-transcriptional Regulation of TMEM63C Expression by miR-564

We investigated the role of miRNAs in the regulation of TMEM63C expression. In a first step, we performed in silico analysis to identify potential miRNAs modulating TMEM63C expression on post-transcriptional level. In silico analysis is based on different computational algorithms, which are using different parameters to predict the probability of a functional miRNA binding site within a given mRNA target [16]. However, the characterization of miRNA-mRNA interactions is challenging and difficult to predict [17]. For this reason, several miRNAs were predicted to regulate TMEM63C expression. For our in vitro experiments, we selected miR-30b and miR-564 as very likely candidates for TMEM63C regulation. Both were predicted by at least 3 different prediction tools. In this study, we showed a direct reduction of TMEM63C expression by miR-564 treatment in renal cells, while miR-30b inhibited TMEM63C possibly rather indirectly. Both miRNAs were shown to be expressed in kidney cells [18].

Some miRNAs are already known to be significant participants in renal pathologies, such as miR-21 or miR-192 in kidney fibrosis [10]. In addition, previous studies described a modulating influence of miRNAs, such as miR-21, miR-22, or miR-566, in the genesis or prevention of renal cell cancer [11–13]. So far, miR-564 has not been identified in the context of renal pathologies, but various studies reported on the relevance of miR-564 and its function in different cancer biology. In this regard, miR-564 was demonstrated to induce cell apoptosis and to suppress cell proliferation in osteosarcoma cells by targeting protein kinase B [19].

Kidney and Blood Pressure Research

Kidney Blood Press Res 2020;45:850–862

DOI: 10.1159/000508477

Mutlu et al. [20] showed an inhibitory effect of miR-564 on cell proliferation in breast cancer cells due to suppression of phosphoinositide 3-kinase and mitogen-activated protein kinase. In addition, ectopic expression of miR-564 was described to stop EMT and reduce the migration and invasion of breast cancer cells [20]. In further studies, miR-564 was found to modulate TGF-β in different cell types [21, 22]. Jiang et al. [21] showed that miR-564 reduced TGF-β expression in glioblastoma cells. In another experimental setting, Xiao and Colleagues [22] presented an upregulation of miR-564 to be associated with an increased TGF-β expression in hypertrophic scars. So far, the role of miR-564 in the kidney, and especially in the context of renal pathologies, is unknown. However, miR-564 and its regulative function on TGF-β and EMT may not only be important in cancer, but could also be relevant in the modulation of renal fibrosis. In our study, miR-564 suppressed the expression of TMEM63C. For this reason, we investigated the effects of reduced TMEM63C expression on renal cells and studied the impact of TGF-β on TMEM63C expression.

Expression Regulation and Functional Effects of TMEM63C in HEK 293

Schulz et al. [7] showed the importance of TMEM63C expression for the maintenance of GFB in zebra fish models and demonstrated its potential relevance in patients with focal segmental glomerulosclerosis in translational studies. However, until now, the expression regulation of TMEM63C is widely unexplored. In our experiments, we used HEK 293 – due to its high transfection efficiency – to examine the expression regulation and impact of TMEM63C. The recent report already showed impaired cell viability due to suppression of TMEM63C in hPC [7]. In our study, we found downregulation of TMEM63C to be associated with reduced viability also in other renal cells (HEK 293). These results suggest that TMEM63C may have a beneficial effect on renal cell survival. Next, we analyzed the impact of TGF-β on TMEM63C expression. TGF-β is known as regulator and initiator of EMT and has been described as key mediator of glomerular and tubulointerstitial pathobiology in CKD [23, 24]. In CKD, TGF-β led to tubulointerstitial fibrosis and dysfunction of podocytes [25]. Previous studies showed that miR-564 is involved in the regulation of TGF-β [21, 22]. In this study, we found TGF-β to affect TMEM63C expression in a concentration-dependent manner. Further, we observed an inhibiting effect of miR-564 on TMEM63C generation. For this reason, we also studied the potential role of TMEM63C in EMT. In EMT, cells lose progressively their epithelial characteristics and acquire markers of mesenchymal phenotype [26]. Therefore, the ratio of epithelial and mesenchymal marker proteins is changed [27]. Typical epithelial markers are E-cadherin and fibronectin, whereas typical mesenchymal proteins are N-cadherin, α-SMA, and vimentin [27]. HEK 293 were shown to express both epithelial and mesenchymal marker proteins [28]. Therefore, we used these cells as suitable model to study the change of epithelial characteristics by altered TMEM63C expression. We found reduced TMEM63C expression to be associated with an increased ratio of α-SMA versus E-cadherin in HEK 293. This changing ratio of α-SMA versus E-cadherin is discussed as an indicator for tubular EMT [29]. However, the precise role of TMEM63C in EMT of renal tubular epithelial cells remains uncertain and should be investigated in further experiments. In conclusion, we found siTMEM63C to reduce cell viability in HEK 293. In addition, we showed an association between reduced TMEM63C expression and a changing expression of proteins that are involved in EMT. Therefore, the increased expression of TMEM63C by TGF-β might reflect a potential protective mechanism of TMEM63C in renal cells under pathophysiological conditions, such as the development of renal fibrosis.

Expression Regulation and Functional Effects of TMEM63C in hPC

Similar to HEK 293, TGF-β treatment increased TMEM63C expression in a concentration-dependent manner in hPC. Enhanced TGF-β concentration is associated with podocyte apoptosis and detachment from the glomerular basement membrane, EMT, and the development

Kidney and Blood Pressure Research

Kidney Blood Press Res 2020;45:850–862

DOI: 10.1159/000508477

of glomerulosclerosis [30]. For EMT studies in podocytes, it is important to consider that these cells have been described as atypical epithelial cells with a different expression of epithelial and mesenchymal proteins [31]. EMT in podocytes, also referred to as "podocyte disease transformation," is associated with a decrease in proteins such as podocin, nephrin, and P-cadherin and an increase in α-SMA and N-cadherin [31, 32]. Moreover, Ghiggeri et al. [33] indicated that nephrin elimination may trigger EMT in hPC. We showed that reduced TMEM63C expression is associated with decreased generation of nephrin in hPC. These data support our suspicion that TMEM63C may play a potential role in modulation of EMT in renal cells. Further, nephrin is known as an essential structural protein of the slit diaphragm and is pivotal for the preservation of GFB function as well as podocyte viability [2]. Langham et al. [34] also showed reduced nephrin expression to be associated with proteinuria in relevant kidney diseases such as diabetic nephropathy. We found reduced nephrin expression by inhibiting TMEM63C. For this reason, the current data support our previous observations linking TMEM63C to the development of albuminuria [7]. Altogether, our results demonstrated that TMEM63C is regulated by miR-564 and TGF-β in hPC and affects the expression of nephrin and could therefore influence the preservation of renal filter function.

Conclusion

In this study, we identified TMEM63C as a direct target of miR-564 in human renal cells. Moreover, the current study demonstrated that TMEM63C is regulated by TGF-β and could be involved in EMT. However, the effects of TMEM63C on EMT have not yet been clarified and should be investigated in further experiments. These experiments may include in vivo studies or at least studies in primary kidney cells, since experiments in immortalized cell lines, although important for mechanistic studies, should be viewed with some caution due to a potential permissive oncogenic phenotype for EMT studies [35]. Moreover, the role of EMT per se in the context of renal fibrosis has been questioned [36] and has been a matter of controversy [37]. Nevertheless, more recent studies indicated that at least partial EMT may be sufficient to promote renal fibrosis [38, 39] although evidence for human CKD is scant [37].

Our current results also support recently reported findings linking TMEM63C-expression to GFB function and albuminuria [7]. In the latter study, downregulation of TMEM63C resulted in albuminuria in zebra fish models and reduced cell viability of hPC, indicating a potential protective effect of TMEM63C for renal filter function [7]. In line with these findings, the current study showed siTMEM63C to reduce nephrin, a pivotal protein for the preservation of GFB function as well as podocyte viability [2]. Moreover, siRNA-mediated downregulation of TMEM63C led to a reduced cell viability of HEK 293. On the other hand, downregulation of TMEM63C in HEK293 was linked to EMT by increasing the α-SMA/E-cadherin ratio and was thus associated with the activation of pro-fibrotic mechanisms [37]. In this regard, our finding demonstrating an upregulation of TMEM63C by TGF-β, which is a major driver of renal fibrosis, may reflect a counter-balancing mechanistic link between TMEM63C and TGF-β. Taken together, our data indicate that TMEM63C is not only linked to GFB function but may also be involved in EMT control. Therefore, TMEM63C is a novel functional candidate with potential impact for the development and progression of CKD.

Acknowledgements

We thank Claudia Plum, Petra Karsten, Sarah Podlech, Dr. Anja Brehm, and Marie Käbel for experimental and technical support.

Kidney and Blood Pressure Research

Kidney Blood Press Res 2020;45:850–862

DOI: 10.1159/000508477

Conflict of Interest Statement

The authors have no conflicts of interest to declare.

Funding Sources

This study was supported by the DFG (German Research Foundation) – Project number 394046635-SFG 1365 and the Open Access Publication Funds of Charité – Universitätsmedizin Berlin.

Author Contributions

M.O., A.G., J.S., K.B., and A.E. carried out the cell culture studies. K.B., M.O., and A.E. participated in the PCR tests. M.O. and A.E. performed the statistical analysis. M.O., A.E., and R.K. conceived the study, participated in its design and coordination, and drafted the manuscript. A.G., J.S., and K.B. revised the manuscript critically. All authors read and approved the final manuscript. All authors agree to be accountable for all aspects of the work and to ensure that questions relating to the accuracy or integrity of any part of the work have been appropriately investigated and resolved.

TMEM63C, transmembrane protein 63C; GAPDH, glyceraldehyde-3-phosphate dehydrogenase; α-SMA, α-smooth muscle actin.

References

1 Reiser J, Sever S. Podocyte biology and pathogenesis of kidney disease. Annu Rev Med. 2013;64:357–66.
2 Li X, Chuang PY, D'Agati VD, Dai Y, Yacoub R, Fu J, et al. Nephrin preserves podocyte viability and glomerular structure and function in adult kidneys. J Am Soc Nephrol. 2015;26(10):2361–77.
3 Podgorski P, Konieczny A, Lis L, Witkiewicz W, Hruby Z. Glomerular podocytes in diabetic renal disease. Adv Clin Exp Med. 2019;28(12):1711–5.
4 Brinkkoetter PT, Ising C, Benzing T. The role of the podocyte in albumin filtration. Nat Rev Nephrol. 2013;9(6):328–36.
5 Lambers Heerspink HJ, Gansevoort RT. Albuminuria is an appropriate therapeutic target in patients with CKD: the pro view. Clin J Am Soc Nephrol. 2015;10(6):1079–88.
6 Abbate M, Zoja C, Remuzzi G. How does proteinuria cause progressive renal damage? J Am Soc Nephrol. 2006;17(11):2974–84.
7 Schulz A, Müller NV, van de Lest NA, Eisenreich A, Schmidbauer M, Barysenka A, et al. Analysis of the genomic architecture of a complex trait locus in hypertensive rat models links Tmem63c to kidney damage. eLife. 2019;8:e42068.
8 Trionfini P, Benigni A. MicroRNAs as master regulators of glomerular function in health and disease. J Am Soc Nephrol. 2017;28(6):1686–96.
9 Trionfini P, Benigni A, Remuzzi G. MicroRNAs in kidney physiology and disease. Nat Rev Nephrol. 2014;11(1):23.
10 Chung AC, Lan HY. MicroRNAs in renal fibrosis. Front Physiol. 2015;6:50.
11 Fan B, Jin Y, Zhang H, Zhao R, Sun M, Sun M, et al. MicroRNA21 contributes to renal cell carcinoma cell invasiveness and angiogenesis via the PDCD4/cJun (AP1) signalling pathway. Int J Oncol. 2020 Jan;56(1):178–92.
12 Gong X, Zhao H, Saar M, Peehl DM, Brooks JD. miR-22 regulates invasion, gene expression and predicts overall survival in patients with clear cell renal cell carcinoma. Kidney Cancer. 2019;3(2):119–32.
13 Pan X, Quan J, Li Z, Zhao L, Zhou L, Jinling X, et al. miR-566 functions as an oncogene and a potential biomarker for prognosis in renal cell carcinoma. Biomed Pharmacother. 2018;102:718–27.
14 Eisenreich A, Langer S, Herlan L, Kreutz R. Regulation of podoplanin expression by microRNA-29b associates with its antiapoptotic effect in angiotensin II-induced injury of human podocytes. J Hypertens. 2016;34(2):323–31.
15 Leppert U, Gillespie A, Orphal M, Böhme K, Plum C, Nagorsen K, et al. The impact of α-lipoic acid on cell viability and expression of nephrin and ZNF580 in normal human podocytes. Eur J Pharmacol. 2017;810:1–8.

Kidney and Blood Pressure Research

Kidney Blood Press Res 2020;45:850–862

DOI: 10.1159/000508477

16 Kuhn DE, Martin MM, Feldman DS, Terry AV Jr., Nuovo GJ, Elton TS. Experimental validation of miRNA targets. Methods. 2008;44(1):47–54.
17 Riffo-Campos ÁL, Riquelme I, Brebi-Mieville P. Tools for sequence-based miRNA target prediction: what to choose? Int J Mol Sci. 2016;17(12):1987.
18 Argyropoulos C, Wang K, Bernardo J, Ellis D, Orchard T, Galas D, et al. Urinary microRNA profiling predicts the development of microalbuminuria in patients with type 1 diabetes. J Clin Med. 2015;4(7):1498–517.
19 Ru N, Zhang F, Liang J, Du Y, Wu W, Wang F, et al. MiR-564 is down-regulated in osteosarcoma and inhibits the proliferation of osteosarcoma cells via targeting Akt. Gene. 2018;645:163–9.
20 Mutlu M, Saatci Ö, Ansari SA, Yurdusev E, Shehwana H, Konu Ö, et al. miR-564 acts as a dual inhibitor of PI3K and MAPK signaling networks and inhibits proliferation and invasion in breast cancer. Sci Rep. 2016;6:32541.
21 Jiang C, Shen F, Du J, Hu Z, Li X, Su J, et al. MicroRNA-564 is downregulated in glioblastoma and inhibited proliferation and invasion of glioblastoma cells by targeting TGF-β1. Oncotarget. 2016;7(35):56200–8.
22 Xiao L, Tang T, Huang Y, Guo J. MiR-564 promotes hypertrophic scar via up-regulating TGF-β1. G Ital Dermatol Venereol. 2019 Apr;154(2):186–91.
23 Bottinger EP, Bitzer M. TGF-beta signaling in renal disease. J Am Soc Nephrol. 2002;13(10):2600–10.
24 Loeffler I, Wolf G. Transforming growth factor-β and the progression of renal disease. Nephrol Dial Transplant. 2014;29(Suppl 1):i37–45.
25 Gewin L, Zent R. How does TGF-β mediate tubulointerstitial fibrosis? Semin Nephrol. 2012;32(3):228–35.
26 Seccia T, Caroccia B, Piazza M, Rossi GP. The key role of epithelial to mesenchymal transition (EMT) in hypertensive kidney disease. Int J Mol Sci. 2019;20(14):3567.
27 Moustakas A, Heldin CH. Mechanisms of TGFβ-induced epithelial-mesenchymal transition. J Clin Med. 2016;5(7):63.
28 Inada M, Izawa G, Kobayashi W, Ozawa M. 293 cells express both epithelial as well as mesenchymal cell adhesion molecules. Int J Mol Med. 2016;37(6):1521–7.
29 Du T, Zou X, Cheng J, Wu S, Zhong L, Ju G, et al. Human Wharton's jelly-derived mesenchymal stromal cells reduce renal fibrosis through induction of native and foreign hepatocyte growth factor synthesis in injured tubular epithelial cells. Stem Cell Res Ther. 2013;4(3):59.
30 Lee HS. Mechanisms and consequences of TGF-ß overexpression by podocytes in progressive podocyte disease. Cell Tissue Res. 2012;347(1):129–40.
31 May CJ, Saleem M, Welsh GI. Podocyte dedifferentiation: a specialized process for a specialized cell. Front Endocrinol. 2014;5:148.
32 Ying Q, Wu G. Molecular mechanisms involved in podocyte EMT and concomitant diabetic kidney diseases: an update. Ren Fail. 2017;39(1):474–83.
33 Ghiggeri GM, Gigante M, Di Donato A. Constitutional nephrin deficiency in conditionally immortalized human podocytes induced epithelial-mesenchymal transition, supported by beta-catenin/NF-kappa B activation: a consequence of cell junction impairment? Inter J Nephrol. 2013;2013:457490.
34 Langham RG, Kelly DJ, Cox AJ, Thomson NM, Holthöfer H, Zaoui P, et al. Proteinuria and the expression of the podocyte slit diaphragm protein, nephrin, in diabetic nephropathy: effects of angiotensin converting enzyme inhibition. Diabetologia. 2002;45(11):1572–6.
35 Wang Y, Chen S, Yan Z, Pei M. A prospect of cell immortalization combined with matrix microenvironmental optimization strategy for tissue engineering and regeneration. Cell Biosci. 2019;9(1):7.
36 Humphreys BD, Lin SL, Kobayashi A, Hudson TE, Nowlin BT, Bonventre JV, et al. Fate tracing reveals the pericyte and not epithelial origin of myofibroblasts in kidney fibrosis. Am J Pathol. 2010;176(1):85–97.
37 Liu BC, Tang TT, Lv LL, Lan HY. Renal tubule injury: a driving force toward chronic kidney disease. Kidney Int. 2018;93(3):568–79.
38 Lovisa S, LeBleu VS, Tampe B, Sugimoto H, Vadnagara K, Carstens JL, et al. Epithelial-to-mesenchymal transition induces cell cycle arrest and parenchymal damage in renal fibrosis. Nat Med. 2015;21(9):998–1009.
39 Grande MT, Sánchez-Laorden B, López-Blau C, De Frutos CA, Boutet A, Arévalo M, et al. Snail1-induced partial epithelial-to-mesenchymal transition drives renal fibrosis in mice and can be targeted to reverse established disease. Nat Med. 2015;21(9):989–97.

Lebenslauf

Mein Lebenslauf wird aus datenschutzrechtlichen Gründen in der elektronischen Version meiner Arbeit nicht veröffentlicht.

Publikationsliste

Subrova J, Böhme K, Gillespie A, Orphal M, Plum C, Kreutz R, Eisenreich A. (2022). “MiRNA-29b and miRNA-497 Modulate the Expression of Carboxypeptidase X Member 2, a Candidate Gene Associated with Left Ventricular Hypertrophy.” Int J Mol Sci. 18(4):2263.

Impact Factor: 5,924

Grabowski K, Herlan L, Witten A, Qadri F, Eisenreich A, Lindner D, Schädlich M, Schulz A, **Subrova J**, Mhatre KN, Primessnig U, Plehm R, van Linthout S, Escher F, Bader M, Stoll M, Westermann D, Heinzel FR, Kreutz R. (2022). "Cpxm2 as a novel candidate for cardiac hypertrophy and failure in hypertension." Hypertens Res. 45(2):292-307.

Impact Factor: 2,941

Orphal M, Gillespie A, Böhme K, **Subrova J**, Eisenreich A, Kreutz R. (2020). “TMEM63C, a Potential Novel Target for Albuminuria Development, Is Regulated by MicroRNA-564 and Transforming Growth Factor beta in Human Renal Cells.” Kidney Blood Press Res. 45(6):850-862.

Impact Factor: 2,687

Danksagung

Für die intensive Betreuung und Unterstützung bei der Durchführung der Experimente sowie bei der Veröffentlichung der Ergebnisse möchte ich mich beim Herrn PD Dr. rer. nat. Andreas Eisenreich bedanken. Mit seiner Hilfe konnte ich verschiedene biochemische Labormethoden erlernen und diese im Rahmen meiner Doktorarbeit anwenden. Danke. Ebenfalls danke ich meinem Doktorvater Herrn Prof. Dr. med. Reinhold Kreutz für seine tatkräftige Unterstützung meines Promotionsvorhabens. Weiter möchte ich Frau Dr. Katja Grabowski für die nette und erfolgreiche Zusammenarbeit und das Zurverfügungstellen der Gewebeproben sowie Frau Anna Sonnenburg für die Durchführung der durchflusszytometrischen Messungen danken. Mein Dank gehört auch Frau Karen Böhme und Frau Claudia Plum für ihre Hilfsbereitschaft im Labor. Dem gesamten Team des Instituts für Klinische Pharmakologie und Toxikologie der Charité möchte ich danken, dass ich ein Teil davon werden konnte. Außerdem danke ich meinen Eltern, die sich stets für meine Arbeit interessiert haben und mich nicht selten auch fachlich beraten haben.